Stony Brook University

Elucidation of mechanisms of *Yersinia pestis* survival in macrophages by examination of phagosomal acidification and negative selection screening

A dissertation presented

by

Kathryn Anne Klein

to

The Graduate School

In partial fulfillment of the

Requirements

For the degree of

Doctor of Philosophy

in

Genetics

Stony Brook University

August 2009

Stony Brook University

The Graduate School

Kathryn Anne Klein

We, the dissertation committee for the above candidate for the

Doctor of Philosophy degree, hereby recommend

acceptance of this dissertation.

James B. Bliska, Ph.D. – Dissertation Advisor
Professor, Department of Molecular Genetics and Microbiology

Martha B. Furie, Ph.D. – Chairperson of Defense Committee
Professor, Department of Pathology, Department of Molecular Genetics and Microbiology

Michael A. Frohman, M.D., Ph.D.
Professor, Department of Pharmacological Sciences

David G. Thanassi, Ph.D.
Associate Professor, Department of Molecular Genetics and Microbiology

Craig R. Roy, Ph.D.
Professor, Section of Microbial Pathogenesis, Yale University

This dissertation is accepted by the Graduate School

Lawrence Martin
Dean of the Graduate School

Abstract of the Dissertation

Elucidation of mechanisms of *Yersinia pestis* survival in macrophages by examination of phagosomal acidification and negative selection screening

by

Kathryn Anne Klein

Doctor of Philosophy

in

Genetics

Stony Brook University

2009

Yersinia pestis, the causative agent of plague, is able to survive and replicate within the phagosomes of murine macrophages. However, the mechanism by which *Y. pestis* promotes its intracellular survival is not well understood. Previous studies demonstrated that *Y. pestis*-containing vacuoles (YCVs) acquire markers of late endosomes or lysosomes in macrophages, suggesting that the phagosomes mature. Thus, further investigation was performed to characterize how *Y. pestis* modifies its phagosomal environment in order to promote its survival within macrophages. A negative selection screen was also performed to identify genes that are important for the survival of *Y. pestis* in macrophages.

Studies were undertaken to investigate the mechanism of *Y. pestis* survival in phagosomes of macrophages. Fluorescence microscopy of infected macrophages showed that *Y. pestis* does not colocalize with markers of acidic vacuoles. The pH of YCVs was determined by microscopic imaging of infected macrophages, and these pH

measurements indicated that YCVs fail to acidify below a pH of 7 in macrophages. Additionally, YCVs did not colocalize with markers of the lysosomal vacuolar ATPase required for phagosomal acidification. Thus, it appears that *Y. pestis* prevents acidification of its phagosome to promote its survival in the macrophage, potentially by interfering with the vacuolar H+ ATPase.

To identify genes that are important for *Y. pestis* survival in macrophages, a transposon library of *Y. pestis* mutants was subjected to negative selection in primary murine macrophages. Several genes were identified as potentially important in the intracellular survival of *Y. pestis*. One of these genes is predicted to encode a glucose-1-phosphate uridylyltransferase (*galU*), which plays a role in the biosynthesis of the lipooligosaccharide outer core. Viable count assays verified that a *Y. pestis galU* mutant is defective for survival in murine macrophages. Further characterization showed that the *Y. pestis galU* mutant is susceptible to antimicrobial peptides. Therefore, *galU* appears to encode an enzyme important for production of the bacterial lipooligosaccharide core and is required for *Y. pestis* survival in macrophages.

Table of Contents

List of Abbreviations.....vi-vii
List of Figures.....viii-ix
List of Tables.....x
Acknowledgements.....xi-xii
Chapter 1 – Introduction.....1-20
Yersinia Pathogenesis.....1
Macrophage Biology.....4
Pathogens subvert macrophage functions to survive intracellularly.....10
Y. pestis survival and trafficking within macrophage phagosomes.....14
Figures and Tables.....17
Chapter 2 – To examine if *Y. pestis* prevents acidification of its vacuoles as an intracellular survival strategy.....21-43
Summary.....21
Introduction.....22
Experimental Procedures.....22
Results.....27
Discussion.....30
Figures and Tables.....34
Chapter 3 – To examine the importance of Rab GTPases to the trafficking of *Y. pestis*-containing phagosomes in macrophages.....44-59
Summary.....44
Introduction.....44
Experimental Procedures.....45
Results.....47
Discussion.....50
Figures and Tables.....53
Chapter 4 – To identify and characterize genes important for *Y. pestis* to promote intracellular survival.....60-84
Summary.....60
Introduction.....60
Experimental Procedures.....62
Results.....67
Discussion.....71
Figures and Tables.....75
Chapter 5 – Concluding Remarks.....85-91
Summary.....85
Open questions.....86
References.....92-103

List of Abbreviations

BMM – bone marrow-derived macrophage

CFU – colony forming unit

FACS - fluorescent-activated cell sorting

FBS – fetal bovine serum

FITC - fluorescein isothiocyanate

HI – heart-infusion

HRP – horseradish peroxidase

IPTG - isopropyl-β-D-1-thiogalacto-pyaranoside

LB – Luria-Bertani

LOS - lipooligosaccharide

LPS – lipopolysaccharide

mag – *magellan3* mini-transposon

MOI – multiplicity of infection

ORF – open reading frame

pCD1 – 70kb virulence plasmid

PFA – paraformaldehyde

pgm locus – pigmentation locus

Pla – plasminogen activator

RAVE - regulator of the ATPase of vacuolar and endosomal membranes

SDS - sodium dodecyl sulfate

T3SS – Type III secretion system

TraSH – transposon-site hybridization

vATPase – vacuolar H+ ATPase

YCV – *Yersinia*-containing vacuole

List of Figures

Figure 1.1 - Structure of the vATPase.....18

Figure 1.2 - Model for trafficking of YCV.....19

Figure 1.3 – General Structure of the LPS.....20

Figure 2.1 - Measurement of YCV acidification using Lysotracker and fluorescence microscopy.....35-36

Figure 2.2 - Prevention of YCV acidification is not due to known virulence factors.....37

Figure 2.3 - The ability to prevent YCV acidification is shared among *Yersinia* species.....38

Figure 2.4 - Measurement of YCV pH using live cell ratiometric imaging.....39

Figure 2.5 - *De novo* protein synthesis is not required for KIM5 to prevent phagosome acidification.....40

Figure 2.6 – *Y. pestis* is unable to globally prevent YCV acidification within a macrophage.....41-42

Figure 2.7 - YCVs containing live bacteria do not colocalize with vATPase.....43

Figure 3.1 - Colocalization of Rab proteins with YCVs.....54-55

Figure 3.2 - Polyclonal Rab27 is less specific than the monoclonal Rab27 antibody.....56

Figure 3.3 - Polyclonal Rab27 antibody cross-reacts with *Y. pestis*.....57

Figure 3.4 – Extracellular bacteria are detected after macrophages competent or deficient for Rab27 are infected.....58

Figure 3.5 - Rab27 does not contribute to block in phagosome acidification.....59

Figure 4.1. Design of the TraSH screen.....80-81

Figure 4.2 – Analysis of KIM6+ mutants for defects in intracellular survival.....82

Figure 4.3 - *galU* is important for the survival of *Y. pestis* in macrophages.....83

Figure 4.4 – Analysis of KIM mutants for defects in preventing phagosome acidification.....84

List of Tables

Table 1.1 – Features of *Y. pestis* KIM strains.....17

Table 2.1 - *Yersinia* strains used in Chapter 2.....34

Table 3.1 - *Yersinia* strains used in Chapter 3.....53

Table 4.1 - *Yersinia* strains used in Chapter 4.....75

Table 4.2 - Primers used to create gene knockouts.....76

Table 4.3 - Negative selection screen results showing 25 genes with the highest negative fold change.....77

Table 4.4 - Gene mutation effects on intracellular survival of *Y. pestis* in macrophages.....78

Table 4.5 - *galU* is important for resistance to polymyxin B.....79

Acknowledgements

General Acknowledgements

First and foremost, I would like to express my deepest gratitude toward my advisor Dr. James Bliska for accepting me into his lab and guiding me throughout my dissertation research. I am appreciative of Jim's availability to provide advice and assistance, as well as his willingness to give me freedom in my work.

I would also like to thank the members of the Bliska lab for making the lab environment both fun and productive. I would especially like to thank Maya Ivanov and Galina Romanov for all of their technical assistance during my research, Hana Fukuto for all of the scientific discussion and advice regarding my dissertation work, and to Betty Noel for general help and support during my time in the lab.

I am grateful to the members of my committee first for agreeing to serve on my committee. I am incredibly thankful for all of the useful scientific suggestions given during committee meetings.

Great thanks go out to my family and friends for their love and support during my time in graduate school. I am particularly indebted to my father for instilling in me a desire to learn, as well as a love of all things related to science.

Last but certainly not least, I would like to thank my wonderful fiancé Dr. Patrick Wagner. Words cannot express how happy I am to have him in my life. I am grateful for his love, friendship, patience, devotion, support and understanding during these years of our respective post-graduate educations.

Research-specific Acknowledgements

I thank Xiao Wu, who created CO92Δpgm/GFP and A1122/GFP, as well as tested the *Yersinia* strains via Lysotracker Red assay (results shown in Figure 2.3) when she was a rotation student in the lab. I am grateful to Dr. Satoshi Sato for the gift of the vATPase OSW2 antibody. I thank Dr. Lance Palmer for analysis of the ratiometric pH data seen in Chapter 2, as well as analysis of the microarray data found in Chapter 4. I am grateful to Dr. Hana Fukuto for advice regarding general TraSH screen setup and analysis. I appreciate the assistance of Adam Rosebrock in designing the microarray sample conditions, and thank Hong Wang for processing the microarrays. I thank Jens Grabenstein for creating the KIM10+ *galU* strains. I thank Amanda Smith, a high school student in the Intel Science Technology and Research Preparatory program, for constructing the KIM6+ Δ*y0157-y0159* mutant. I thank Hannah Volkman from the University of Washington for protocols concerning the THP-1 human monocyte cell line, and Rebecca Rowehl from the Stony Brook Cell Culture/Hybridoma Facility for assistance with and advice on THP-1 cell culture. I thank Galina Romanov for excellent technical assistance in isolating BMMs.

Chapter 1: Introduction

Yersinia pathogenesis

***Yersinia* history.** There are three species of *Yersinia* that are pathogenic in humans - *Y. pestis*, *Y. pseudotuberculosis*, and *Y. enterocolitica*. *Y. pestis* is best known as the causative agent of plague (101). Three biovars of *Y. pestis* have been identified due to differences in glycerol fermentation and nitrate reduction: Antiqua, Mediaevalis, and Orientalis (160). These differences do not appear to correlate with any variation in virulence, as each biovar has been associated with a major plague epidemic. Biovar Mediaevalis is associated with the most famous pandemic – the Black Death of the fourteenth century, reported to have killed approximately one-third of the human population in Europe (101, 160). Though the incidence of plague in recent times is relatively low, there is still concern due to the emergence of naturally occurring drug-resistant strains (39). There is also a long history of plague being used for biological warfare, from the fourteenth century though the early 1990s (77). As part of an effort to improve responses to bioterrorism, *Y. pestis* has been classified as a CDC category A select agent, since infection with aerosolized bacteria leads to highly contagious and fatal pneumonic plague (123). It is thought that *Y. pestis* evolved from its close genetic relative *Yersinia pseudotuberculosis* as recently as 1,500-20,000 years ago (1).

***Yersinia* virulence factors.** All three *Yersinia* species contain a 70 kb virulence plasmid (pCD1 in *Y. pestis* and pYV in *Y. pseudotuberculosis* and *Y. enterocolitica*) encoding a type III secretion system (T3SS) as well as its effector proteins, known as

Yersinia outer proteins (Yops) (26, 155). YopB and YopD are inserted into the host cell membrane to form a pore through which the effector Yops are translocated into the host cell cytosol (122, 142). LcrV appears to regulate formation of the YopB-D pore, while YopK plays a role in regulating translocation of the effector Yop proteins (6, 58). The effector Yops exhibit a number of different effects on the host. YopE, YopH, YopO, and YopT are involved in promoting resistance to phagocytosis (48, 120). YopE, YopH, and YopJ suppress the proinflammatory response (10, 11, 131). YopE, in addition to these other functions, has been implicated in promoting cytotoxicity (121). YopJ (YopP in *Y. enterocolitica*) also promotes apoptosis of the host cell (92). The function of YopM has yet to be characterized, but this effector localizes to the nucleus (135). The T3SS is thus required for sustained bacterial survival and replication within a host.

Y. pestis has two additional plasmids contributing to its virulence. The pMT1 plasmid codes for the F1 capsule and murine toxin and appears to be involved in flea colonization and transmission, and the pPCP1 plasmid encodes the plasminogen activator (Pla) important for bacterial dissemination into the deeper tissues of the host (23, 141). The T3SS, F1 capsule, and Pla are all upregulated at the host temperature of 37^{o}C. Another factor contributing to the virulence of *Yersinia* is the 102 kb pigmentation (*pgm*) locus located on the bacterial chromosome; this region encodes both the hemin storage genes as well as the genes required for the production of the siderophore yersiniabactin, required for iron acquisition from the mammalian host (53, 99). Most of the strains of *Y. pestis* isolated in nature contain these three virulence plasmids as well as the *pgm* locus (101).

***Yersinia* pathogenesis.** The members of the *Yersinia* genus are Gram-negative bacteria able to survive within macrophages. *Y. pseudotuberculosis* and *Y. enterocolitica* are enteric pathogens that are transmitted via the fecal-oral route (4, 160). Following consumption of contaminated food or water, the bacteria travel to the small intestine, where they are taken up by and transported through the M cells in Peyer's patches (127). From there, the bacteria can be engulfed by macrophages and travel to regional lymph nodes, and in rare cases bacterial infection can become systemic. These pathogens generally cause a self-limiting gastroenteritis in immunocompetent hosts. *Y. pestis* is a bloodborne pathogen, and is maintained in the environment through a rodent reservoir and a flea vector (160). When an infected flea attempts to feed on a rodent or a human, *Y. pestis* is introduced via the flea bite. The bacteria then travel to regional lymph nodes either by trafficking to these sites within macrophages, or utilizing Pla to penetrate into the deeper tissues (73, 110). Once in the lymph nodes, the bacteria will replicate and cause the lymph nodes to swell, a classical sign of bubonic plague. If left untreated, bubonic plague has a 50-90% mortality rate (107). *Y. pestis* can disseminate from the bubo into the blood stream, causing septicemia, and once in the blood travel to secondary lymphoid organs such as the liver and spleen. The bacteria may also travel to the lung, which gives rise to secondary pneumonic plague. This form of plague is easily transmitted to other hosts through respiratory droplets, resulting in primary pneumonic plague. Both septicemic and pneumonic forms of plague show high morbidity and mortality if left untreated, and the fatality rate of pneumonic plague is nearly 100% in the absence or delay of antibiotic therapy (60).

Macrophage Biology

Macrophages are professional phagocytes crucial to the innate immune system, their role being to destroy foreign objects in the body (63). These phagocytes reside in nearly all tissues of the body, having particularly significant populations in secondary lymphoid organs as well as tissues highly exposed to foreign particles such as the lung and gastrointestinal tract. In addition to their role in the innate immune response, macrophages also play a role in adaptive immunity by producing cytokines and by presenting antigens to lymphocytes, stimulating antibody production (63). A macrophage is able to recognize a pathogen through various cell-surface receptors, which initiates phagocytosis of said pathogen (72). Once a macrophage interacts with and degrades a pathogen, for example through recognition of bacterial ligands by Toll-like receptors, the macrophage can then process and present antigens to CD4 T cells (63). The T cells then produce interferon gamma, which activates macrophages (83, 95). A consequence of macrophage activation is the oxidative burst, which results in the production of reactive oxygen intermediates. These reactive oxygen species can activate the transcription factor NF-κB, which then leads to upregulation of proinflammatory cytokines; in addition, these oxygen intermediates are highly microbicidal (52, 119).

Phagosome maturation. Once a foreign particle is phagocytosed by a macrophage, it is engulfed in a vacuole termed a phagosome. The phagosome will interact and fuse with vacuoles of the endocytic pathway to mature into a phagolysosome, which has a hostile environment that can destroy the pathogen (156). No more than five minutes after internalization, phagosomes gain markers of early endosomes such as early endosome

antigen 1 (EEA1) (93). Within thirty minutes, the maturing phagosome contains characteristics of late endosomes (2). The final fusion of the maturing phagosome with lysosomes gives rise to a phagolysosome, which has a low pH and contains degradative enzymes and antimicrobial peptides from the lysosome; these serve to destroy the foreign particle (105). Both late endosomes and lysosomes contain similar markers such as cathepsins and lysosomal-associated membrane proteins (LAMPs), making these vesicles difficult to distinguish.

Phagosome maturation is a complex process, requiring several classes of proteins for the orchestration of the intermediate fusion events. ADP-ribosylation factor (ARF) GTPases regulate vesicle assembly in the endocytic pathway. Soluble *N*-ethylmaleimide-sensitive factor-attachment protein receptors (SNAREs) mediate fusion of vesicles with their target membranes (22). However, since these proteins lack a degree of specificity, Rab GTPase proteins are required to properly target and dock vesicles to the correct membranes in a selective way (156). Phosphoinositides (PI) interact with many of these proteins to regulate endocytic trafficking. For instance, enrichment of PI on a phagosome containing Rab5 recruits effectors necessary for fusion to late endosomes (67). PI also interact with ARF proteins to direct actin cytoskeleton rearrangements such as those seen with phagocytosis (72). Research suggests that phagosome maturation is also a dynamic process, occurring through multiple transient fusion and fission events (32). These brief phagosome-endosome interactions allow a transfer of luminal contents, and limit the comingling of the different components of the membrane compartments. There is evidence that some types of receptor-mediated phagocytosis can drive phagosome

maturation. For instance, Toll-like receptors, which act as coreceptors for bacteria, appear to induce a much faster rate of phagosome maturation than usual (9).

Phagosomal pH. Phagosome maturation appears to be an active process, regulated in part by pH. For instance, phagosomes do not fuse with lysosomes until the phagosomal environment is partially acidified (87). There is evidence that pH not only controls endocytic trafficking, but also plays a role in regulating exocytosis of secretory vesicles. An increase in lysosomal pH can cause secretion of lysosomal enzymes (150).

The vacuolar H^+ ATPase (vATPase) is a proton pump necessary for acidification of the phagosome and endocytic compartments (36). It is a multisubunit complex comprised of at least 14 subunits arranged in two domains (Figure 1.1). The V_1 domain is cytoplasmic and is responsible for the hydrolysis of ATP, and the V_o subunit is membrane-bound and is responsible for proton translocation into the lumen (78, 80). The a subunit plays a role in both domains – its N terminus helps form the peripheral stalk to which V_1 is bound, and its C terminus is located in the membrane and plays a crucial role in proton translocation (66, 74). Stator subunits A and B of V_1 alternate to form a hexameric structure, and ATP hydrolysis occurs at the interface between these two subunits (166). Protons enter the V_o rotary machinery through subunit a. ATP hydrolysis by V_1 then drives rotation of the V_o proteolipid ring, comprised of multiple subunits of c and one subunit each of c' and c" (106). Each of these hydrophobic subunits contains a single glutamate amino acid buried within a transmembrane domain (57). The ATP-driven rotation forces protons to be translocated through c, c', and c" subunits via protonation of the glutamate residues, and through interactions with the arginine 735 of

subunit a the protons are displaced into the lumen (66) (Figure 1.1). The activity of the vATPase can be regulated by reversible dissociation of the two domains. Dissociation is known to require an intact microtubule network and can occur under glucose depletion (162). Conversely, addition of glucose can lead to assembly of the domains back into the complete vATPase. The regulator of the ATPase of vacuolar and endosomal membranes (RAVE) complex, which appears to complex with and act as a chaperone for dissociated V_1, is essential for stable assembly of the vATPase (138, 139). RAVE interacts with subunit C, which appears to play a regulatory role in the association between V_1 and V_o (168). Recent data suggests that the vATPase may act as a pH sensor - the vATPase can recruit ARF proteins to early endosomes only when the endosomes are acidic (59). There is also some indication that Rab GTPases may play a role in vATPase localization and trafficking (27).

Rab GTPases. The Rab family is part of the Ras superfamily of small GTPases. Rab proteins are important regulators of intracellular vesicle trafficking (49). Over 60 Rabs have been identified in humans, indicating how important Rabs are in regulating the complex intracellular trafficking pathways found in higher eukaryotes. Rabs are anchored to intracellular membrane surfaces, and when activated to a GTP-bound state recruit and bind effector proteins to carry out trafficking tasks related to membrane fusion events. Rab5, a marker of early endosomes, regulates the fusion of phagosomes with early endosomes (16). The functions of Rab7, associated with late endosomes and lysosomes, are less well understood than those of Rab5; Rab5 may regulate the transition from early to late endosomes (35) and/or fusion of late endocytic compartments (17). Progression

from early to late endosomes requires a near-simultaneous removal of Rab5 from the vesicle surface and acquisition of Rab7 to the surface; this process is known as Rab conversion (115).

Rab27, on the other hand, regulates the exocytosis of secretory vesicles (158). A mutation in Rab27 results in a rare autosomal recessive disease named Griscelli syndrome. Symptoms of this disorder include T cell malfunction in granule secretion and hemophagocytic syndrome, an uncontrolled activation of macrophages and T lymphocytes (88). Research has revealed that Rab27 is required for the action of several secretory cells; these include insulin secretion by pancreatic islet cells (164), dense core secretion by platelets (133), and lytic granule secretion in cytotoxic T lymphocytes (146). It is currently unclear what role Rab27 plays in macrophages.

Antimicrobial peptides. Antimicrobial peptides are a highly conserved group of molecules that play a key role in innate immunity (163). These peptides exhibit potent microbicidal activities, and are thus considered to be "natural antibiotics" (116). Some of these molecules also show dedicated antifungal activity (81). They are located within the granules of immune cells and are found in nearly every tissue that is exposed to microorganisms (38). Several classes of antimicrobial peptides are <50 amino acids, and have a conserved amphipathic structure composed of a positively charged region and a hydrophobic region (86, 116); the structure determines both the antimicrobial activity of as well as the target specificity of the peptide (114). Antimicrobial peptides are synthesized and stored as propeptides, and upon infection of the host cell they are then cleaved into a mature form (165). They can inactivate the pathogen in a number of ways,

including by disruption of bacterial cell membranes and inhibition of DNA synthesis (12, 43). A peptide can display selective toxicity for a microorganism. Many types of antimicrobial peptides can be found within a given tissue-specific immune cell, which suggests that redundancy may exist among the different peptides (116). In addition to microbicidal activity, antimicrobial peptides have demonstrated other functions. Some types of cathelicidins and defensins seem to act as chemoattractants for leuckocytes as well as play a role in activating the adaptive immune response (71, 151).

Bactericidal peptides most commonly cause cell membrane permeabilization; the charged region interacts with the cell membrane or lipid A of lipopolysaccharide (LPS), while the hydrophobic region is inserted into the membrane lipid bilayer, causing disruption (163). It has been reported that pathogens can develop resistance to antimicrobial peptides, usually due to modification of the bacterial LPS (see below) (51). The two most well characterized groups of bactericidal antimicrobial peptides are cathelicidins and defensins (116). Defensins, by far the largest group, are cationic peptides and share a similar cyclic structure due to six conserved cysteine residues that form three disulfide bridges (29). Cathelicidins have a linear structure due to the lack of disulfide bridges; they contain a conserved signal sequence, but a variable C-terminal antimicrobial domain (29). Both defensins and cathelicidins act by disrupting the cell membrane, but cathelicidins initially inhibit DNA synthesis, indicating differences in the mechanism of action (116). Defensins and cathelicidins can act synergistically in order to clear pathogens from the host cells (94). Expression of cathelicidins can be induced by the reactive oxygen species of phagocytic cells (113). Several bactericidal peptides have been shown *in vitro* to have optimum activity in a slightly alkaline pH (54).

Pathogens subvert macrophage functions to survive intracellularly

Several species of pathogenic bacteria subvert macrophage function in order to survive and replicate. Most commonly, these bacteria either escape from the phagosome and replicate in the macrophage cytosol, or modify the phagosome to prevent destruction. Several bacteria have evolved ways to avoid the acidic environment of the phagolysosome, most commonly by avoiding phagolysosomal fusion. Several pathogenic bacteria promote their intracellular survival by utilizing similar proteins to either resist killing by macrophages, or to modify the host cell response. The mechanisms pathogenic bacteria employ to survive within macrophages can yield hints in the study of *Y. pestis* intracellular survival. Two common bacterial virulence determinants and two model organisms are discussed below.

Lipopolysaccharides. LPS is a large molecule found on the outer membrane of Gram-negative bacteria (Figure 1.3). It is generally comprised of lipids and sugars in a chain formation (90, 130). The fatty acid tail of lipid A anchors the LPS to the bacterial outer membrane. Attached to the sugar portion of lipid A is the core oligosaccharide, which consists of the inner and outer core. The inner core is made up of unique sugars such as heptose, while the outer core contains more common sugars such as glucose and galactose. A series of O antigen repeating subunits termed the O polysaccharide is attached to the outer core. The O polysaccharide is highly variable in the number of repeating subunits seen, and different sizes of O polysaccharide can be detected biochemically (136). LPS is a commonly recognized pathogen-associated molecular pattern ligand via its cellular receptor Toll-like receptor 4. It can also be recognized and

inhibited by some cathelicidins (104). Several pathogenic bacteria have a unique LPS due to modifications of the lipid A, which is usually part of the bacterial defense against host killing (50, 68). This modified lipid A has been shown to be important for resistance to antimicrobial peptides. It has been previously reported that the O antigen of *Y. enterocolitica* can modulate expression of the TTSS (100). However, *Y. pestis* lacks the O polysaccharide due to inactivation of the O antigen gene cluster, and thus has a rough LPS or lipooligosaccharide (LOS) (108). It has been shown that Pla activation in *Y. pestis* actually requires loss of the O antigen (69). The LOS of *Y. pestis* is regulated by temperature. The lipid A of bacteria grown at 28^{o}C induced production of the tumor necrosis factor alpha; when shifted to host cell temperature, the lipid A structure was modified, and the modified lipid A has decreased activation of this proinflammatory cytokine (65).

PhoP. PhoP is part of the regulatory two-component system PhoPQ (47). PhoQ is the sensor kinase located in the inner membrane, and it undergoes autophosphorylation when a low divalent cation concentration is detected in the environment. This kinase then phosphorylates the response regulator PhoP, which then activates transcription of its regulated genes (40). Approximately 40 genes and operons are under the control of PhoP (169). These PhoP-regulated genes are involved in a number of cell processes, including transcriptional regulation, stress responses, and LPS modification. There is some evidence indicating that acidic pH may promote transcription of a subset of these PhoP-activated genes (84). This pH-dependent transcriptional activation may be independent of PhoQ-dependent sensing of Mg^{2+} concentrations within phagosomes, as Mg^{2+}

measurements have found concentrations of Mg^{2+} in SCVs to be similar to human serum Mg^{2+} concentrations (84). However, most research studies on the subject altered the concentration of Mg^{2+} in cultures, as opposed to investigating Mg^{2+} within the phagosome. PhoP has been shown to be essential for the virulence of several pathogens, including *S.* Typhimurium and *M. tuberculosis* (85, 91). It is known that PhoP as well as several PhoP-regulated genes are important for the intracellular survival of *Y. pestis* in macrophages, perhaps by promoting resistance to antimicrobial peptides and by promoting survival under low Mg^{2+} conditions (46, 98). The concentration of Mg2+ in phagosomes is unknown.

***Salmonella* Typhimurium.** *Salmonella enterica* serovar Typhimurium is an enteric pathogen that is able to infect both phagocytic and nonphagocytic cells (14). Bacterial infection leads to gastroenteritis in humans and causes a typhoid fever-like disease in mice. *S.* Typhimurium modifies its phagosome to avoid destruction by host cells. The *Salmonella*-containing vacuole (SCV) initially interacts with the endocytic pathway, but then appears to inhibit phagolysosomal fusion. There is some evidence that *S.* Typhimurium actually promotes initial fusion events of the SCV with endocytic vacuoles as a method of directing phagosome maturation; these fusion events may be mediated in part by effectors of the T3SS located on the *Salmonella* Pathogenicity Island (SPI) 1 (143). It is thought that induction of the T3SS located on SPI-2 may play a role in blocking this final fusion step by subverting endosome transport (153). The transcriptional activator PhoP has also been implicated in blocking fusion of lysosomes with the SCV (41). In addition, PhoP-regulated genes also play a role in remodeling the

lipid A of the *Salmonella* LPS (50). This modification of lipid A is required for resistance to antimicrobial peptides and cationic peptides (132). *Salmonella* appear to regulate expression of Rab proteins to avoid lysosomal fusion (55). Induction of the SPI-2 T3SS causes formation of *Salmonella*-induced filaments, which have been associated with maximal intracellular growth of the bacteria (8).

Mycobacterium tuberculosis. *Mycobacterium tuberculosis* is the causative agent of tuberculosis. Approximately one-third of the human population is infected with the bacterium, and the disease causes 1.6 million deaths a year (103). The bacteria are transmitted via respiratory droplets. Once in the lungs, bacteria are phagocytosed by alveolar macrophages. However, *M. tuberculosis* very quickly modifies its phagosome by blocking Rab conversion, leading the bacterial phagosome to resemble an early endosome (154). Rab5 is located on the phagosomal surface; however, EEA1 is excluded. Exclusion of EEA1 seems to be due to a *M. tuberculosis* block in calcium flux. In addition, the bacterium further exploits Rab5 in order to acquire iron from sorting endosomes. Bacterial surface lipids like lipoarabinomannan are released and prevent recruitment of phosphatidylinositol 3-phosphate (PI(3)P) to the phagosome. Bacterial proteins like the tyrosine phosphatase PtpA also appear to help prevent accumulation of Rab7 on the phagosome. All of these mechanisms are employed to maintain the block in phagolysosomal fusion. Recent evidence suggests that *M. marinum*, a close genetic relative of *M. tuberculosis*, may utilize the Esx-1 secretion system to escape from the phagosome and reside in the cytosol of the macrophage (161). *M. tuberculosis* may utilize a similar mechanism, as a secretion mutant in *M. marinum* was successfully

complemented with a gene from *M. tuberculosis*. However, the initial inhibition of phagosome maturation is still required in order for the bacteria to survive. Recent studies have also revealed that PhoP may regulate the Esx-1 system; mutation of *phoP* caused attenuation of *M. tuberculosis*, perhaps due to loss of secretion of the T cell antigen ESAT-6 (37).

Yersinia pestis survival and trafficking within macrophage phagosomes

Y. pestis is a Gram-negative bacillus capable of surviving and replicating within macrophages both *in vitro* and *in vivo* (19, 82). However, the mechanism by which *Y. pestis* survives intracellularly is still poorly understood. Recent evidence suggests that *Y. pestis* initially establishes an intracellular replicative niche *in vivo*, and that this step may be required for establishment of an infection within a host (82). Fluorescent-activated cell sorting (FACS) performed on macrophages isolated from the spleens of *Y. pestis*-infected mice found that the bacteria first arrive in the spleen at two days post infection and remain exclusively intracellular between days two and four post infection. Extracellular bacteria only become evident at five days post infection. Research has indicated that the required for intracellular proliferation (*rip*) genes located within the *pgm* locus are necessary for the replication of *Y. pestis* within activated macrophages (111). The plasmid-encoded components such as the T3SS and F1 capsule do not seem to play a major role, if any, in the intracellular survival of *Y. pestis*; in fact, these components promote resistance to phagocytosis. The bacteria are indeed more often found extracellularly within the tissues of an infected host (75), and *Y. pestis* is thus classified as a facultative intracellular pathogen.

Electron microscopy has revealed that several bacteria may be found within a single YCV at later time points post infection; this phenomenon has been termed a spacious phagosome (46). It is unclear what events cause these spacious phagosomes to form. However, it is speculated that *Y. pestis* may utilize the autophagic pathway to acquire membranes for YCV enlargement (112). There is evidence that *Y. pestis* induces some level of apoptotic cell death (79), potentially to escape from the macrophage; however, it is unclear if apoptosis is the only mechanism by which the bacteria may leave the macrophage.

It appears that YCVs interact with components of the late endocytic pathway such as late endosomes and lysosomes (46) (Figure 1.2). Immunofluorescence assays performed in this study showed that the YCV colocalizes with LAMP-1, cathepsin D, and the cell tracer ovalbumin, and that the interaction of the YCV with these markers of late endosomes and lysosomes persisted over time. Colocalization experiments with the lysosomal tracer acridine orange suggested that *Y. pestis* can survive and replicate within a phagolysosome (148). This finding implies that the default endocytic pathway is not affected. Research performed with *Y. pseudotuberculosis*, the close genetic relative of *Y. pestis*, suggested that the phagosomal pH of the YCV is altered (152). The phagosomal pH of YCVs containing live bacteria was measured over time and found to be only slightly acidified (pH ~6.2), while YCVs containing dead bacteria showed an acidic pH (pH ~4.5). Investigation of the biochemical activity of the vATPase on YCVs containing live bacteria revealed that that this activity was inhibited as compared to YCVs containing dead bacteria. $PhoP^-$ mutants exhibit similar intracellular trafficking as compared to wild type *Y. pestis* (46). It is currently unknown if PhoP may play a role in

affecting phagosomal pH. PhoP also plays a role in regulating the biosynthesis of the core oligosaccharide of *Y. pestis* (68). It has been shown in *Y. enterocolitica* that LPS plays a role in resistance to antimicrobial peptides (137), and that mutation of this structure in other pathogenic bacteria results in a loss of virulence (21, 96).

The strain of *Y. pestis* utilized in these studies was originally isolated from a Kurdistan Iran man (KIM) in the Middle East (33). This strain belongs to the biovar Mediaevalis, and was identified as being particularly virulent. Since fully virulent *Y. pestis* may be studied only under Biosafety Level 3 conditions, several attenuated strains have been created for scientific research (Table 1.1) (13).

The research performed in this dissertation was twofold. The first was to further the understanding of how *Y. pestis* manipulates its intracellular environment to survive in macrophages. To this end, experiments were carried out to elucidate how *Y. pestis* might modify its phagosome in order to survive intracellularly. The second was to further identify genes that play a role in the intracellular survival of *Y. pestis* in macrophages. A negative selection screen was performed to identify candidate genes, and these candidates were characterized for their ability to survive intracellularly. Through these two aims I hoped to further the understanding of the mechanisms *Y. pestis* employs to promote its survival within macrophages.

Table 1.1. Features of *Y. pestis* KIM strains.

	pCDI (TTSS)	pMT1 (F1 capsule)	pPCP1 (Pla)	*pgm* locus (iron acquisition)
KIM5	+	+	+	-
KIM6+	-	+	+	+
KIM6	-	+	+	-
KIM10	-	+	-	-

Figure 1.1. Structure of the vATPase.

VATPase is a multisubunit complex arranged in two domains. The cytoplasmic domain V_1 is responsible for ATP hydrolysis. The catalytic site is located at the interface between subunits A and B (solid red arrow). The membrane-bound V_o domain is responsible for proton translocation (red dashed arrow). The proton enters a hemi-channel in subunit a. ATP hydrolysis then drives rotation of the proteolipid ring comprised of subunits c, c', and c". The rotation (direction indicated by black arrows) forces the proton to be translocated through each of the subunits in this ring via protonation of glutamate residues, and the proton is then displaced into the luminal hemi-channel through interactions with the arginine 735 of subunit a and subsequently exits the vATPase into the lumen. Adapted by permission from Macmillan Publishers Ltd: Nature Reviews Molecular Cell Biology (36), copyright 2007.

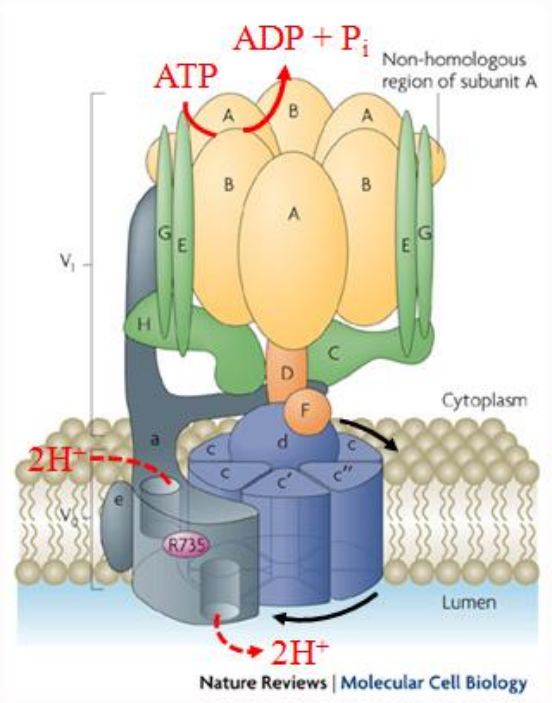

Figure 1.2. Model for trafficking of YCV.

A *Y. pestis* bacterium is engulfed by a macrophage into a phagosome. This YCV interacts with components of the endocytic pathway, and gains markers of late endosomes (LAMP-1, Rab7) and lysosomes (cathepsin D, vATPase). The YCV appears to exist within a phagolysosome-like compartment, but the bacterium continues to persist and replicate. Some YCVs exhibit a spacious phenotype beginning at 8 hours post infection. The YCV may hijack the regulated exocytic pathway via Rab27 as a mechanism of escape from the host cell.

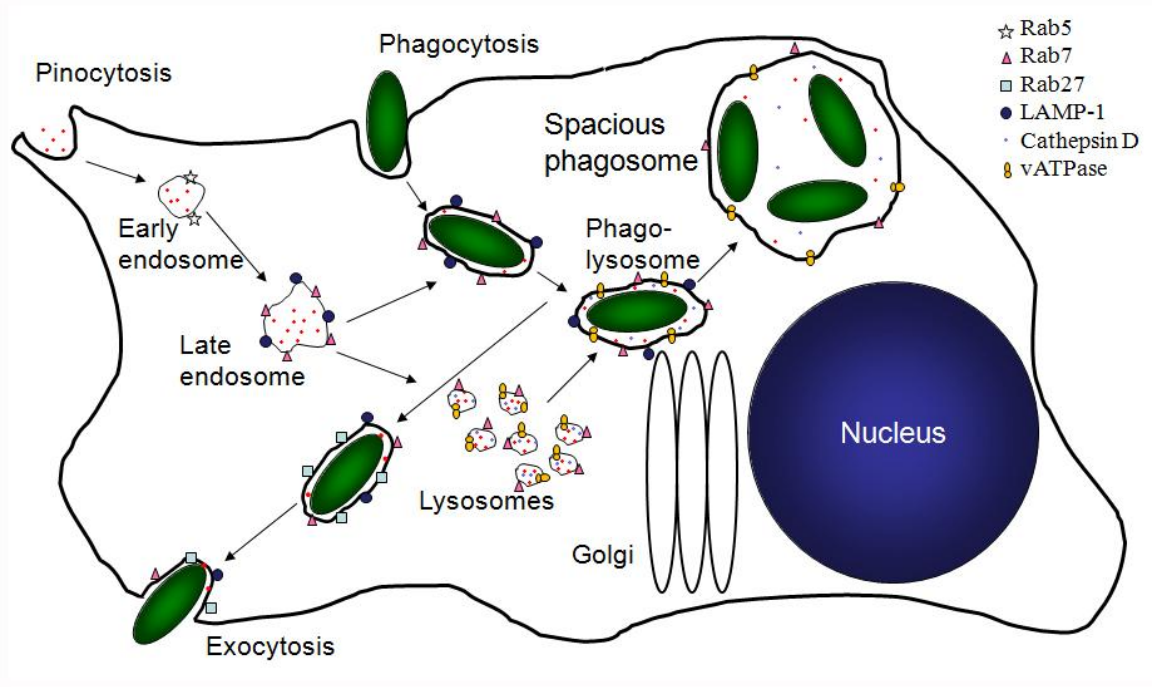

Figure 1.3. General structure of the LPS.

The LPS is comprised of lipid A, which anchors the LPS to the bacterial membrane, a core oligosaccharide made up of the inner and outer core, and the O polysaccharide, which consists of repeated subunits of the O antigen. *Y. pestis* lacks the O polysaccharide, and this truncated LPS formed of the lipid A and the core oligosaccharide is termed LOS. Adapted by permission from Macmillian Publishers Ltd: Nature Reviews Microbiology (90), copyright 2005.

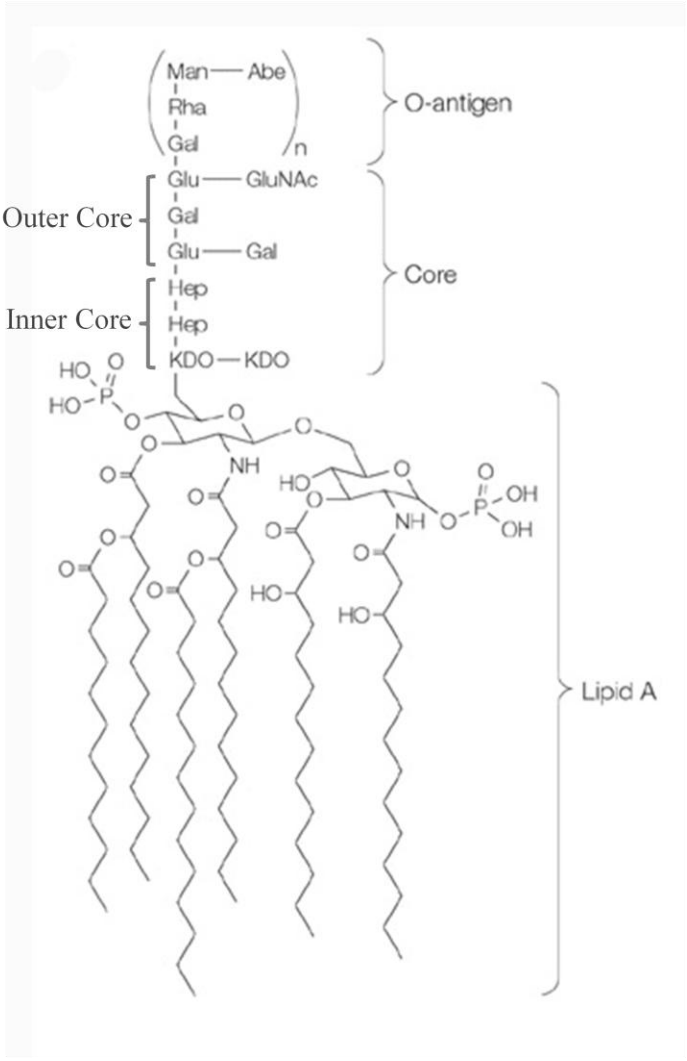

Chapter 2: To examine if *Yersinia pestis* prevents acidification of its vacuoles as an intracellular survival strategy.

Summary

YCVs appear to fuse with late endosomes and lysosomes, and yet the bacteria survive within these compartments. Given this survival phenotype, it is possible that *Y. pestis* affects its phagosomal environment in order to survive. Since a main feature of a phagolysosome is an acidic pH, we decided to examine the pH of the YCV. Microscopic observations utilizing the acidic vacuolar tracer Lysotracker Red revealed that phagosomes containing live *Y. pestis* KIM5 do not colocalize with Lysotracker, indicating that the pH of these phagosomes is higher than 5.5. Phagosomes containing paraformaldehyde-fixed KIM5, on the other hand, showed an increase in colocalization with Lysotracker, suggesting that dead bacteria are reduced in their ability to affect their phagosomal pH. Ratiometric pH measurements confirmed that YCVs containing live bacteria fail to acidify below a pH of 7, while YCVs containing fixed-killed *Y. pestis* acidify to a pH of 4.5. Additional Lysotracker studies showed that the ability to prevent acidification of the YCV appears to be conserved among the three pathogenic *Yersinia* species. Further microscopic investigation showed that YCVs containing live bacteria did not colocalize with an antibody to the vATPase, suggesting that the vATPase is either inactivated or excluded on these vacuoles. These results indicate that *Y. pestis* blocks phagosome acidification of its vacuole to promote its intracellular survival, potentially through the disruption of the vATPase.

Introduction

Several pathogenic bacteria block phagosome maturation as a mechanism to survive within macrophages (70). As a consequence, the phagosomal environment of these vacuoles does not acidify. It was previously reported that *Y. pestis* colocalizes with markers of late endosomes and lysosomes, indicating that the YCV interacts with these compartments (46). Furthermore, some evidence suggested that *Y. pestis* survives within a phagolysosome (148). However, the mechanism by which *Y. pestis* survives within such a compartment is not characterized.

It has been reported that phagosomes containing live *Y. pseudotuberculosis* are not well acidified, and that this lack of acidification may be due to an inhibition of the vATPase (152). The vATPase is a proton pump necessary for the acidification of the phagolysosome, and is found on various components of the endocytic pathway, including lysosomes. In this chapter, I investigated the possibility that *Y. pestis* manipulates its phagosomal environment to prevent phagosome acidification, and obtained evidence that blocking acidification is how *Y. pestis* survives within macrophage phagosomes.

Experimental Procedures

Bacterial strains and growth conditions. The bacterial strains used in this study are listed in Table 2.1. *Yersinia* strains were grown at 28^{o}C either on heart infusion (HI) agar or Luria-Bertani (LB) agar. *Yersinia* cultures were grown at 28^{o}C in LB or HI broth. Ten μg/ml chloramphenicol and 25 μg/ml ampicillin were added to media for growth of *Y. pestis*, and 30 μg/ml chloramphenicol and 100 μg/ml ampicillin were added to media for

growth of *Y. pseudotuberculosis* as necessary unless otherwise indicated. Isopropyl-β-D-1-thiogalacto-pyaranoside (IPTG) was added to cultures at a final concentration of 500 μM to pre-induce GFP expression.

Cell culture. Macrophage-like murine cell line J774A.1 was cultured in Dulbecco's modified Eagle's medium ((DMEM), Gibco) containing GlutaMAX and a high glucose concentration and supplemented with 10% fetal bovine serum (FBS) and 1 mM sodium pyruvate, and incubated at 37°C with 5% CO_2. Cells were grown to confluence and detached from the dishes, and 2 x 10^5 cells were seeded into wells of 24-well tissue culture plates and incubated overnight before experimental use. For fluorescence microscopy, the cells were incubated on acetone-washed round glass coverslips. For some experiments, 2 x 10^5 cells in a low volume of medium were seeded into 35 mm glass bottom culture dishes according to the manufacturer's instructions (MatTek). The THP-1 human monocyte cell line was cultured in suspension in RPMI-1640 (Invitrogen) supplemented with 10% FBS, 1 mM sodium pyruvate, and 0.05 mM β-mercaptoethanol. Three days prior to experimental use, cells were seeded into 24-well plates at a concentration of 2.2 X 10^5 cells/well and differentiated into adherent macrophages in RPMI supplemented with 10% FBS and containing 100 nM phorbol 12-myristate 13-acetate (PMA) for 48 hours. The cells were then washed with plain RPMI to remove the PMA and incubated with fresh medium for 24 hours before infection.

Macrophage infection assay. After overnight growth, 1 ml of *Yersinia* culture was centrifuged at 1400 x *g* for 4 minutes and washed with phosphate buffered saline (PBS). As a negative control, 1ml of bacteria was collected and killed by fixation with 2.5%

paraformaldehyde in PBS (PFA) and washed 3 times with PBS prior to infection. The concentration of the bacteria was determined using absorbance at OD_{600}. Macrophages were infected at a multiplicity of infection (MOI) of 10 bacteria per macrophage. The infected plates were centrifuged at 200 x *g* for 5 minutes and incubated at 37°C with 5% CO_2 for 10 minutes. Infected macrophages were washed 2 times with PBS, and fresh DMEM containing 8 µg/ml gentamicin was applied. IPTG (500 µM) was also added to induce expression of green fluorescent protein (GFP). After one hour the cells were again washed, and DMEM containing either 2 µg/ml gentamicin (for *Y. pestis*) or 4.5 µg/ml gentamicin (for *Y. pseudotuberculosis*) and 500 µM IPTG was applied for the remainder of the infection.

Immunofluorescence assay. For immunofluorescence analysis, the infected cells were fixed in 2.5% PFA for at least 30 minutes and washed 3 times with PBS. Coverslips were inverted and mounted onto glass slides using Prolong Gold antifade reagent (Invitrogen) and allowed to dry. Coverslips were cleaned with 70% ethanol just prior to analysis. Samples were analyzed using a Zeiss inverted Axiovert 200 M microscope with a 100X objective. Images were captured and analyzed with Adobe Photoshop.

Lysotracker Red assay. The macrophage infection assay was performed as described above. Cells were incubated on coverslips prior to infection. Lysotracker Red DND-99 (Molecular Probes) was added at a concentration of 50 nM 1 hour prior to fixation and analysis of samples. After fixation, cells were incubated in PBS for one hour prior to mounting on slides to reduce background red staining on coverslips. In some experiments, 30 µg/ml chloramphenicol was added to the cells at the time of infection

and maintained throughout the time course to inhibit bacterial protein synthesis during infection.

GFP induction assay. The macrophage infection assay was performed as described above with the following modifications. Bacteria were not pre-induced to express GFP. Rather, 500 μM IPTG was added to the medium after 1.25 hours of infection, to ensure that only intracellular bacteria expressed GFP. In some experiments, macrophages were incubated in medium containing 30 μg/ml chloramphenicol to inhibit bacterial protein synthesis during infection. Samples were fixed and analyzed as described above.

Macrophage co-infection assay. Co-infection experiments were performed as follows. KIM5/GFP bacteria were induced with IPTG and then fixed. Macrophages were infected at a MOI of 5 with fixed KIM5/GFP and unlabeled live KIM5 (total MOI = 10). Infected macrophages were labeled with Lysotracker as described above. At 1.25 hours post infection cells were fixed, blocked with 3% bovine serum albumin (BSA) in PBS, and permeabilized with 0.1% saponin in blocking buffer for two 10 minutes washes. Samples were then stained with rabbit polyclonal anti-*Yersinia* SB349 primary antibody (1:1,000) (Cocalico Biologicals) and goat anti-rabbit Alexa Fluor 350 secondary antibody (1:500) (Molecular Probes). Coverslips were then mounted onto slides and analyzed as described above.

Ratiometric pH measurements. The YCV pH was measured by ratiometric imaging (43). Both live and fixed-killed *Y. pestis* KIM5 as well as *Y. pseudotuberculosis* 32777 bacteria were labeled with fluorescein isothiocyanate (FITC) (Sigma) at a final

concentration of 1 mg/ml in PBS (pH 8) for 30 minutes. After three washes in PBS, the bacteria were used to infect J774A.1 cells seeded in 35-mm glass coverslip dishes. The infection was performed in a low volume of 100 µl for 30 minutes at 37°C with 5% CO_2. Afterward, the cells were washed and maintained as described above. A Zeiss LSM 510 META microscope was used for live cell analysis. Images were captured at excitation wavelengths of both 488 nm and 458 nm throughout the time course. At least fifty individual intracellular bacteria for each time point were then gated, and the fluorescence intensities at each wavelength were gathered using Zeiss LSM software. The intensities at each wavelength were background-corrected, and the 488/458 nm average ratio was compared to a pH calibration curve. To generate the pH calibration curve, infected cells were bathed in pH calibration buffer (130 mM KCl, 1 mM $MgCl_2$, 15 mM Hepes, 15 mM MES) at pH 7, 6.5, 6, 5.5, 5, 4.5, or 4. The buffer contained 10 µM each of the sodium and potassium antiporters monensin and nigericin, respectively, to equilibrate intra- and extraphagosomal pH (43). Images were captured and analyzed for each pH to generate the calibration curve. The pH of YCVs was extrapolated from this calibration curve.

Vacuolar ATPase colocalization. The macrophage infection assay was carried out and samples were fixed as described above. Samples were blocked with 3% BSA in PBS. J774A.1 samples were permeabilized with 0.1% saponin in blocking buffer for two 10 minute washes, then stained with a rabbit polyclonal primary antibody to the B subunit of the vATPase (1:250) (Santa Cruz Biotechnology, Inc.) and goat anti-rabbit Alexa Fluor 594 secondary antibody (1:1,000) (Molecular Probes). THP-1 samples were permeabilized with 0.2% Triton X-100 for 10 minutes, then stained with mouse

monoclonal antibody OSW2 to the a subunit of the vATPase (1:100) (129) and goat anti-mouse Alexa Fluor 594 secondary antibody (1:500). Coverslips were then mounted onto slides as described above.

Results

YCVs containing live bacteria do not colocalize with Lysotracker Red. *Y. pseudotuberculosis* has been previously shown to inhibit acidification of phagosomes in primary murine macrophages (152). To determine if *Y. pestis* shows a similar phenotype, Lysotracker DND-99, a probe specific for acidic vacuoles such as lysosomes, was utilized. When J774A.1 macrophages were infected with KIM5/GFP (Table 2.1) in the presence of Lysotracker Red, very few GFP-positive YCVs colocalized with Lysotracker Red up to 5.25 hours post infection (Figure 2.1). In contrast, phagosomes containing fixed-killed KIM5/GFP showed a rapid increase in the colocalization with Lysotracker Red over time (Figure 2.1). This result suggested that the phagosomal environment of live *Y. pestis* was greater than a pH of 5.5, the threshold of detection for Lysotracker Red. Further, this finding indicated that the ability of *Y. pestis* to prevent phagosomal acidification was not due to the *pgm* locus, which is lacking in KIM5. Strains of KIM lacking pCD1 and pPCP1 also did not colocalize with Lysotracker Red (Figure 2.2), suggesting that the factor(s) responsible for this phenotype are independent of the T3SS and Pla. A *Y. pestis phoP* mutant known to be defective for intracellular survival was also examined, but did not colocalize with Lysotracker Red (Figure 2.2), implying that the factor(s) responsible also is independent of the PhoP regulon. As a large increase in the colocalization of fixed-killed bacteria with Lysotracker Red is seen at 1.25 hours post

infection, this time point was used in further experiments. Three strains of *Y. pestis* representing two biovars, six strains of *Y. pseudotuberculosis* representing three serogroups, and one strain of *Y. enterocolitica* were further examined to determine if this potential to prevent phagosomal acidification was conserved among the pathogenic yersiniae (Figure 2.3). None of the strains tested showed any significant colocalization with Lysotracker Red, suggesting that the ability to prevent phagosomal acidification is shared among the three pathogenic yersiniae.

YCVs containing live bacteria do not acidify. To more accurately define the pH of the YCVs, live cell ratiometric measurements were performed (43). Both *Y. pestis* KIM5 and *Y. pseudotuberculosis* 32777 were labeled with the acid-sensitive fluorescent dye FITC to measure the pH of the YCV over a time course. The pH of phagosomes containing live KIM5 became increasingly alkaline to a pH of ~8 over the 5.25 hour infection time period (Figure 2.4). The pH measurements confirmed the Lysotracker Red assay results, and further demonstrated that *Y. pestis* inhibits phagosome acidification. Similar results were obtained for *Y. pseudotuberculosis* 32777 (Fig. 2.4), verifying that this property is shared by the two *Yersinia* species. In contrast, the pH of YCVs containing fixed-killed KIM5 decreased to ~4.5 within 2.5 hours (Fig. 2.4). These results showed that *Y. pestis* inhibits acidification of its phagosomes.

***De novo* protein synthesis is not required for prevention of YCV acidification.** To determine if de novo bacterial protein synthesis is required for *Y. pestis* to inhibit phagosome acidification, the bacteriostatic antibiotic chloramphenicol was added to the infection medium at a concentration 30 μg/ml. To verify that this concentration of

chloramphenicol is effective at inhibiting *de novo* protein synthesis, a GFP induction assay was performed. Bacterial GFP expression was inhibited in chloramphenicol-treated macrophages following addition of IPTG as compared to the untreated control (data not shown), showing that the antibiotic blocked de novo protein synthesis at this concentration. A Lysotracker Red assay was performed in the presence of chloramphenicol, and results showed that there was no difference in the ability of KIM5 to inhibit phagosome acidification in the presence or absence of chloramphenicol (Figure 2.5).

To determine if the factor responsible for preventing phagosome acidification can act globally, a co-infection experiment with live and fixed-killed KIM5 was performed in the presence of Lysotracker Red. The experiment showed that live bacteria were unable to prevent colocalization of Lysotracker with phagosomes containing fixed bacteria when they were in the same macrophage (Figure 2.6). Taken together, these results suggest that *Y. pestis* is able to inhibit phagosome acidification using a factor(s) that is produced by the pathogen prior to phagocytosis, and that this factor does not act globally within the macrophage to inhibit phagosome acidification.

YCVs containing live bacteria do not colocalize with vATPase. Since *Y. pseudotuberculosis* is reported to affect the vATPase (152), colocalization studies using antibodies to the vATPase were performed. A mouse monoclonal antibody to the a subunit of the vATPase was first employed (129). The a subunit is part of the V_o domain and plays a role in proton translocation, but also forms part of the peripheral stalk to which V_1 is bound (36). This antibody does not cross-react with the mouse protein, so

differentiated human THP-1 macrophages were infected and analyzed for vATPase colocalization. However, THP-1 cells were infected only to a small degree, and colocalization studies with the monoclonal antibody were unsuccessful due to the limited number of intracellular bacteria available for analysis. A rabbit polyclonal antibody to the c terminus of the B subunit of the vATPase was then utilized in J774A.1 cells to determine if a difference in colocalization could be seen between YCVs containing live or fixed-killed bacteria. The B subunit is part of the V_1 cytoplasmic domain of the vATPse, which hydrolyzes ATP to drive proton translocation into the vacuole and is thus required for phagosomal acidification (36). Phagosomes containing live KIM5 bacteria showed very little colocalization with the vATPase antibody, while YCVs containing fixed-killed bacteria had a high degree of colocalization with the vATPase antibody (Figure 2.7). This result suggests that *Y. pestis* affects the localization of the V_1 domain of the vATPase to the vacuolar membrane in order to prevent phagosomal acidification.

Discussion

Previous colocalization studies indicated that YCVs appear to follow the typical phagosome maturation pathway (46, 148). These studies suggested that *Y. pestis* might interfere with the phagosome maturation pathway without inhibiting fusion of endocytic compartments with the YCV, and further hinted that the bacteria may affect the final step of phagosome maturation – that is, fusion of the phagosome with lysosomes. A defining aspect of this final maturation step is phagosomal acidification. Measurements of pH and vATPase activity suggested that phagosomes containing *Y. pseudotuberculosis* are not completely acidified, perhaps due to inhibition of the vATPase (152). Thus, research was

undertaken to determine if *Y. pestis* prevents phagosome acidification to survive intracellularly.

Initial studies with Lysotracker Red, a cell tracer fluorescent only in acidic (pH ≤ 5.5) compartments, showed that phagosomes containing KIM5 have a pH higher than 5.5. Ratiometric live cell imaging was used to further investigate the phagosomal PH of the YCV. These results indicate that phagosomes containing live *Y. pestis* have a neutral to alkaline pH (pH 6.7-7.9), while phagosomes containing fixed-killed *Y.* pestis as a control show an expected acidic pH (pH 5.2-4.5). Phagosomes containing live *Y. pseudotuberculosis* showed a similar pH to those containing live KIM5. These results are similar to what has been previously reported in *Listeria monocytogenes* (7). However, the pH of the YCVs containing live bacteria was surprising, as previous results in *Y. pseudotuberculosis* indicated that the phagosomes were at least partially acidified (152). However, there have been reports that phagosomes containing *Listeria* remain at neutral pH (7), and that phagosomes containing yeast particles transiently become slightly alkaline during phagolysosome formation (42). These results showed that *Y. pestis* inhibits acidification of its phagosomes, a process likely to prevent maturation of these vacuoles.

Further work was carried out to identify the bacterial factor(s) responsible for preventing phagosomal acidification. Lysotracker Red analysis suggested that this factor is common to all three pathogenic *Yersinia* species. Colocalization experiments with Lysotracker Red also indicated that the factor(s) is not a component of the T3SS or the *pgm* locus, nor is it encoded on pPCP1. This result suggests that the factor(s) responsible for phagosomal acidification is encoded on the chromosome. It is feasible that the factor

in *Y. pestis* may be located on pMT1, but we currently do not have a pMT1$^-$ KIM strain to determine this possibility. Experiments using the bacteriostatic antibiotic chloramphenicol indicated that *de novo* protein synthesis is not required for inhibition of phagosome acidification. Since the bacteria are grown at 28^{o}C prior to infection, the factor(s) is likely not expressed in response to the host environment. In addition, the factor is not able to act globally throughout the macrophage, as fixed-killed bacteria still colocalized with Lysotracker Red in a co-infection assay. However, multiple bacteria were not detected within a single phagosome by this assay, so it is unknown if this factor might be able to act upon multiple bacteria within the same compartment. At present the factor remains unknown and uncharacterized.

A KIM *phoP* mutant exhibits a defect in intracellular survival. It is known that PhoP-regulated genes play a role in promoting resistance to antimicrobial peptides found in lysosomes, and that these genes are also important for the intracellular survival of *Y. pestis* (46). The Lysotracker Red assay was used to test if PhoP may also affect the pH of the YCV. However, phagosomes containing a *phoP* mutant do not colocalize with this marker, and thus *phoP* is not a factor directing the block in phagosomal acidification. Though there are a subset of PhoP-regulated genes that are activated in a pH-dependent manner (84), there have not been reports that PhoP plays a regulatory role in phagosome acidification. This result also suggests that inhibition of phagosomal acidification is not sufficient for the survival of *Y. pestis* in macrophages. Instead, resistance to antimicrobial peptides may play a larger role in promoting the intracellular survival of the bacteria.

Live-bacteria containing YCVs do not colocalize with a subunit of the cytoplasmic V_1 domain of the vATPase. The vATPase can be reversibly dissociated and reassembled, and this process (139, 162). *Y. pestis* may interfere with the assembly of the V_1 and V_o subunits vATPase in order to inhibit the function of the vATPase and thus inhibit phagosomal acidification. It is possible that *Y. pestis* may disrupt localization of the V_1 domain to the phagosome membrane either directly or by interfering with the RAVE complex chaperone necessary for vATPase reassembly (139); however, more research needs to be done in this area to characterize the interaction of *Y. pestis* with the vATPase.

Figures and Tables

Table 2.1. *Yersinia* strains used in Chapter 2.

Strain Name	Relevant Characteristics	Reference
KIM5	*Y. pestis* biovar Mediaevalis, *pgm*$^-$, Ap^r	(44)
KIM5/GFP	*Y. pestis* biovar Mediaevalis, *pgm*$^-$, pMMB207GFP3.1, Ap^r, Cm^r	(46)
KIM5 *phoP*Δ/GFP	KIM5 *phoP*Δ127-429	(46)
KIM6+/GFP	*Y. pestis* biovar Mediaevalis, pCD1$^-$, p67GFP3.1, Ap^r	(46)
KIM6/GFP	*Y. pestis* biovar Mediaevalis, pCD1$^-$, *pgm*$^-$, p67GFP3.1, Ap^r	
KIM10/GFP	*Y. pestis* biovar Mediaevalis, pCD1$^-$, pPCP1$^-$, *pgm*$^-$, p67GFP3.1, Ap^r	(109)
CO92Δpgm/GFP	*Y. pestis* biovar Orientalis, *pgm*$^-$, p67GFP3.1, Ap$^{r\,-}$	This work
EV76.7/GFP	*Y. pestis* biovar Orientalis, pCD1$^-$, p67GFP3.1, Ap^r	
A1122/GFP	*Y. pestis* biovar Orientalis, pCD1$^-$, p67GFP3.1, Ap^r	This work
32777	*Y. pseudotuberculosis* serogroup O1, pYV$^-$, p67GFP3.1, Ap^r	(25)
32777c/GFP	*Y. pseudotuberculosis* serogroup O1, pYV$^-$, p67GFP3.1, Ap^r	(167)
IP2790c/GFP	*Y. pseudotuberculosis* serogroup O1, pYV$^-$, p67GFP3.1, Ap^r	(134)
yP137/GFP	*Y. pseudotuberculosis* serogroup O3, pYV$^-$, p67GFP3.1, Ap^r	
IP2515c/GFP	*Y. pseudotuberculosis* serogroup O2, pYV$^-$, p67GFP3.1, Ap^r	
IP2666c/GFP	*Y. pseudotuberculosis* serogroup O3, pYV$^-$, p67GFP3.1, Ap^r	
IP2775c/GFP	*Y. pseudotuberculosis* serogroup O1, pYV$^-$, p67GFP3.1, Ap^r	
8081/GFP	*Y. enterocolitica* serogroup O8, pYV$^-$, p67GFP3.1, Ap^r	

Figure 2.1. Measurement of YCV acidification using Lysotracker and fluorescence microscopy.

J774A.1 macrophages were infected with live or fixed/killed KIM5/GFP at a MOI of 10. The Lysotracker Red assay was performed over a 5.25-hour infection time course. Representative images at 1.25 hours post infection for live KIM5 (A-C) and fixed-killed KIM5 (D-F) are shown, corresponding to KIM5/GFP (A and D), the Lysotracker Red (B and E), or an image merging the two signals (C and F). The arrow indicates colocalization of bacteria with Lysotracker Red. Percent colocalization of the bacteria with Lysotracker Red was quantified (G). Colocalization was defined at the bacterium being completely enclosed by a halo of the marker studied. At least 50 YCVs over three fields were analyzed for each time point over three independent experiments, results were averaged, and the error bars indicate standard deviations. Reproduced with permission from American Society for Microbiology, copyright 2009 (112).

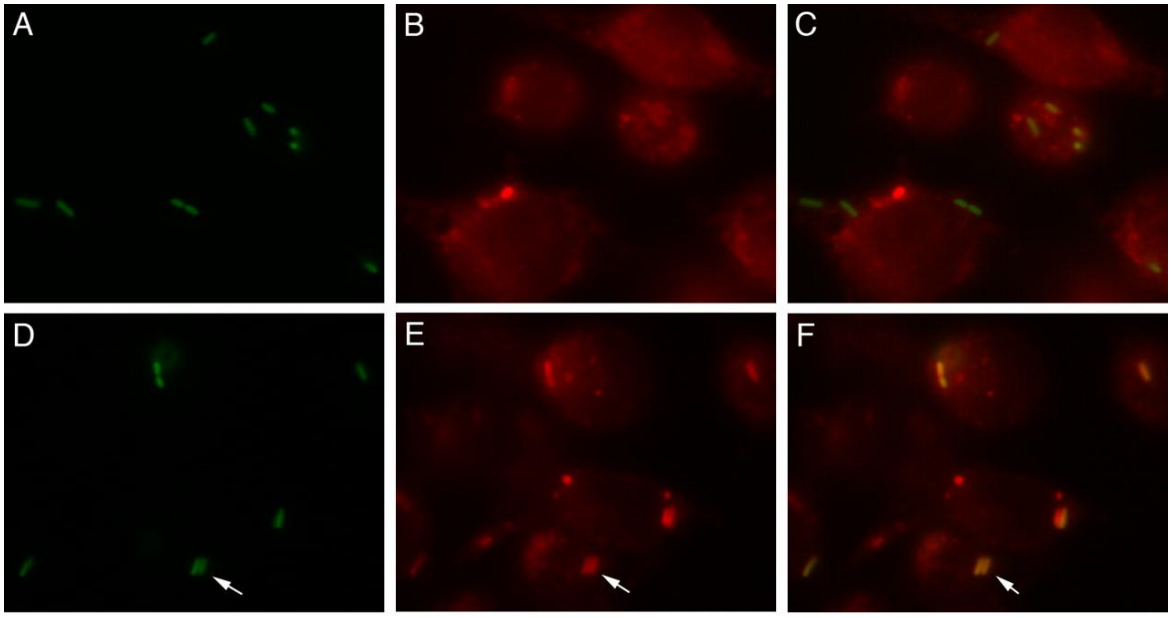
A
B
C
D
E
F

G

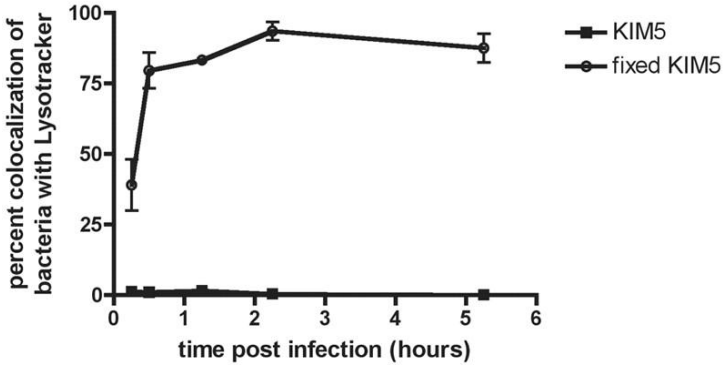
percent colocalization of bacteria with Lysotracker
100
75
50
25
0
0
1
2
3
4
5
6
time post infection (hours)
KIM5
fixed KIM5

Figure 2.2. Prevention of YCV acidification is not due to known virulence factors.

J774A.1 macrophages were infected with GFP-expressing strains of *Y. pestis* lacking pCD1 and/or pPCP1, as well as the *phoPΔ* mutant at a MOI of 10. A time course was performed to evaluate bacterial colocalization with Lysotracker Red as described in the legend to Figure 2.1. KIM5 and fixed-killed KIM5 are shown as controls. Time points post infection are indicated in the legend. Results for one experiment are shown.

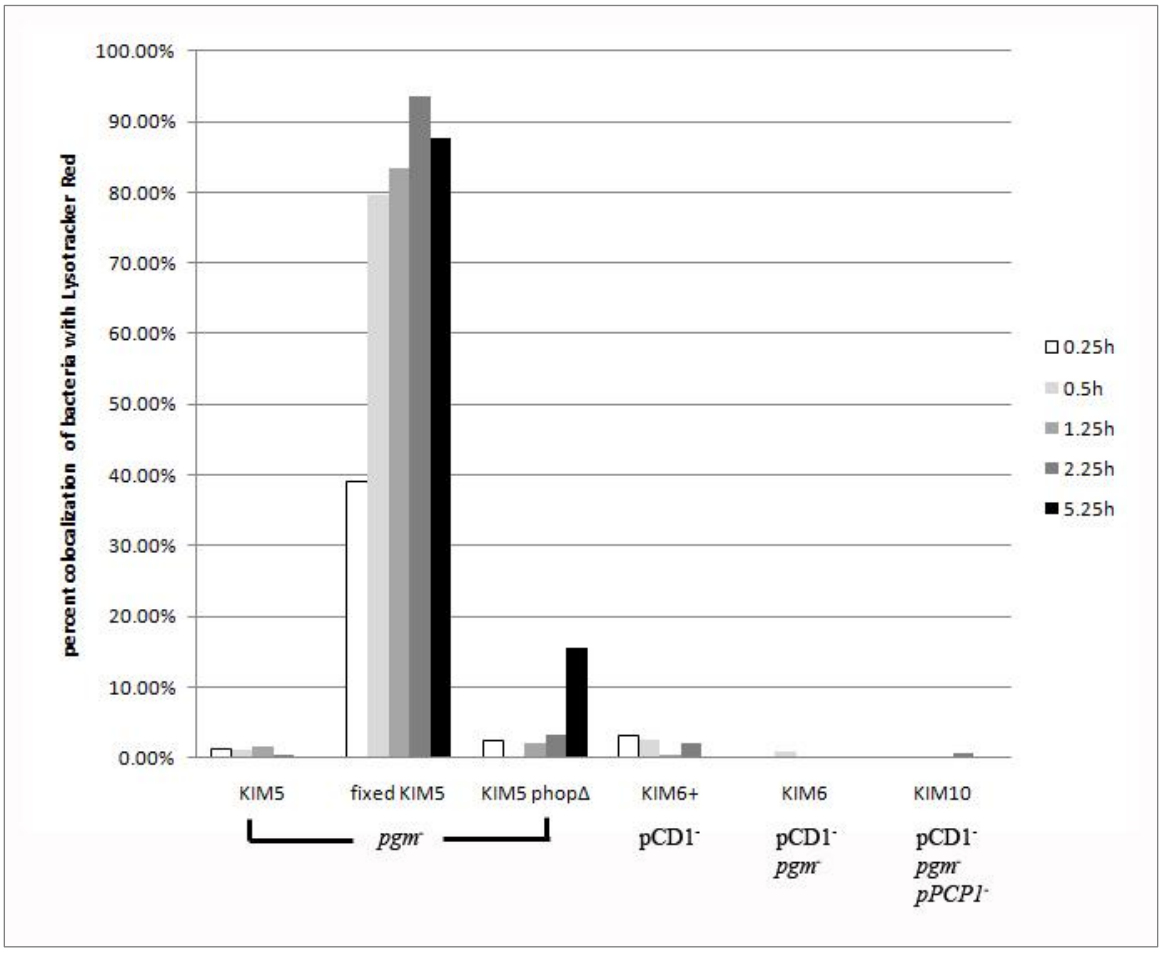

Figure 2.3. The ability to prevent YCV acidification is shared among *Yersinia* species.

GFP-expressing strains of *Y. pestis, Y. pseudotuberculosis,* and *Y. enterocolitica* were infected into J774A.1 macrophages at a MOI of 10 and tested via Lysotracker Red for their ability the prevent phagosome acidification. At 1.25 hours post infection samples were collected and analyzed as described in the legend to Figure 2.1. KIM5 and fixed-killed KIM5 were used as controls. Three strains of *Y. pestis* representing two biovars, six strains of *Y. pseudotuberculosis* representing three serogroups, and one strain of *Y. enterocolitica* are shown. The results of one experiment are shown.

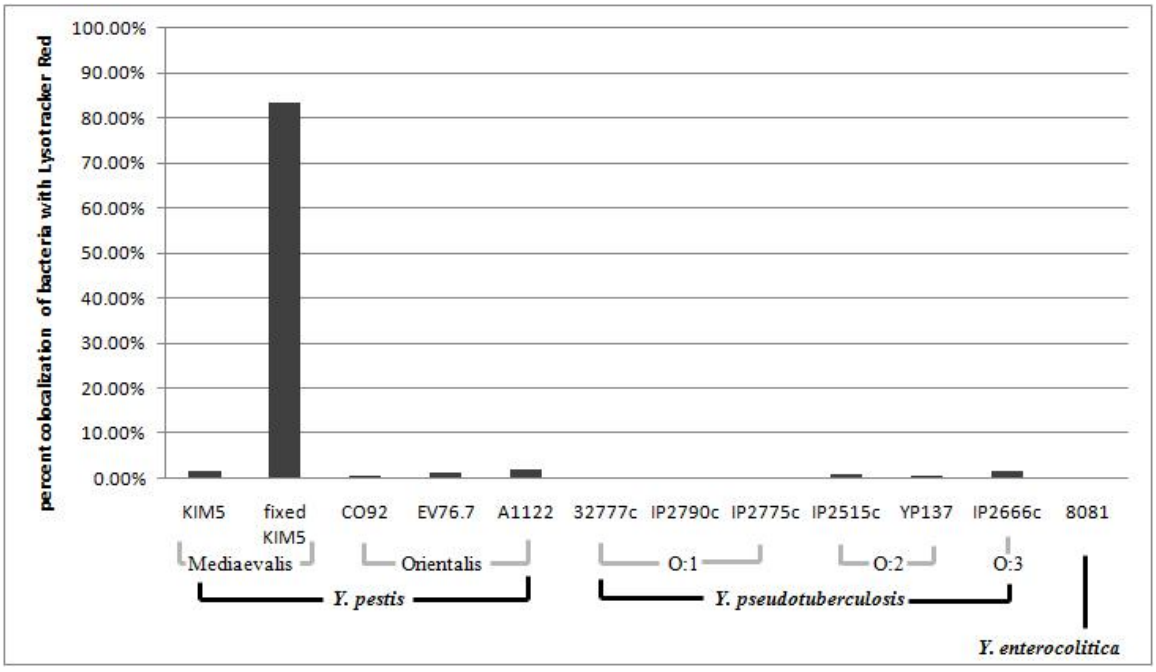

Figure 2.4. Measurement of YCV pH using live cell ratiometric imaging.

Live *Y. pestis* KIM5, fixed-killed KIM5, or live *Y. pseudotuberculosis* 32777 bacteria were labeled with FITC and used to infect J774A.1 macrophages at a MOI of 10. Images were obtained on living infected cells by using excitation wavelengths of 488 nm and 458 nm. Comparison of the 488 nm/458 nm ratio to the pH calibration curve was used to estimate the pH of YCVs. The symbols indicate the averages of three experiments (for 32777) or of five experiments (for KIM5 and fixed KIM5), and the error bars indicate standard deviations. Reproduced with permission from American Society for Microbiology, copyright 2009 (112).

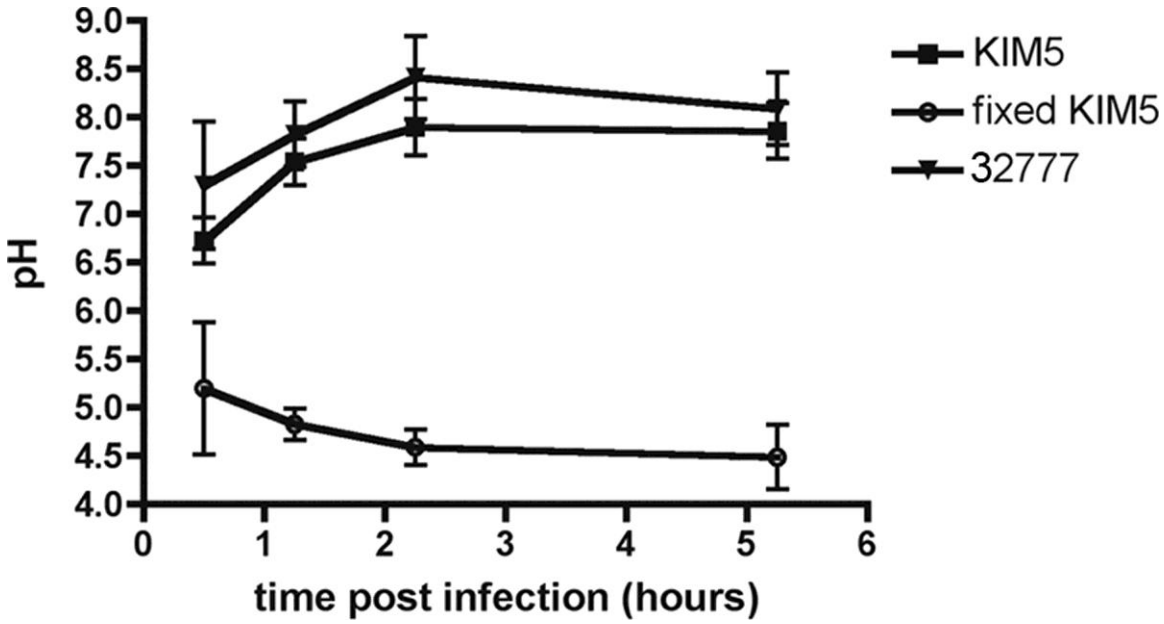

Figure 2.5. *De novo* protein synthesis is not required for KIM5 to prevent phagosome acidification.

A Lysotracker Red assay was performed on J774A.1 macrophages infected with KIM5/GFP in the absence or presence of chloramphenicol (Cam). Samples were collected at 1.25 hours post infection and analyzed. At least 50 phagosomes over three fields were counted over two independent experiments. Results were averaged and error bars represent standard deviation.

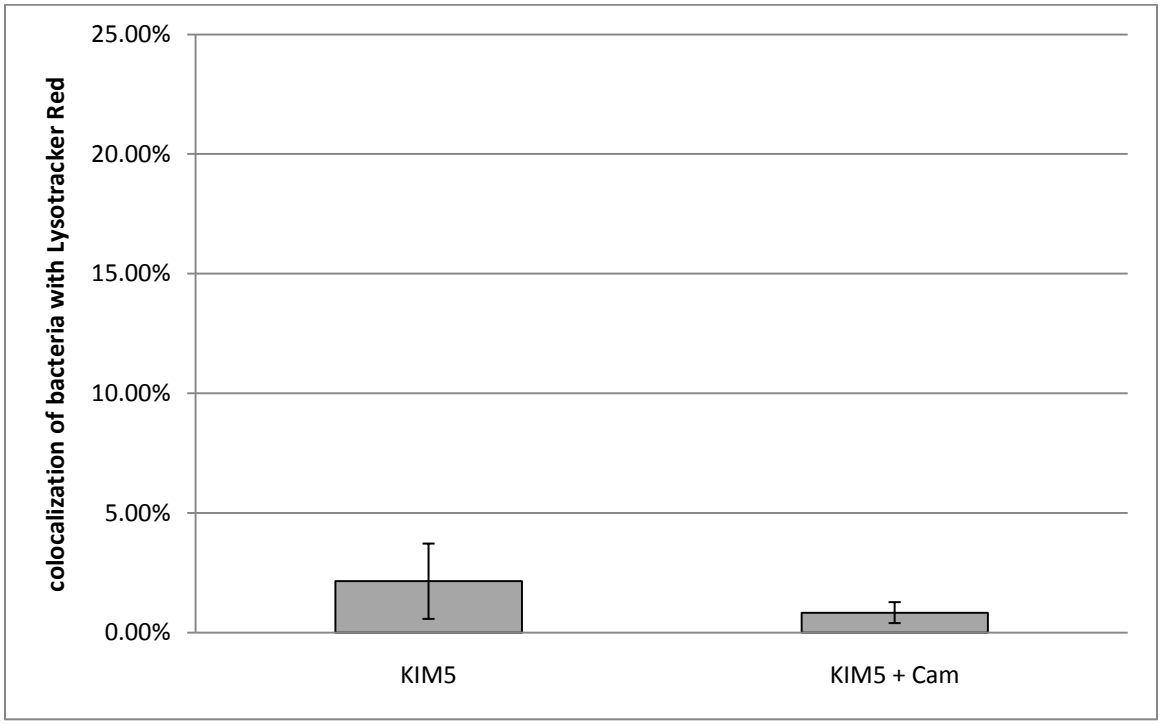

Figure 2.6. *Y. pestis* is unable to globally prevent YCV acidification within a macrophage.

J774A.1 macrophages were either co-infected with unlabeled live KIM5 and fixed/killed KIM5/GFP at an MOI of 5 per strain, or each strain singly at an MOI of 10. Samples were collected at 1.25 hours post infection. Samples were permeabilized with 0.1% saponin, then stained with rabbit anti-*Yersinia* primary antibody (1:1,000) and goat anti-rabbit Alexa Fluor 350 secondary antibody (1:500) prior to imaging. Four live bacteria (arrows) are single-stained with Alexa Fluor 350, while three fixed-killed bacteria (arrowheads) are dual-detected with GFP and Alexa Fluor 350 in the image series. At least 50 phagosomes per strain were evaluated over three fields as seen in the quantitation below. The results of one experiment are shown.

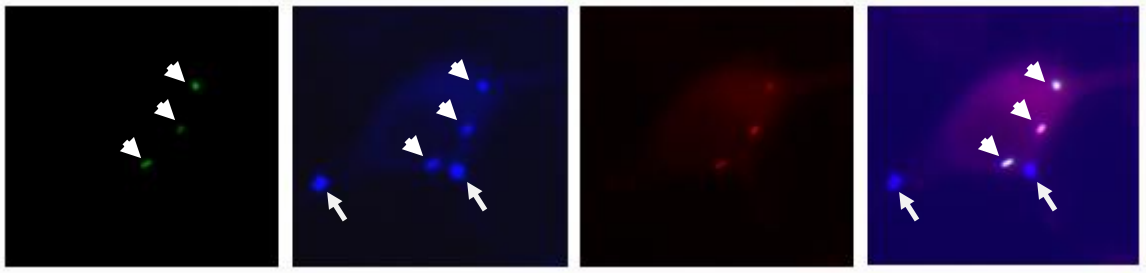

Fixed-killed KIM5 α-*Yersinia* AF350 Lysotracker Red merge

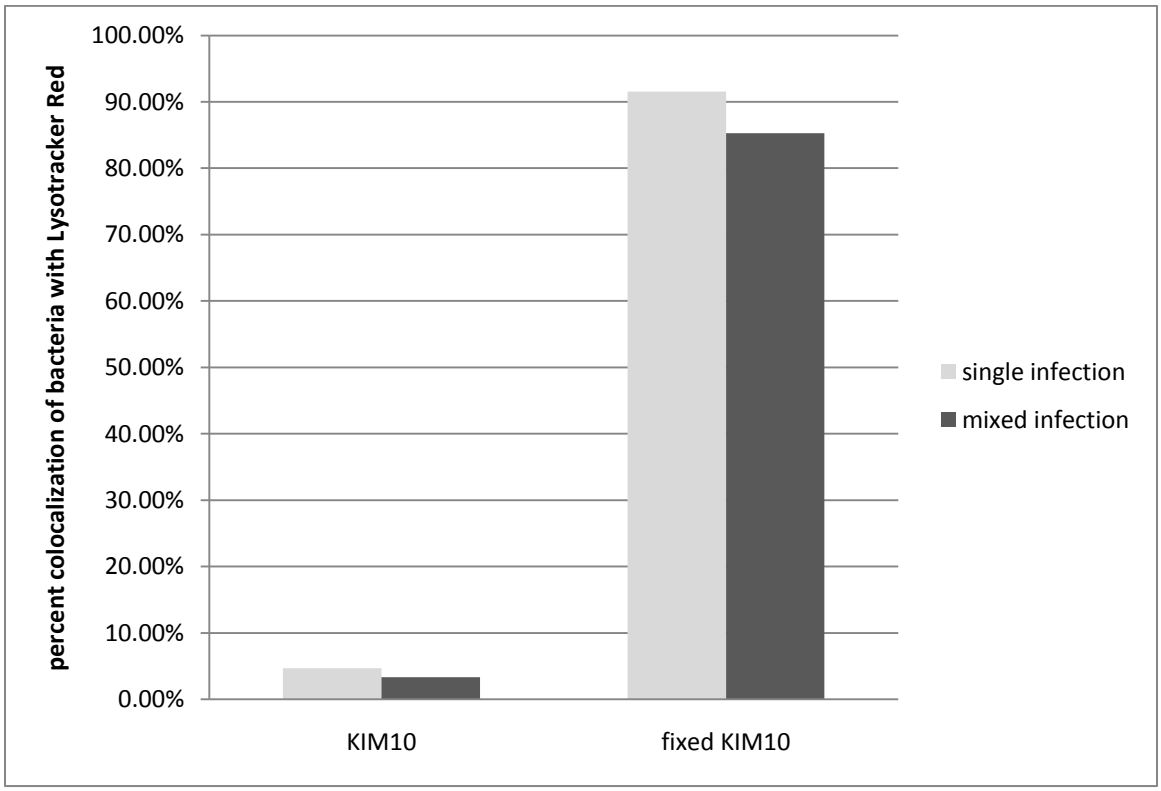

Figure 2.7. YCVs containing live bacteria do not colocalize with vATPase.

J774A.1 macrophages were infected with live or fixed-killed KIM5/GFP at a MOI of 10, and collected over a 5.25 hour time course for analysis. Cells were permeabilized with 0.1% saponin and stained with a rabbit polyclonal antibody to the B subunit of the vATPase. At least 50 bacteria over three fields were evaluated. The average of three independent experiments is graphed below, and the error bars represent standard deviation.

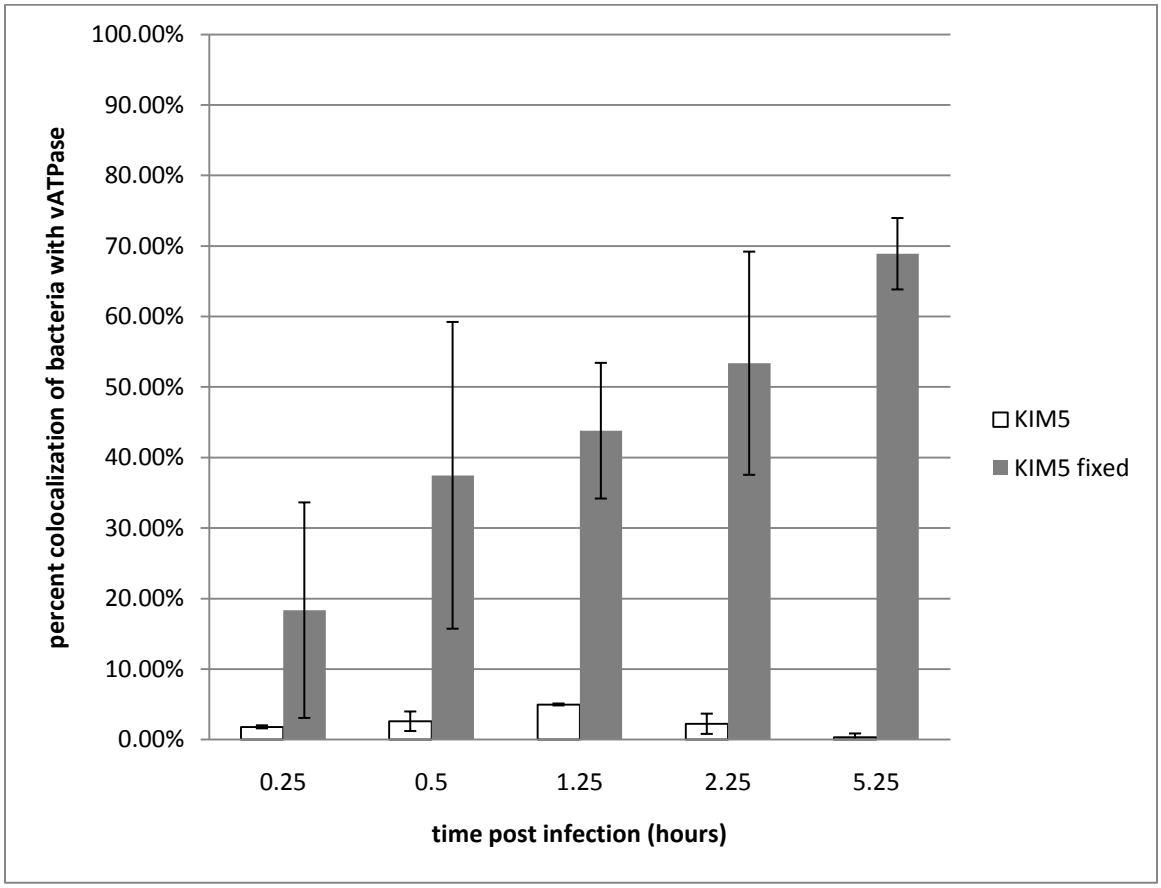

Chapter 3: To examine the importance of Rab GTPases to the trafficking of *Yersinia pestis*-containing phagosomes in macrophages.

Summary

YCVs appear to follow along the typical phagosome maturation pathway. Rab GTPases are essential mediators of this process and regulate fusion of endocytic compartments. I investigated the possibility that *Y. pestis* manipulates these proteins in order to alter its phagosomal environment and ultimately to promote its intracellular survival. Immunofluorescence assays indicated that YCVs may interact with Rab7 and Rab27. However, further investigation of Rab27 by use of macrophages deficient for this protein revealed that Rab27 does not influence the ability of *Y. pestis* to prevent phagosome acidification, nor does the bacterium control Rab27 to escape from the macrophage. These results indicate that Rab27 does not play a role in the intracellular survival and trafficking of *Y. pestis*.

Introduction

Pathogenic bacteria like *S.* Typhimurium and *M. tuberculosis* have been shown to prevent acidification of their vacuoles through regulation of or by blocking acquisition of Rab GTPases (55, 154). Rab GTPases play a key role in regulating fusion of endocytic compartments. Two key mediators in this process are Rab5, found on early endosomes, and Rab7, located on late endosomes and lysosomes (156). Since *Y. pestis* appears to

interact with the endocytic pathway, it is possible that the bacterium manipulates these proteins in order to alter its phagosomal environment and ultimately to promote its intracellular survival. Rab proteins are also important in the regulated exocytosis of secretory vesicles from the cell (158). Rab27 is a key protein in this process. Rab27 regulates melanosome transport and also mediates the exocytosis of lysosome-related organelles and secretory vesicles (61). It is known that *Y. pestis* can exit from the macrophage to replicate extracellularly (82), but this mechanism is not well understood. The goals of these experiments were to determine if *Y. pestis* interacts with Rab GTPases that regulate either endocytic or exocytic pathways, and whether this interaction promotes intracellular survival within macrophages and/or exocytosis from these cells.

Experimental Procedures

Bacterial strains and growth conditions. The bacterial strains used in this study are listed in Table 3.1. *Yersinia* strains were grown at 28^{o}C on heart infusion (HI) agar. *Yersinia* cultures were grown at 28^{o} C in HI broth. Ten μg/ml chloramphenicol and 25 μg/ml ampicillin were added to media for growth of *Y. pestis*.

Cell culture. Macrophage-like murine cell line J774A.1 and human monocyte cell line THP-1 were cultured as described earlier. Bone marrow-derived macrophages were isolated from C3H/HeSn-Rab27a^{ash}/J (Rab27a$^{-/-}$) mice and congenic control C3H/HeSnJ mice (Jackson Laboratory). Bone marrow derived macrophages (BMMs) were isolated from both femurs of each mouse, resuspended into DMEM containing GlutaMAX and a high glucose concentration and supplemented with 20% FBS, 30% L cell-conditioned

medium, and 1 mM sodium pyruvate. The cells were then seeded into four 100 mm tissue culture dishes incubated at 37°C with 5% CO_2 for five days. The cells were then harvested and resuspended into DMEM containing GlutaMAX and a high glucose concentration and supplemented with 10% FBS, 15% L cell-conditioned supernatant, and 1 mM sodium pyruvate, and seeded into 24-well plates as described earlier.

Antibodies. Rabbit polyclonal antibodies to Rab5, Rab7, or Rab27 were obtained from Santa Cruz Biotechnologies. Mouse monoclonal antibodies to Rab5 and Rab27 were obtained from BD Pharmingen.

Rab immunofluorescence assays. The macrophage infection assay described earlier was carried out. At various time points, the samples were washed and fixed with paraformaldehyde/lysine/periodate (PLP) fixative for 30 minutes. After fixation the cells were washed three times with 5% sucrose in PBS, then permeabilized with 0.2% Triton X-100. The samples were either stained with rabbit polyclonal antibodies to Rab5, Rab7, or Rab27 (Santa Cruz Biotechnologies) and goat anti-rabbit Alexa Fluor 594 secondary antibody, or a mouse monoclonal antibody to Rab27 (BD Pharmingen) and goat anti-mouse Alexa Fluor 594.

Escape assay. The escape assay was performed similarly to the macrophage infection assay. One hour after the addition of medium containing 2 µg/ml gentamicin, cells were washed, and fresh DMEM without gentamicin was added to the macrophages. To assay for extracellular bacteria, live cell imaging was performed at the indicated time points using a Zeiss Axiovert S100 microscope with a 32X objective.

Western blot. Bacteria (2 X 10^6) or macrophage cells (2 X 10^5) were collected and suspended into boiling Laemmli buffer for lysis, and samples of the resulting lysates were used for analysis. Samples were run in duplicate on a 15% (SDS)-polyacrylamide gel at 40 mA for 2.5 hours and transferred to a nitrocellulose membrane at 30 V overnight. The membrane was blocked in 1X TBS-Tween and sodium dodecyl sulfate incubated with primary antibody (1:500) for one hour. The membrane was divided into two. One half was incubated with the rabbit polyclonal Rab27 antibody (1:500), and the other was incubated with the mouse monoclonal Rab27 antibody (1:500) for one hour. Membranes were washed extensively with TBS-Tween and incubated with horseradish peroxidase (HRP) goat anti-rabbit (1:10,000) or HRP goat anti-mouse (1:5,000) secondary antibodies. Blots were extensively washed and incubated with an enhanced chemiluminescence reagent (Perkins-Elmer), then immediately developed.

Lysotracker Red assay. The Lysotracker Red assay was performed as described earlier.

Results

Epitopes recognized by Rab7 and Rab27 antibodies colocalize with YCVs. To examine if YCVs colocalize with Rab proteins important for phagosome maturation or regulated exocytosis, KIM5/GFP-infected macrophages were stained with polyclonal antibodies to Rab5, Rab7, or Rab27 (Figure 3.1). Colocalization of the anti-Rab5 with YCVs was not detected at any point of the time course. This result suggests either that Rab5 does not interact with the YCV, or that any colocalization with Rab5 could be occurring too quickly to observe. Rab7 did appear to colocalize with KIM5/GFP, and

this colocalization peaked at 30 minutes post infection. However, the level of colocalization seen was rather low (~25%). Colocalization of anti-Rab27 with KIM5/GFP persisted through the time course of the experiment, but peaked at 0.25 hours post infection (~35%). These results together indicate that Rab7 and Rab27 may have some interaction with YCVs. However, at early time points (< 15 minutes) post infection, some extracellular bacteria were also observed to colocalize with both of these Rabs, giving rise to concern that crosstalk might be occurring between these antibodies and the bacteria.

Rabbit polyclonal Rab27 antibody is not specific. From the immunofluorescence work in J774A.1 macrophages, Rab27 appears to colocalize with YCVs. To verify this interaction, a Western blot comparing uninfected versus KIM5-infected J774A.1 cells was performed. However, a number of protein bands were detected non-specifically, in addition to a 25 kDa size band at which Rab27 is predicted to migrate (Figure 3.2). This result furthered the concern that the polyclonal Rab27 antibody was not specific. A Western blot utilizing a mouse monoclonal antibody to probe lysates of human THP-1 macrophages was performed (Figure 3.2). Only one band was detected, and it was at the expected size, suggesting that the antibody was specific. This antibody was then used in the Rab immunofluorescence assay, comparing uninfected versus infected THP-1 macrophages. The results of this assay were inconclusive, as the THP-1 cells were infected only to a small degree, and thus colocalization studies with the monoclonal antibody were unsuccessful due to the limited number of intracellular bacteria available for analysis. To resolve the question of the specificity of the rabbit polyclonal Rab27

antibody, wild-type and Rab27a$^{-/-}$ macrophages were stained with the rabbit polyclonal antibody. The imaging showed that colocalization between Rab27 and KIM5/GFP was observed even in Rab27a$^{-/-}$ macrophages (Figure 3.3). This finding revealed that the polyclonal antibody utilized in the initial immunofluorescence assays is nonspecific, perhaps reacting with a surface epitope on the bacteria.

Rab27 and bacterial escape from the macrophage. Though *Y. pestis* survives intracellularly, there is evidence that the bacteria can escape and survive extracellularly (82). It is possible that *Y. pestis* may hijack the regulated exocytic pathway as a mechanism to escape from the macrophage without inducing cell death. Rab27 is a key mediator of regulated exocytosis, making it a likely target for such subversion. To test this prospect, live cell imaging was utilized in an escape assay to monitor and compare the ability of KIM5/GFP to escape from either wild-type or Rab27a$^{-/-}$ macrophages over time (Figure 3.4). The results from this experiment showed that extracellular KIM5/GFP became apparent with both wild-type and Rab27-deficient macrophage samples starting at 12 hours after gentamicin removal. This finding suggested that KIM5/GFP was able to escape from macrophages both competent and deficient for Rab27.

Rab27 does not play a role in regulating phagosomal pH. It has recently been reported that Rab27 regulates the pH of dendritic cell phagosomes (62). To examine this possibility in macrophages, C3H/HeSnJ and Rab27a$^{-/-}$ BMMs were infected with live or fixed-killed KIM5/GFP in the presence of Lysotracker Red (Figure 3.5). No difference was seen in the colocalization of live or fixed-killed bacteria with Lysotracker Red in

either the wild-type or Rab27-deficient macrophages. This result suggests that Rab27 does not play a role in regulating phagosomal acidification.

Discussion

Rab GTPases are key regulators of phagosome maturation (156). Many pathogenic bacteria alter Rab colocalization to inhibit phagosome maturation. *M. tuberculosis* inhibits Rab conversion, thereby preventing Rab7-mediated fusion of late endosomes to its phagosome (31). *S.* Typhimurim, on the other hand, appears to recruit Rab7-positive vacuoles to its phagosome and acquire markers of late endosomes such as LAMP-1, but do not fuse with lysosomes (89). Since phagosomes containing *Y. pestis* appear to interact with compartments of the endocytic pathway, I investigated whether YCVs interact with Rab GTPases located on early and late endosomes. Colocalization of bacteria with the early endosome marker Rab5was not detected; however, Rab5 appeared to stain throughout the macrophage in an even distribution, even at later time points, and colocalization with KIM5/GFP was not detected. Given that YCVs interact with late endocytic compartments and that phagosome maturation is a progressive process, it is possible that interactions of Rab5 with the YCV occur too quickly to detect (156). Dominant-negative or constitutively active mutants of Rab5 have been extensively used in overexpression studies to examine the localization of Rab5 to phagosomes and early endosomes (117, 118, 144). Since Rab7 is expected to be located on late endosomes, colocalization with *Y. pestis* is expected to be seen at starting within 30 minutes or later post infection. Colocalization of Rab7 with the YCV peaked at 30 minutes post infection. This observation is expected, and the timing is similar to observations utilizing

bacteria known to colocalize with Rab7 (124). A dramatic decrease in colocalization is seen at later time points; a similar finding has also been reported for *S.* Typhimurium (89). However, overall colocalization of the YCV with Rab7 was lower than expected. These observations may not be accurate, as there is suspicion that the Rab7 polyclonal antibody utilized may exhibit a degree of crosstalk with the bacteria. If these results could be verified through use of Rab7 fusion constructs (157), it is possible that Rab7 may be excluded from YCVs after the interaction of late endosomes with the phagosome occurs. This possibility differs from the events in *S.* Typhimurium; SCV colocalization with Rab7 is observed for several hours post infection (15). From these experiments it is unclear if *Y. pestis* interferes with endocytic Rab GTPases to promote its intracellular survival.

It is known that *Y. pestis* can exit from the macrophage to replicate extracellularly (82), but this mechanism is not well understood. I investigated whether *Y. pestis* utilizes the Rab27-mediated exocytic pathway as a mechanism to escape from the macrophage. Rab 27 plays a key regulatory role in melanosome transport and exocytosis of secretory granules (61). Rab27 has not been previously identified to play such a role in bacterial infection, but loss of Rab27 is correlated to an increase of bacterial infections in patients due to disregulation of macrophage activation (88) Rab27 showed a higher level of colocalization with *Y. pestis* at 15 and 30 minutes post infection, but decreased at later time points. Since Rab27 is a key regulator of exocytosis, the levels of Rab27 colocalization might indicate that *Y. pestis* is usurping the activity of this Rab to escape from the macrophage shortly after phagocytosis. My research became focused on furthering this finding. Western blots indicated that the polyclonal Rab27 antibody used

for the initial colocalization experiments was not specific; use of Rab27a$^{-/-}$ macrophages confirmed that this antibody cross-reacted to a surface epitope of *Y. pestis*, rendering the initial experiments invalid. Further use of Rab27a$^{-/-}$ macrophages indicated that Rab27 does not affect the ability of *Y. pestis* to prevent phagosomal acidification. This result was not surprising, as Rab27 has not been ascribed a function in phagosome maturation. Extracellular *Y. pestis* were found after gentamicin was removed from infected macrophages competent or deficient for Rab27. This could suggest that *Y. pestis* was able to escape from the macrophages regardless of the absence of Rab27. However, this type of assay is very difficult to interpret, as the bacteria replicate after being found extracellularly. Other bacteria have been reported to exit the macrophage; this is usually dependent on cell death (70), but has been found to occur intermittently in *Salmonella* infection due to the action of flagella (126). It is known that *Y. pestis* promotes apoptosis of host cells (79), and it is possible that cell death is the primary mechanism by which the bacteria exit the macrophage. Based on these results, it appears that *Y. pestis* does not utilize Rab27 to prevent phagosome acidification, but it remains unclear if Rab27-mediated exocytosis may be exploited as a mechanism of escape from the macrophage.

Figures and Tables

Table 3.1. *Yersinia* strains used in Chapter 3.

Strain Name	Relevant Characteristics	Reference
KIM5	*Y. pestis* biovar Mediaevalis, *pgm*$^-$	(44)
KIM5/GFP	KIM5, pGFP Ap^r	(46)

Figure 3.1. Colocalization of Rab proteins with YCVs.

J774A.1 macrophages were infected with KIM5/GFP at a MOI of 10, and at different times thereafter the samples were fixed and stained with antibodies to Rab5 (A-C), Rab7 (D-F), or Rab27 (G-I); images shown that were captured by phase and fluorescence microscopy correspond to 30 minutes post infection. The percent colocalization of GFP signals (A, D, G) with each Rab antibody signal (B, E, H) were quantified at the time points indicated in the graph (J) below. At least 50 YCVs over three fields were analyzed for each time point. One experiment is shown.

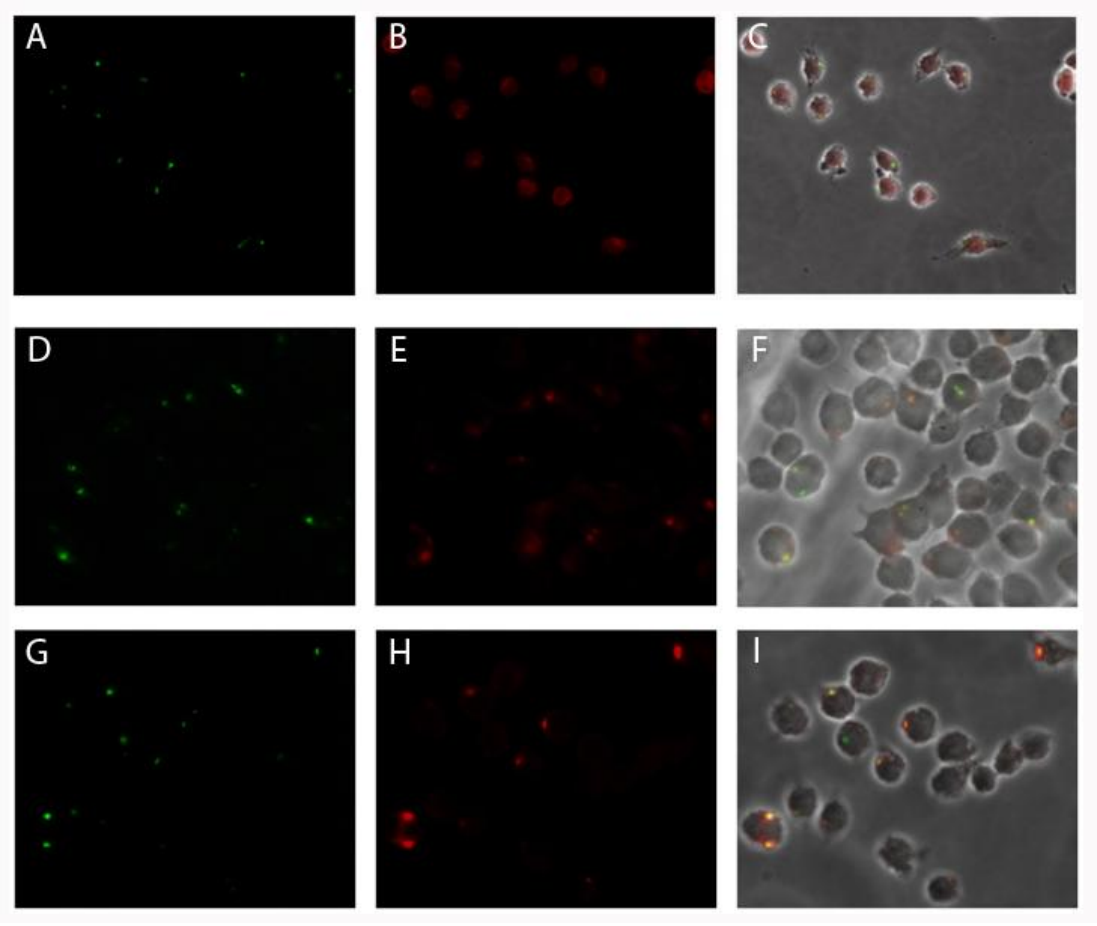

J

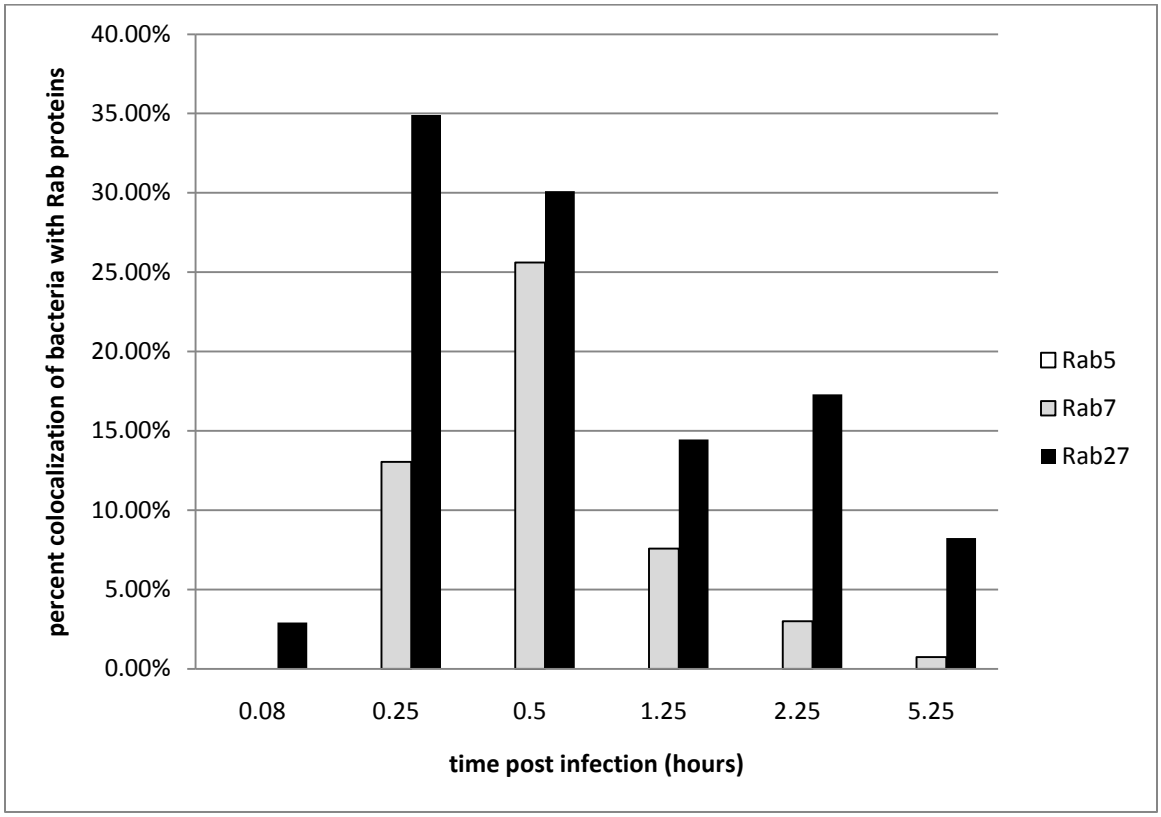
40.00%
35.00%
30.00%
25.00%
20.00%
15.00%
10.00%
5.00%
0.00%
percent colocalization of bacteria with Rab proteins
0.08
0.25
0.5
1.25
2.25
5.25
time post infection (hours)
Rab5
Rab7
Rab27

Figure 3.2. Polyclonal antibody toRab27 is less specific than the monoclonal Rab27 antibody.

Samples of lysate derived from 1 X 10^6 bacterial cells or 2 X 10^5 mammalian cells were loaded onto a 16.5% SDS-polyacrylamide gel in duplicate. Mammalian cells included J774A.1 murine macrophage-like cells, THP-1 human monocyte suspension, of THP-1 monocytes differentiated into adherent macrophages. The gel was transferred to a nitrocellulose membrane and divided. The membranes were probed with either a polyclonal or monoclonal antibody to Rab 27, then secondary antibodies conjugated to HRP. Blots were incubated with chemiluminescence reagent and immediately developed for one minute. Positions of molecular weight standards in kDa are shown the left.

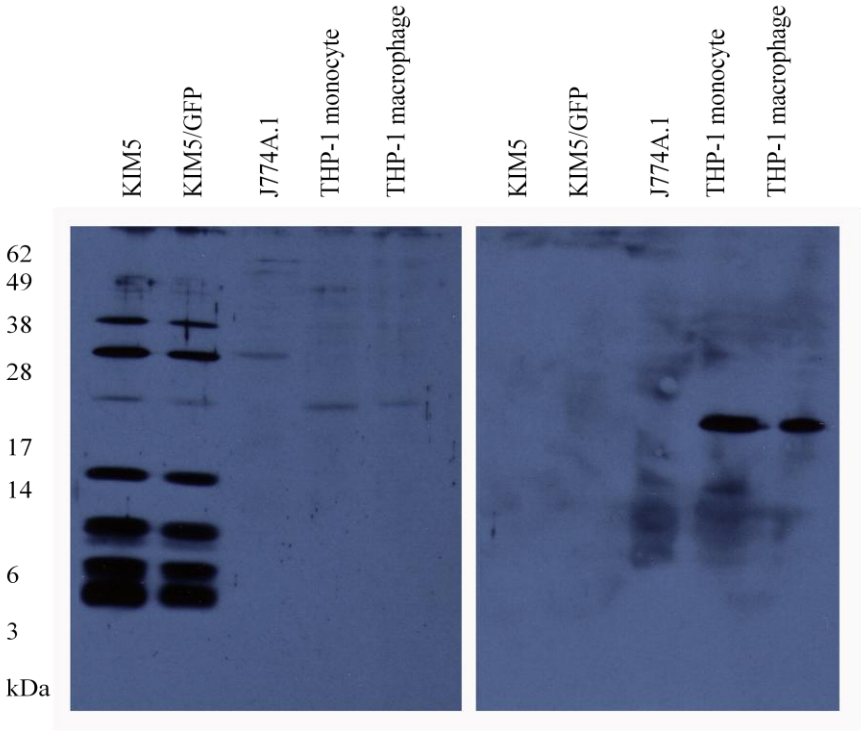

Figure 3.3. Polyclonal Rab27 antibody cross-reacts with *Y. pestis*.

C3H/HeSnJ (A-C) or Rab27a$^{-/-}$ (D-F) macrophages were infected with KIM5/GFP at and MOI of 10, fixed and then stained with a rabbit polyclonal antibody to Rab27. GFP fluorescence (A, D) and Rab27 staining (B, E) were visualized by fluorescence microscopy. Colocalization (C, F) was observed at the 1.25 hour time point with 100X objective.

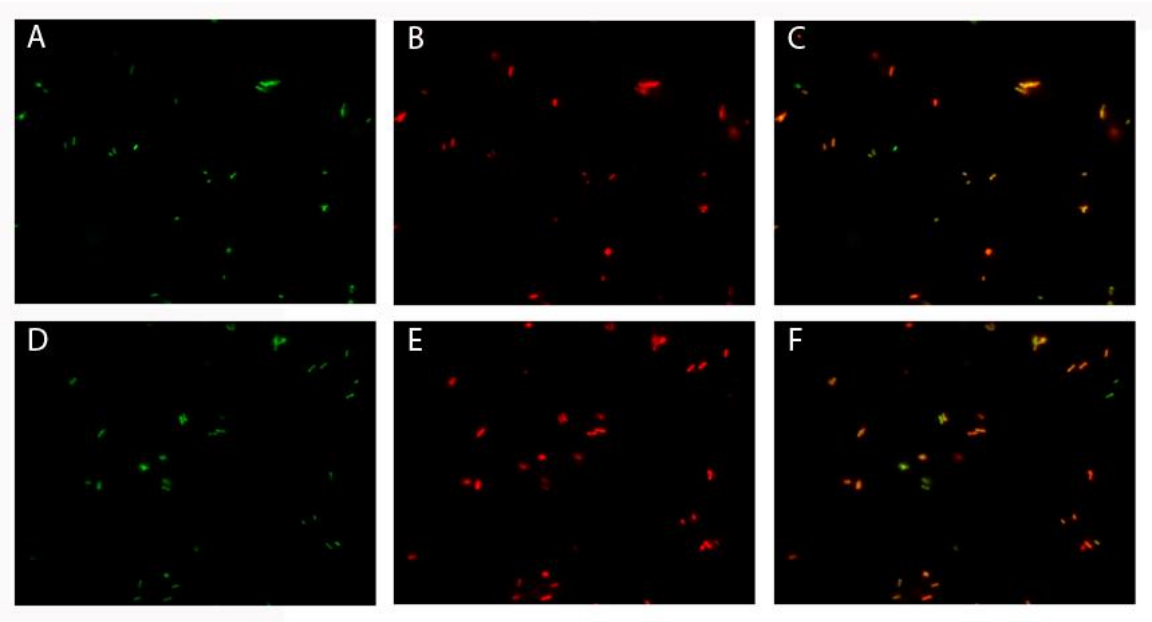

Figure 3.4. Extracellular bacteria are detected after macrophages competent or deficient for Rab27 are infected.

C3H/HeSnJ (A-C) and Rab27a$^{-/-}$ (D-F) macrophages were infected with KIM5/GFP. At 2.25 hours post infection, gentamicin was removed from the medium, and cells were monitored by live cell microscopic imaging for bacterial escape. 32X merged images of the phase and GFP channels show infected macrophages at the time of gentamicin removal (A, D), 12 hours after gentamicin removal (B, E), and 18 hours after gentamicin removal (C, F).

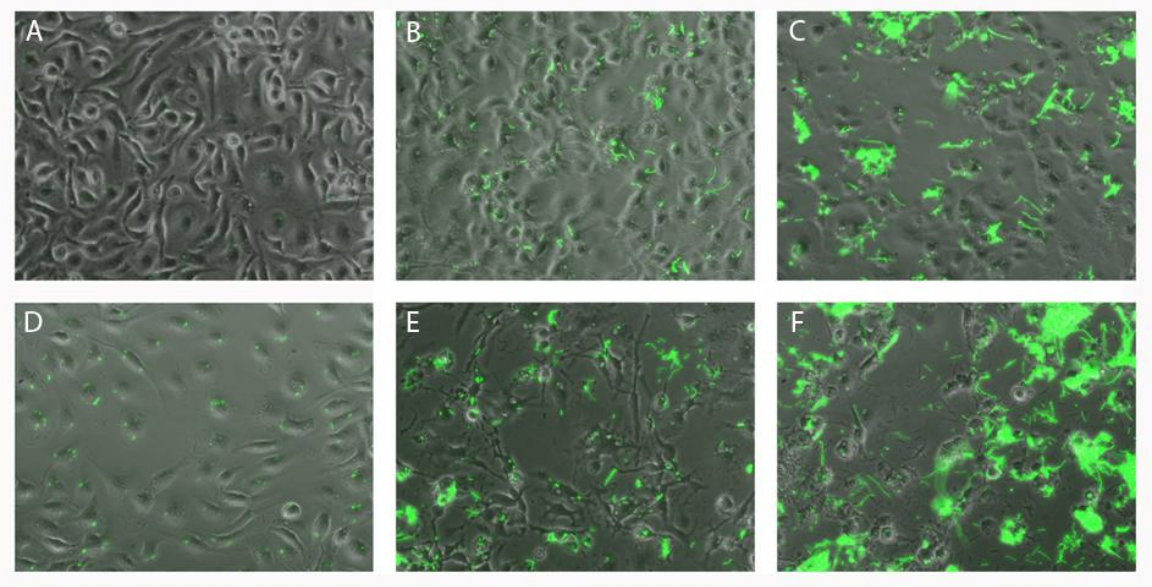

Figure 3.5 Rab27 does not contribute to inhibition of phagosome acidification.

C3H/HeSnJ and Rab27a$^{-/-}$ macrophages were infected with live or fixed-killed KIM5/GFP at a MOI of 10 and tested via Lysotracker Red for their ability to prevent phagosome acidification over a time course. At least 50 phagosomes from three fields were analyzed. Time post infection is indicated in the legend. The results of one experiment are shown.

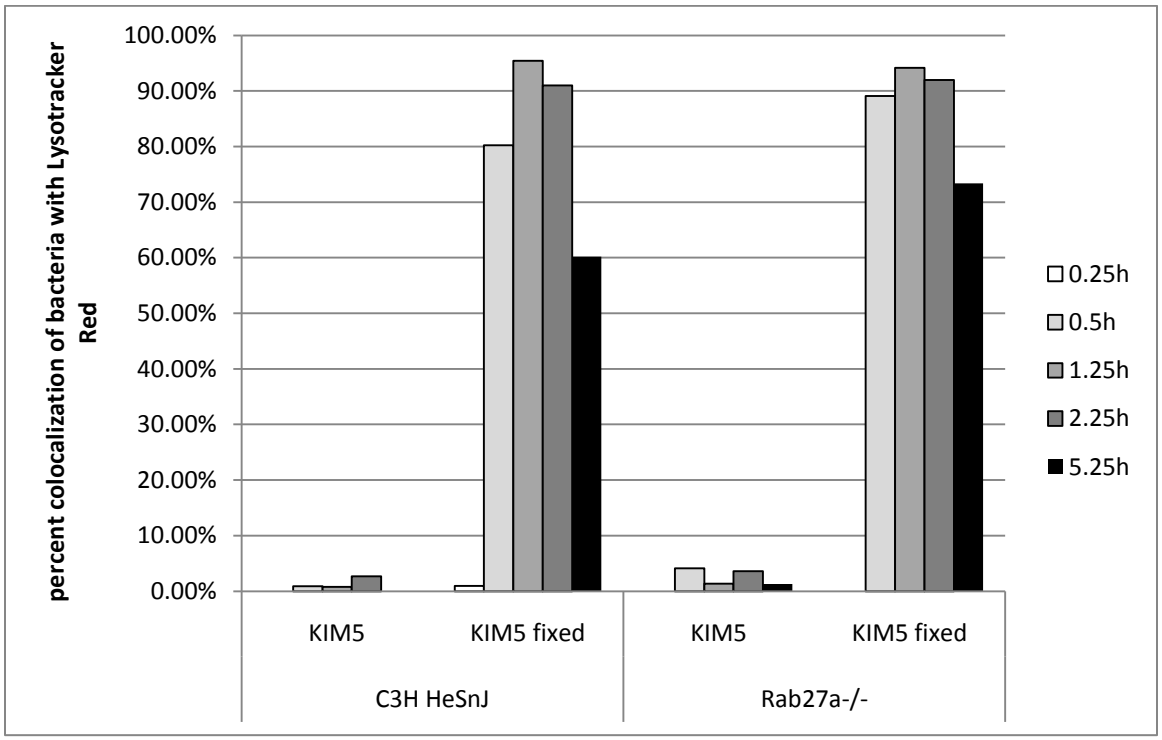

Chapter 4: To identify and characterize genes important for *Yersinia pestis* to promote intracellular survival.

Summary

Recent advances in microarray technology have allowed for approaches to examine a bacterial genome to identify genes important for survival under different selection conditions (128). Transposon site hybridization (TraSH) is a method that combines transposon mutagenesis with microarray hybridization technology to allow for high throughput screening of mutant libraries after negative selection. TraSH has been employed to identify mycobacterial genes required for growth under certain nutrient conditions (128) as well as to identify genes contributing to the survival of *S.* Typhimurium within murine macrophages (20). In this study we performed a negative selection screen to identify genes that are important for the survival of *Y. pestis* in macrophages. Several genes were identified as potentially playing a role in the intracellular survival of *Y. pestis*. We identified the gene *galU* from this screen and characterized its role in the intracellular survival of *Y. pestis* in macrophages.

Introduction

Y. pestis is able to survive and replicate within murine macrophages (19, 147). However, the basis for this is still poorly understood. It is known that the transcriptional activator PhoP as well as some of the PhoP-regulated genes are important for the intracellular survival of *Y. pestis* in macrophages, perhaps by promoting resistance to

antimicrobial peptides and by promoting survival under low Mg^{2+} conditions (46). The *pgm* locus contains an operon called *ripCBA* that promotes the survival of the bacteria within activated macrophages (111). However, it is not known how this region promotes *Y. pestis* survival in macrophages. These genes are not known to be involved in the trafficking of the YCV and do not explain the phenotypes involved, such as a lack of phagosomal acidification. Thus, it is unlikely that the genes responsible for allowing *Y. pestis* to survive intracellularly have all been identified.

Recent advances in microarray technology have allowed for approaches to examine a bacterial genome to identify genes important under different selection conditions (128). TraSH is a method that combines transposon mutagenesis with microarray technology to allow for high throughput screening of mutant libraries after negative selection (Figure 4.1). TraSH has been employed to identify mycobacterial genes required for growth under certain nutrient conditions (128) as well as to identify genes contributing to the survival of *Salmonella enterica* serovar Typhimurium within murine macrophages (20).

In this study I performed a negative selection screen to further identify genes that are important for the survival of *Y. pestis* in macrophages. Several genes were identified as potentially playing a role in the intracellular survival of *Y. pestis*. We identified the gene *galU* from this screen and characterized its role in the intracellular survival of *Y. pestis* in macrophages.

Experimental Procedures

Bacterial strains and growth conditions. The bacterial strains used in this study are listed in Table 4.1. *Escherichia coli* strains were grown at 37^{o}C either on Luria-Bertani (LB) agar or in LB broth. *Yersinia* strains were grown at 28^{o}C either on HI agar or LB agar. *Yersinia* cultures were grown at 28^{o}C in LB or HI broth. Tetracycline (20 µg/ml) and kanamycin (25 µg/ml) were added to media as necessary. Ten µg/ml chloramphenicol and 25 µg/ml ampicillin were added to media for growth of *Y. pestis*, and 30 µg/ml chloramphenicol and 100 µg/ml ampicillin were added to media for growth of *Y. pseudotuberculosis* and *E. coli* as necessary unless otherwise indicated.

Cell culture. BMMs were cultured as described earlier. BMMs were prepared from the femurs of 6-8 week old female C57BL/6 mice (Jackson laboratories). The macrophage-like cell line J774A.1 was cultured as described earlier.

Construction of transposon library. *Y. pestis* KIM6+ was conjugated to *E. coli* S17λpir containing pMar2xT7/TyK, which includes a *Himar1* element flanked by outward-reading T7 promoters, and was modified by replacing the gentamicin resistance cassette of pMar2xT7 (76) with a kanamycin cassette. The transconjugants were plated on *Yersinia*-selective medium (YSM) (Oxoid) containing 100 µg/ml kanamycin, and the resultant ~31,500 colonies were pooled together in LB broth with 50% glycerol and frozen at -80^{o}C.

Negative selection in bone marrow macrophages. The negative selection screen was performed in a manner similar to previously published reports (9, 51). Briefly, the

transposon library was grown in culture from frozen stock at 28^{o}C overnight. Bacteria grown at 28^{o}C were harvested as an unselected input control. BMMs (10^{7}) were infected at a MOI of 2 for 15 minutes, washed with PBS, and incubated with medium containing gentamicin. At 8 hours post infection, the BMM cells were lysed with 0.1% Triton X-100, and the bacteria were harvested by centrifugation and resuspended in HI, and an outgrowth step was performed overnight at 28^{o}C with shaking. The bacteria were then collected as the selected output condition. Four independent experiments were performed.

Genomic DNA processing and in vitro transcription. Genomic DNA (gDNA) was isolated using the Qiagen Genomic-tip 100/G protocol. 20 µg of purified gDNA was sheared by sonication and precipitated with ammonium acetate and ethanol. 2 µg of sheared purified gDNA was used for transcription with the Ambion amino-allyl MessageAmpII kit, allowing the transcription reaction to proceed for 14 hours at 37^{o}C to make amino allyl-modified amplified RNA. The RNA was purified using the Qiagen nucleotide removal kit. For two experiments, the control condition RNA was labeled with Cyanine 3 (GE Healthcare) and the negatively selected condition RNA was labeled with Cyanine 5, and the reciprocal was done with the remaining two experiments.

Microarray hybridization and processing. The 70-mer oligonucleotide microarrays representing all open reading frames (ORFs) from *Y. pestis* were obtained from TIGR. The microarray slides were prehybridized, washed, and dried immediately before hybridization by using the protocol recommended by the Pathogen Functional Genomics Resource Center of the J. Craig Venter Institute

(http://pfgrc.jcvi.org/index.php/microarray/protocols.html). For hybridization, RNA samples labeled with Cy3 or Cy5 were dye-matched so that each sample had the sample amount of dye present (200-250 pmol) and resuspended in 130µl of hybridization solution containing 25% (vol/vol) formamide, 5X SSC, 0.1% SDS, and 300 µg/ml of sheared salmon sperm DNA (1X SSC is 0.15 M NaCl plus 0.015 M sodium citrate). Samples were heated at 95^{o}C for 10 minutes prior to hybridization. Hybridization was performed on a Tecan HS4800 Pro hybridization station as per manufacturer's instructions. Hybridized arrays were sequentially washed with 5X SSC-0.1% SDS, 2X SSC-0.1% SDS, 0.1X SSC-0.1% SDS, 0.1% SDS, 95% ethanol, and deionized water. Arrays were directly scanned after the last wash using an Agilent G2505B DNA Microarray scanner controlled by Agilent scan control software, with a pixel size of 5 µm on a single-pass sequential line. The laser power was set to 100% for both red and green channels, and photomultiplier gains were automatically adjusted by the scanner. Slide spots were gridded using GenePix Pro 6 software. Lossless image files were stored for later analysis.

Microarray statistical analysis. Statistical analysis on the microarray data was done as described previously (46). Briefly, the microarray data were analyzed using the Limma module of the Bioconductor package for the R statistical environment (140). The microarray datum for each gene was fitted to a linear model, and statistics were generated using the lmFit and eBayes functions. The *P* values displayed were adjusted for multiple testing using the Benjamini and Hochberg method within Limma. Genes with *P* values of <0.05 and a negative fold change of less than -1 were considered negatively selected.

Annotations for microarray data were derived from The Institute for Genomic Research type annotation files.

Construction of *Yersinia* mutants. Deletions of KIM6+ ORFs (Table 4.1) were generated using suicide plasmids constructed by recombinant polymerase chain reaction (PCR) (56). Following two rounds of PCR (159) with two pairs of tailed primers, DNA fragments were generated which contained completed deletions of the desired open reading frames flanked by 5' and 3' sequences. The resulting DNA fragments were inserted into the suicide plasmid pSB890 (64). A list of the primers used can be found in Table 4.2. The KIM6+ mutants were generated through allelic exchange as previously described (97) and verified by PCR. *Y. pseudotuberculosis* IP2790c *galU::mag* was created through conjugation with S17λpir carrying the *mariner*-based *magellan3* mini-transposon (*mag)* on pFD1 (125). A KIM10+ *galU::mag* mutant was created using the lambda red recombinase system (28, 30), amplifying *galU::mag* from IP2790c *galU::mag* using the appropriate primers. pGalU was created by PCR amplifying the wild type *galU* ORF and inserting the gene into pMMB67EH (American Type Culture Collection), placing *galU* under the control of the *tac* promoter. Both pGalU and the empty vector were introduced into KIM10+ *galU::mag* via conjugation (46). Plasmid pMMB207gfp3.1 (chloramphenicol resistant), used to express green fluorescent protein (GFP), was introduced into the indicated strains by conjugation.

Colony forming unit assay. The CFU assay was performed as described earlier with the following modifications. BMMs were seeded in 24-well tissue culture plates at a concentration of 1.5 X 10^5 cells/well. Cells were infected with *Y. pestis* at a MOI of 10,

and 0.05 mM IPTG was added to the medium throughout the course of infection when appropriate. At the time points indicated, the cells were washed with PBS and 500 µl of 0.1% Triton X-100 was added to each well and incubated at 37^{o}C for ten minutes to allow for lysis of the macrophages. The wells were scraped with a pipet, the supernatant was collected into Eppendorf tubes, and the wells were washed with 500 µl of LB and combined with the Triton X-100 supernatants. Samples were serially diluted onto HI agar directly after sample collection. Statistical analysis was performed using one-way analysis of variance and the Dunnett's posttest (GraphPad Prism version 4.0c for Macintosh, GraphPad Software, San Diego California USA, www.graphpad.com).

Polymyxin B MIC assay. The minimum inhibitory concentration (MIC) was determined as follows. Polymyxin B (Sigma) was diluted two-fold into HI broth with 0.05 mM IPTG at concentrations from 0.122-250 µg/ml. Each dilution (100 µl) was aliquoted into 96-well plates. Overnight cultures of *Y. pestis* were diluted and added to wells at a concentration of ~1 X 10^{6} CFU/ml. Plates were placed at 28^{o}C for 20 hours with shaking, and then examined for growth and compared to a control grown in HI broth with no polymyxin B. The MIC was taken as the lowest antibiotic concentration at which there was no visible growth.

Lysotracker Red assay. Colocalization of YCVs containing *Y. pestis* with Lysotracker Red was determined using J774A.1 cells as described earlier.

Results

Use of a negative selection screen to identify genes important for the intracellular survival of *Y. pestis* in macrophages. When a mutant library is exposed to a selection condition, it is expected that a subset of mutants will be unable to survive and thus be lost from the library. Microarray technology can detect the negatively-selected mutants by comparison with the unselected library (128). This approach was utilized to identify genes important for the survival of *Y. pestis* within murine macrophages (Figure 4.1). A transposon library was created with ~31,500 *Y. pestis* KIM6+ insertion mutants, which is equal to approximately 7.3X coverage of the KIM6+ genome. KIM6+ was utilized in this screen because the *pgm* locus is known to encode genes that are important for the survival of *Y. pestis* in macrophages (111). Also, the bacteria are grown at 28^{o}C prior to infection, and under this growth condition expression of the TTSS is bypassed. This library was subjected to selection via infection of BMMs, and the surviving bacteria were collected and compared to the nonselected library to identify genes that may play a role in the survival of *Y. pestis* in macrophages. Four independent experiments were performed, with two experiments per dye swap to correct for dye bias (24). This screen differed from previous screens (20, 128) in that the PCR amplification utilizing a linker sequence was omitted, and the RNA was not reverse transcribed to cDNA but was hybridized directly to microarray slides. The steps of PCR amplification and reverse transcription were excluded in order to minimize any selective amplification leading to subsequent loss of data. BMMs were infected at an MOI of 2; at this MOI approximately 50% of the macrophages were infected, and the majority of those cells contained only

one bacterium. This was done to mitigate any possible effects from multiple bacteria within a cell. The screen revealed 525 genes that had a greater than -1 fold change as compared to the unselected control, indicating loss of the gene in the selected condition as compared to the unselected control. The 25 genes with the highest negative fold changes are shown in Table 4.3. The genes *phoP* and *phoQ* had a high negative fold change, as well as members of the PhoP-regulated *pmr* operon. As these genes had been previously characterized as being important for the survival of *Y. pestis* in macrophages (46), they acted as internal controls for as well as validated the methodology of the screen.

Construction and analysis of mutants to assess importance of genes for survival in macrophages. From the microarray data, a number of genes were selected for mutational inactivation in *Y. pestis* (Tables 4.3 and 4.4). From Table 4.3, three genes or operons were selected, *gshA*, *y0157-y0159*, *and y0144.* Six additional genes or operons, *y0021*, *y0036*, *y0228*, *y0230-y0235*, *y0297*, and *y4047*, were chosen based upon the predicted functions of their products (Table 4.4). The resultant KIM6+ mutants all exhibited growth rates similar to parental *Y. pestis* KIM6+ in HI broth at 28°C and were tested via CFU assay to assess viability within primary murine macrophages. However, except for the strain lacking *galU* (discussed below), none of the mutants examined at 24 hours post infection showed a significant defect in intracellular survival as compared to the wild type control (Table 4.4, Figure 4.2).

A *Y. pestis galU* mutant is defective for survival in macrophages. The *galU* locus was second on the list of negatively selected genes (Table 4.3). The *galU* gene encodes a

glucose-1-phosphate uridylyltransferase (accession number NP_669934). This enzyme catalyzes the addition of UMP to glucose-1-phospate yielding UDP-glucose and release of pyrophosphate. UDP-glucose is a metabolic intermediate in the biosynthesis of the LPS core. Genomic sequence analysis indicated that in *Y. pseudotuberculosis* and *Y. pestis galU* is the first gene in a two-gene operon (*galUF*). The *galF* gene most likely encodes a UDP-galactose transferase (accession number NP_669933).

It has been shown for several gram-negative bacteria, such as *Vibrio cholerae* (96) and *Klebsiella pneumonia* (21), that inactivation of *galU* results in an attenuation of virulence. The *galU* gene was previously identified in a separate *mag* transposon mutagenesis screen investigating genes required for *Y. pseudotuberculosis* IP2790c to grow under low Mg^{2+} conditions (45, 125). The IP2790c *galU* mutant showed a defect in intracellular survival *in vitro* (45). A KIM10+ *galU* mutant had been previously constructed based on the results of this low $Mg2^{+}$ screen, and was utilized in the studies outlined here. To determine if a *Y. pestis galU* mutant was also attenuated *in vitro*, a CFU assay was performed. BMMs infected with KIM10+*galU::mag*/pMMB67EH were found to have ~2 log fewer bacteria at 8 hours post infection as compared to the wild type-infected cells (Fig. 4.3). This defect in intracellular survival is comparable to what is seen with *Y. pestis* Δ*phoP*-infected macrophages (46). Thus, *galU* appears to be required for the intracellular survival of *Y. pestis* in murine macrophages. Introduction of the wild type *galU* ORF on a plasmid under the control of the *tac* promoter (pGalU) into KIM10+*galU::mag* mutant resulted in partial complementation of the mutant (Figure 4.3). It is possible that the plasmid-encoded *galU* is being overexpressed and producing a

toxic effect on the bacteria, thus reducing viability and leading to this intermediate phenotype.

A *Y. pestis galU* mutant shows no defect in preventing phagosomal acidification. It has been previously determined that YCVs containing live *Y. pestis* do not acidify (112). To determine if loss of *galU* affects acidification of the YCV, a colocalization experiment using the acidic tracer Lysotracker Red DND-99 was performed. J774A.1 macrophage-like cells were infected with either KIM10+/GFP or KIM10+*galU::mag*/GFP in the presence of Lysotracker, and colocalization was assayed via fluorescence microscopy. As was reported with YCVs containing KIM5/GFP (112), YCVs containing KIM10+ or the *galU* mutant showed very little colocalization with Lysotracker (Fig 4.4). This indicates that *galU* does not have a role in preventing phagosome acidification. The colocalization of KIM6+ and the various KIM6+ ORF mutants constructed (Table 4.1) with Lysotracker was examined as well; however, these YCVs also did not acidify (Fig. 4.4).

A *Y. pestis galU* mutant shows reduced resistance to polymyxin B. It has been previously reported that loss of *galU* in *Vibrio cholerae* causes an increase in susceptibility to antimicrobial peptides (96). More recently, it was shown that *Y. enterocolitica* mutants lacking the outer portion of the core oligosaccharide suffer defects in resistance to the cationic microbial peptide polymyxin B (137). This peptide has a hydrophobic tail, similar to other microbial peptides, that interacts with the bacterial cell membrane to cause membrane permeabilization. To determine if a similar trait is seen in the *Y. pestis galU* mutant, KIM10+ strains were diluted into HI containing different concentrations of polymyxin B and further incubated to assess the MIC.

KIM10+*galU::mag*/pMMB67EH showed an increased susceptibility to polymyxin B as compared to the wild type and complemented strains (Table 4.5). This suggests that *galU* is necessary for an intact. *pestis* LOS, which in turn confers resistance to cationic microbial peptides.

Discussion

The aim of this study was to identify genes that contribute to the survival of *Y. pestis* inside murine macrophages. A transposon library of 31,500 KIM6+ mutants was created and negative selection was performed using primary murine macrophages. Genes previously identified as being required for the intracellular survival of *Y. pestis* in macrophages (46) were identified from the screen, suggesting that the screen was functioning properly. However, several mutants created based on the results of the screen showed no defect in intracellular survival. That several of the mutants tested failed to show an intracellular defect indicates that the screen results have a number of false positives. One possible explanation is that this is due to the outgrowth step of the selected pool in culture. It could be that some mutants are slow-growing as compared to wild type bacteria, and are unable to replicate sufficiently by the endpoint of the negative selection. These mutants would be lost from the selected output in a fashion not due to the macrophage selection condition. This could explain why a number of housekeeping genes required for the maintenance of the bacterium, such as genes encoding ribosomal proteins, were identified in the screen (see Table 4.3). However, this is not the case with the KIM6+ mutants that we tested, as all mutants showed comparable growth to the wild type strain in HI media. Another possibility is that there may be a subtle survival defect,

and that this defect was amplified during negative selection due to competition from the multiple transposon mutants in the screen. It is possible that if the output from each experiment was passaged and reselected to enhance the signal as was previously reported for *Salmonella* (20), this enrichment would result in a reduction of noise from the screen. To our knowledge, this is the first time that a TraSH-based negative selection screen has been performed in *Yersinia*. The methodology behind this screen can be applied to the newly created KIM6+ transposon library to identify genes that are essential under specific conditions in *Y. pestis*. This type of screen has been utilized in identifying genes important *in vivo* through passage in mice (20). A TraSH screen could be used to identify genes that play a role in the resistance to antimicrobial peptides. The transposon library could be passaged through macrophages from mice deficient for the cathelicidin-related antimicrobial peptide (CRAMP) (5) to identify candidates that may be involved in bacterial resistance to this peptide.

One gene with a high negative fold change, *galU*, was found to be important for survival in macrophages. GalU is predicted to be a glucose-1-phosphate uridylyltransferase, which catalyzes the conversion of glucose-1-phosphate to UDP-glucose. UDP-glucose is a metabolite used in the synthesis of sugars added to the core oligosaccharide of the LPS. The LPS consists of the bacterial membrane anchor lipid A linked to the core oligosaccharide, which is linked to the O polysaccharide. Loss of the core allows antimicrobial peptides to interact with lipid A and ultimately compromise bacterial membrane integrity (90). Loss of the O polysaccharide has also been associated with sensitivity to antimicrobial peptides (137). However, *Y. pestis* has an LOS due to the absence of O polysaccharide (108). It has been suggested that the

inability of *galU* mutants to synthesize a complete core oligosaccharide leads to an attenuation in virulence (21, 96). Previous study of the KIM10+ *galU* mutant LOS showed some differential staining patterns via silver stain as compared to wild type KIM10+ LOS (45). Further examination of the mutant revealed an increased susceptibility to the cationic microbial peptide polymyxin B. That *galU* plays a role in the formation of a complete outer core, and that a fully formed outer core is necessary for resistance to antimicrobial products, has also been described in other bacterial species (96, 137). A *Y. pseudotuberculosis* IP2790c *galU* mutant showed a similar phenotype as the *Y. pestis galU* mutant in the CFU assays, which suggests that *galU* plays a similar role in both *Yersinia* species. It is interesting to note that *galU* has been reported to be essential in *Y. enterocolitica* (137). This is clearly not the case for *Y. pestis* and *Y. pseudotuberculosis*, suggesting a divergent role for *galU* in *Y. enterocolitica*. The organization of the gene cluster containing *galU* is significantly different in *Y. enterocolitica* as compared to either *Y. pestis* or *Y. pseudotuberculosis*. Other bacterial species also have an organization of this gene cluster that is different from *Y. pestis* and *Y. pseudotuberculosis*, and yet *galU* mutants were able to be constructed (21, 96), indicating that the gene is not essential in these cases. As with the research in this chapter, these other studies show that a *galU* mutant does exhibit decreased resistance to antimicrobial peptides, as well as an altered lipid core structure.

Members of the *pmr* operon, which were previously identified as important for survival of *Y. pestis* in macrophages, were also identified in this screen. Pmr modifies the lipid A of LOS with aminoarabinose to increase bacterial resistance to antimicrobial peptides (34). Since mutations in either *galU* or *pmr* result in a defect in intracellular

survival, this suggests that both are required for the formation of a complete outer core as well as resistance to antimicrobial peptides, and that neither can compensate for the loss of the other.

Figures and Tables

Table 4.1: *Yersinia* strains used in Chapter 4.

Strain Name	Relevant Characteristics	Reference
KIM6+	*Y. pestis* biovar Mediaevalis, pCD1$^-$	(44)
KIM6+ *phoP*Δ	KIM6+ *phoP*Δ127-429	
KIM6+ Δ*y0142-y0145*	KIM6+ *y0142* Δ nucleotide 61- *y0145* nt724	This work
KIM6+ Δ*y0036-y0040*	KIM6+ *y0036* Δ nt31-*y0040* nt1107	This work
KIM6+ Δ*y0230-y0235*	KIM6+ *y0230* Δ nt31-*y0235* nt1029	This work
KIM6+ Δ*y0021-y0022*	KIM6+ *y0021*Δ nt61-*y0022* nt1717	This work
KIM6+ Δ*y0228*	KIM6+ *y0228*Δ19-1329	This work
KIM6+ Δ*y4047*	KIM6+ *y4047*Δ19-484	This work
KIM6+ Δ*y0297*	KIM6+ *y0297*Δ19-1011	This work
KIM6+ Δ*y0157-y0159*	KIM6+ *y0157*Δ nt22-*y0159* nt151	This work
KIM6+ Δ*gshA*	KIM6+ *gshA*Δ40-1560	This work
KIM10+	Biovar Mediaevalis, pCD1$^-$, pPCP1$^-$	(102)
KIM10+*galU::mag*/ pMMB67EH	KIM10$^+$ *galU::magellan3*, pMMB67EH, Kn^R, Ap^R	This work
KIM10+*galU::mag*/pGalU	KIM10$^+$ *galU::magellan3*, pGalU, Kn^R, Ap^R	(45)
KIM10+*galU::mag*/GFP	KIM10$^+$ *galU::magellan3*, p67GFP3.1, Kn^R, Ap^R	(45)
IP2790c	*Y. pseudotuberculosis* serogroup O1, pYV$^-$	(134)
IP2790c*galU::mag*/GFP	IP2790c *galU::magellan3*, p67GFP3.1, Kn^R, Ap^R	(45)
IP2790c*galU::mag*/pGalU	IP2790c *galU::magellan3*, pGalU, Kn^R, Ap^R	(45)

Table 4.2: Primers used to create gene knockouts.

Primer name	Sequence[1] 5' → 3'	Gene/region disrupted
MCE-1F	atgcggatccTAAATTACCATCACAGTAAACAGC	
MCE-2R	AATGTTTGCGCCTCATTTCGAACGTTGATTGAATTG	*y0142-y0145*
MCE-3F	CAATTCAACGTTCAACGTTGCAAATGAGGCGCAAACATT	
MCE-4R	ataaattctagaCACATGCGTTGTGGTTTCCCATGA	
HCP-1F	gccttcgcggccgcTGTCGAAAAAAACCTGTAGGA	
HCP-2R	AAGCAGTAAAGCAGATGTGATGACTGGCGTGCGCCG	*y0036-y0040*
HCP-3F	CGGCGCACGCCAGTCATCACATCTGCTTTACTGCTT	
HCP-4R	gcccggtctagaAAGAGCGCAATGATCCTGACATCC	
y0235-1F	atagtcggatccACACTCAGCTCAAAACACATGAGT	
y0235-2R	AAGATTTCTTACCTTGCAGTCGGGATGGTGTTACGT	*y0230-y0235*
y0235-3F	ACGTAACACCATCCCGACTGCAAGGTAAGAATCTT	
y0235-4R	tataattctagaGATCAACGTAGTCTGCCTAGCCCG	
y0021-1F	ataatttctagaTTTGCACCGAACGAAAATCTGAGC	
y0021-2R	CTGCAAATAAATTTGTTCGTCAGTGGACATGGTAA	*y0021-y0022*
y0021-3F	TTTACCATGTCCACTGACGAACAAATTTATTTGCAG	
y0021-4R	aactttggatccGACAGTTTATTTGAGTAAGACAAC	
y0228-1F	ataatatctagaCGATCTCGTGGCTGATGCGTTTAA	
y0228-2R	ATGCACATGAGCAAATTCGCGTTATTGAGTCAGTAA	*y0228*
y0228-3F	TTACTGACTCAATAACGCGAATTTGCTCATGTGCAT	
y0228-4R	aattagggatccAATCAAATGGGCATCATATTCTGC	
y4047-1F	aataaaggatccGTCTCTGATTTGGTAGGTTTTGGC	
y4047-2R	ATGCATTACAGCTTATTGGACAGGCAAACACCTTAG	*y4047*
y4047-3F	CTAAGGTGTTTGCCTGTCCAATAAGCTGTAATGCAT	
y4047-4R	gacaattctagaTGACGAGTAGCGAGAAACAGCAAT	
y0297-1F	aatattggatccTTATAGGGAACCTCAGAAAGTTGC	
y0297-2R	TTGGAAAATAAGAAAGAAGCTGCGCCTAAACACTAG	*y0297*
y0297-3F	CATAGTGTTTAGGCGCAGCTTCTTTCTTATTTTCCAA	
y0297-4R	ttagtatctagaGTTATTGCTACAACATCCCTCACG	
PTS-1F	acaggctcagaTGAACAAGGCATTATGGTAGCACG	
PTS-2R	ATCCAGCATCAGCAGCGCGTTGGTCATCTCATCTTT	*y0157-y0159*
PTS-3F	AAAGATGAGATGACCAACGCGCTGCTGATGCTGGAT	
PTS-4R	acagaaggatccAGTACGCAAGACCAGTTCTAGTTC	
gshA1F	gaagttggatccCGAGCGAATATGGCAATAGTTGAT	
gshA2R	TAAATACTCTTCAAAGCTATCGACCTCCCGCTCTTG	*gshA (y0887)*
gshA3F	CAGAGCGGGAGGTCGATAGCTTTGAAGAGTATTTA	
gsha4R	taataatctagaAGTGACCTTCAGCACGTCCGCCAT	

[1] Letters in lower case represent nucleotides added to the primer to insert to specific restriction site.

Table 4.3: Negative selection screen results.

	Gene	Symbol	Fold Change	Predicted function
1	y1793	phoQ	-2.993	sensor protein PhoQ
2	y2631	galU	-2.492	glucose-1-phosphate uridylyltransferase
3	y1921	pmrK	-2.322	hypothetical protein
4	y1794	phoP	-2.233	transcriptional regulatory protein
5	y1918	pmrF	-2.134	putative sugar transferase
6	y1919	pmrI	-2.126	hypothetical protein
7	y1920	pmrJ	-2.115	hypothetical protein
8	y0364	wecB	-2.034	UDP-N-acetyl glucosamine -2-epimerase
9	y0157	ptsN	-1.84	phosphotransferase system enzyme IIA
10	y0365	wecC	-1.789	UDP-N-acetyl-D-mannosaminuronic acid dehydrogenase
11	y0887	gshA	-1.76	glutamate--cysteine ligase
12	y4138	atpH	-1.757	ATP synthase subunit D
13	y4140	atpE	-1.706	ATP synthase subunit C
14	y4013	rpsK	-1.692	30S ribosomal protein S11
15	y3321	gshB	-1.688	glutathione synthetase
16	y4137	atpA	-1.682	ATP synthase subunit A
17	y0158		-1.659	hypothetical protein
18	y3984	rpsG	-1.642	30S ribosomal protein S7
19	y0134	rplM	-1.636	50S ribosomal protein L13
20	y0087		-1.631	lipopolysaccharide core biosynthesis glycosyl transferase
21	y0144		-1.631	hypothetical protein
22	y3680	imp	-1.629	organic solvent tolerance protein precursor
23	y4009	rplO	-1.625	50S ribosomal protein L15
24	y4139	atpF	-1.621	ATP synthase subunit B
25	y1922	pmrL	-1.62	hypothetical protein

The 25 genes with the highest negative fold change are shown.

Table 4.4: Gene mutation effects on intracellular survival of *Y. pestis* in macrophages.

Position in screen	Gene	Symbol	Fold Change	Predicted function	Bacterial intracellular survival (reference)
2	y2631	galU	-2.492	glucose-1-phosphate uridylyltransferase	-
4	y1794	phoP	-2.233	transcriptional regulatory protein	- (46)
5	y1918	pmrF	-2.134	putative sugar transferase	- (46)
9	y0157	ptsN	-1.84	phosphotransferase system enzyme IIA	+
11	y0887	gshA	-1.76	glutamate--cysteine ligase	+
18	y0158		-1.659	hypothetical protein	+
21	y0144		-1.631	hypothetical protein	+
60	y0159	ptsO	-1.514	Phosphocarrier protein HPr-like NPr	+
65	y4047		-1.504	hypothetical protein	+
119	y0036		-1.435	hemolysin co-regulated protein	+
218	y0228		-1.339	hypothetical protein	+
219	y0297	cytR	-1.339	regulator for deo operon, edp, cdd, tsx, nupC, and nupG	+
255	y0234		-1.313	putative ATP-binding protein of ABC transporter	+
390	y0232		-1.244	putative permease of ABC transport protein	+
417	y0235		-1.229	putative periplasmic binding protein of ABC transporter	+

The genes mutated in this screen are organized by fold change, and each gene's position in the screen results is indicated. Potential function of the genes is listed, and a summary of testing for intracellular survival is indicated. + indicates bacterial survival in macrophages similar to wild type bacteria, while a - indicates a defect for bacterial survival in macrophages.

Table 4.5. *galU* is important for resistance to polymyxin B.

	MIC of polymyxin B (μg/ml)
KIM10+	125
KIM10+*galU::mag*/pMMB67EH	0.49
KIM10+*galU::mag*/pGalU	125

Bacteria were grown for 20 hours in HI with polymyxin B at concentrations from 0.122-250 μg/ml, and the MIC was determined as the lowest concentration of polymyxin B at which bacterial growth was not seen. Three independent experiments were performed, and all yielded the same result.

Figure 4.1. Design of the TrasH screen.

A. A schematic of the negative selection screen. A pool of transposon-mutagenized *Y. pestis* KIM6+ were either passaged through macrophages as a negative selection condition, or grown *in vitro* without selection. Bacteria were harvested from each option and gDNA was isolated. After *in vitro* transcription, labeled RNA samples were hybridized to microarray slides and analyzed. Genes important for survival in the selective condition will be lost, and the loss of fluorescence signal of these genes is detected as a change in the fluorescence ratio when compared to the unselected control. Reprinted from Current Opinion in Microbiology (18), copyright 2007, with permission from Elsevier.

B. Representation of *in vitro* transcription from the transposon (128). The transposon consists of a *Himar1* element flanked by outward-reading T7 promoters. After the transposon is inserted in the bacterial genome and the gDNA is isolated after selection is performed, the gDNA is sheared to reduce the fragment size for *in vitro* transcription. Transcription is initiated from the outward-reading T7 promoters, and amino-allyl UTP is incorporated. The RNAs are labeled with Cyanine 3 or Cyanine 5 at these modified UPTs, and then purified for microarray hybridization. Copyright 2001 National Academy of Sciences, USA (128).

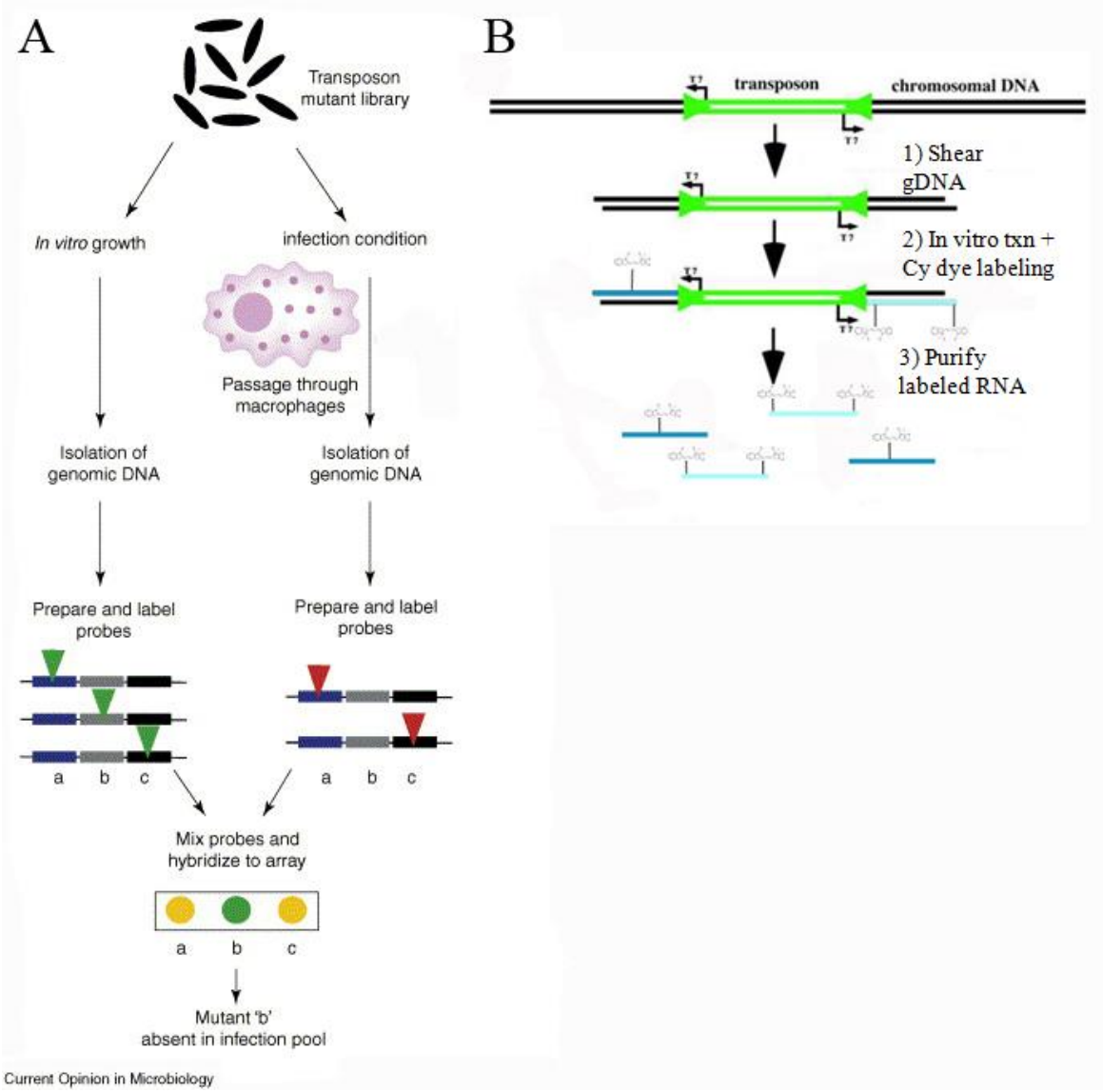

Current Opinion in Microbiology

Figure 4.2. Analysis of KIM6+ mutants for detects in intracellular survival.

BMMs were infected with the KIM6+ strains at an MOI of 10. After 15 minutes of infection the macrophages were washed to remove nonadherent bacteria and then incubated in medium containing gentamicin to kill extracellular bacteria. At the indicated time points cells were washed with PBS and lysed with Triton X-100, and serial dilutions were plated to enumerate CFUs. KIM6+ and KIM6+ *phoPΔ* were used as controls. Time post infection is indicated in the legend.

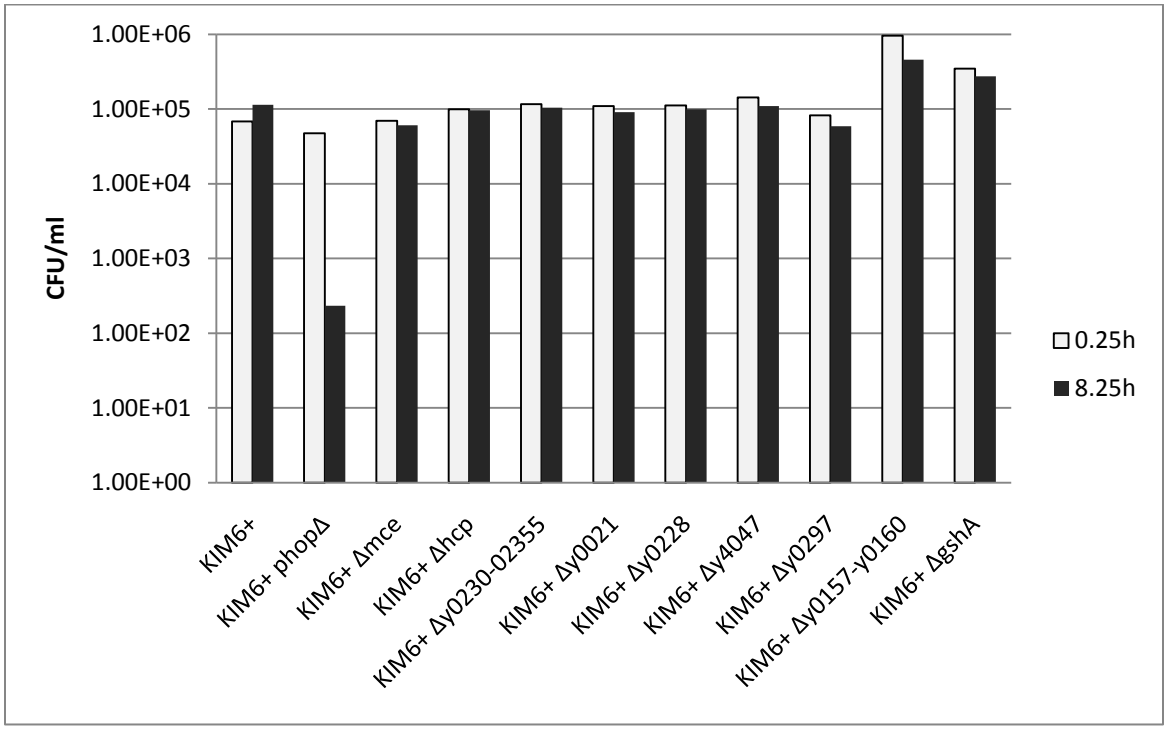

Figure 4.3. *galU* is important for the survival of *Y. pestis* in macrophages.

BMMs were infected with *Y. pestis* KIM10+, KIM10+ *galU::mag* mutant, or KIM10+ *galU::mag* complemented with pGalU at a MOI of 10. Samples were collected as in Figure 4.1, and serial dilutions were plated to enumerate CFUs. The data are averaged from three independent experiments, and the error bars indicate standard deviations. Time post infection (hours) is indicated in the legend. Asterisks indicate a significant difference compared to the data for the 15 minute time point for each strain (one asterisk represents $p < 0.05$, two asterisks represent $p < 0.01$), as determined by one-way analysis of variance with Dunnett's post test.

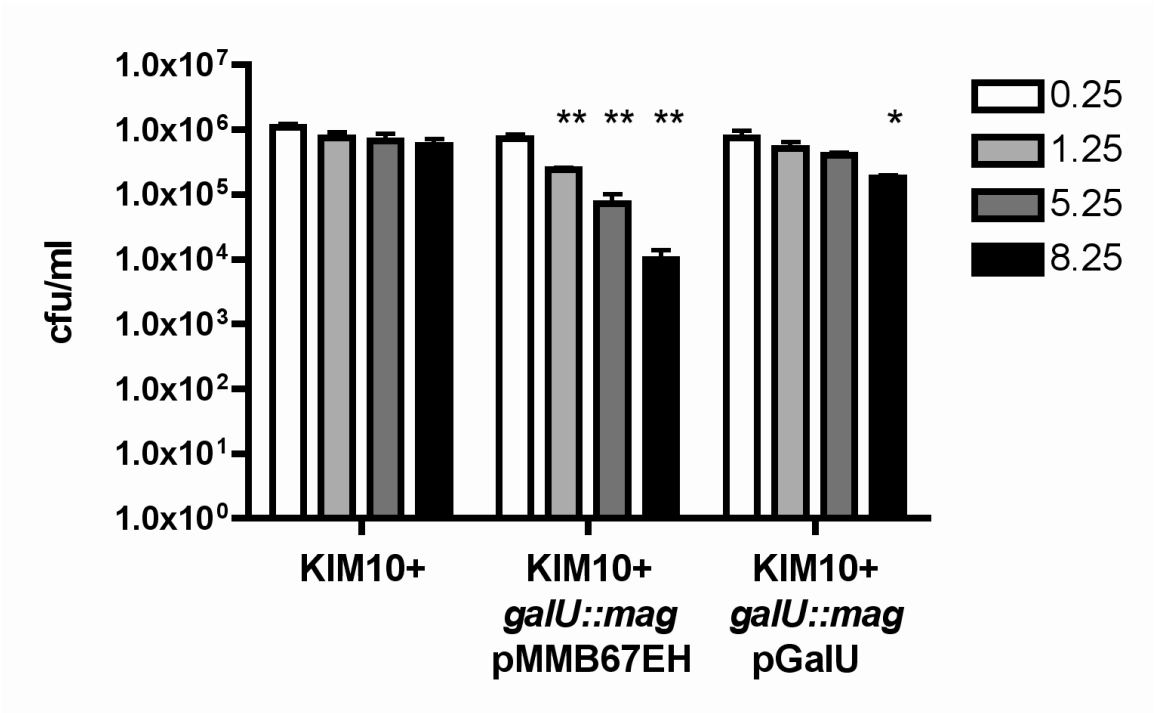

Figure 4.4: Analysis of KIM mutants for defects in preventing phagosome acidification.

J774A.1 macrophages were infected with the KIM mutants listed at a MOI of 10 in the presence of Lysotracker Red. Samples were collected at 1.25 hours post infection and analyzed. At least 50 phagosomes were counted over three fields. One experiment is shown.

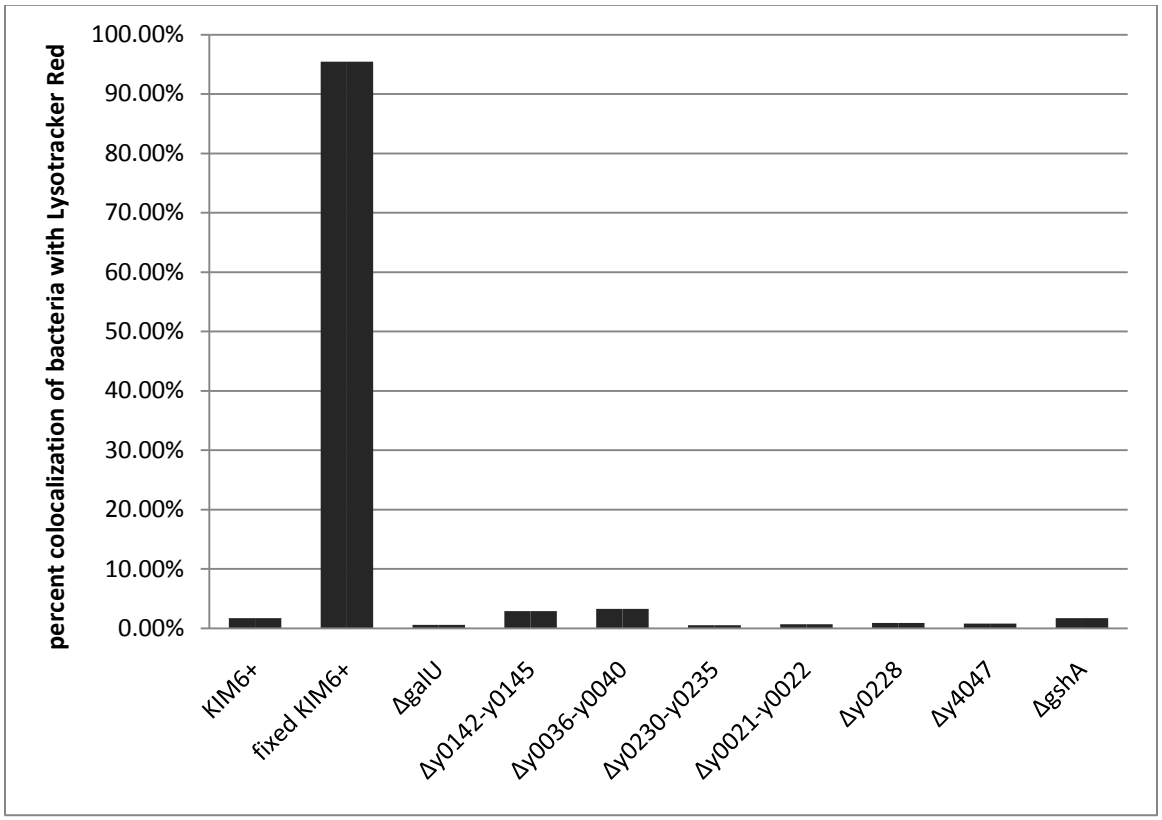

Chapter 5: Concluding remarks

Summary

The aim is this research was twofold - to further our understanding of how *Y. pestis* manipulates its intracellular environment to survive in macrophages and to further identify genes that play a role in the intracellular survival of *Y. pestis* in macrophages. As to the first part, I determined that *Y. pestis* blocks acidification of its phagosome, potentially as a survival mechanism.

Using an acidotropic fluor Lysotracker Red, I was able to show that phagosomes containing *Y. pestis* do not acidify. Previously published observations utilizing antibodies to late endocytic compartments and cell tracers to lysosomes indicated that YCVs interact with late endocytic compartments and may mature into phagolysosomes (46, 148) That YCVs fail to acidify does not necessarily contradict these previous results - *Y. pestis* could very well interact with endosomes, and perhaps lysosomes to a limited extent, even though the compartment cannot be a fully mature phagolysosome due to a lack of acidification. After confirming that the YCV does not acidify, I also found that this property is shared with *Y. pseudotuberculosis* and *Y. enterocolitica*. The factor(s) responsible for this phenotype is thus likely to be conserved among these species. I also found that none of the previously identified virulence determinants tested are required for inhibiting phagosomal acidification, leaving this factor currently unidentified. In addition, I found that *Y. pestis* does not colocalize with a marker to the cytoplasmic V_1 subunit of the vATPase. This could suggest that the vATPase is being inhibited in some fashion in order to prevent phagosomal acidification.

YCVs were also examined for their ability to alter intracellular trafficking through Rab GTPases. Unfortunately, due to technical limitations this topic was unable to be sufficiently studied, and thus remains unresolved. Utilizing macrophages deficient for Rab27, I was able to determine that *Y. pestis* does not subvert regulated exocytosis in order to escape from macrophages.

I performed a negative selection screen that identified a number of candidates that potentially play a role in the survival of *Y. pestis* in macrophages. *phoP* and the PhoP-regulated *pmr* operon were previously found to be important for the intracellular survival of *Y. pestis*; these genes were also among the potential candidates, lending validity to the screen. Several candidate genes were disrupted, and the resultant mutants were studied for their ability to survive in macrophages. Unfortunately, none of these mutants showed a defect in intracellular survival. *galU*, a gene encoding glucose-1-phosphate uridylyltransferase, was also found in this screen. GalU plays a role in the synthesis of the LPS core, and previous studies suggested that loss of this gene in *Y. pestis* led to an altered LOS (45). A *Y. pestis galU* mutant was found to be deficient for surviving in macrophages. In addition, this mutant became sensitive to the antimicrobial peptide polymyxin B, which also suggested that the LOS might be altered in this mutant.

Open Questions

Which bacterial factor(s) is responsible for inhibiting phagosome acidification?

Further understanding of the mechanism by which *Y. pestis* inhibits phagosome acidification requires identification of genes essential for this process. A key step in this quest is to identify mutants defective for preventing phagosomal acidification. I have

screened several strains that are lacking virulence factors and determined that the factor is not part of the T3SS, or encoded within the *pgm* locus or pPCP1. Several genes have now been examined as well (Chapter 2, Chapter 4), and these genes do not play a role in preventing phagosomal acidification. A negative selection screen in *M tuberculosis* recently revealed more genes that may be involved in preventing phagosomal acidification (145). This screen utilizes FACS to identify FITC-labeled bacteria that colocalize with Lysotracker Red. This type of screen could be performed with a mutant library of *Y. pestis* to try to enrich for genes that may play a role in preventing phagosomal acidification. It is quite possible that this factor(s) is a bacterial surface protein or lipid. Since *de novo* protein synthesis is not required for *Y. pestis* to inhibit phagosome acidification, the factor must be present, easily accessible, and not sensitive to the temperature shift between 28^{o}C and 37^{o}C. Surface membrane components could be isolated, and the components mixed with fixed-killed bacteria during infection and examined for colocalization of Lysotracker Red. If dead bacteria no longer colocalize with Lysotracker, biochemical techniques could be used to potentially identify the responsible factor.

How does *Y. pestis* interact with the vATPase?

I found that the YCV does not colocalize with an antibody that recognizes a subunit of the cytoplasmic V_1 domain of the vATPase. Our result offers up a number of possibilities as to the interaction of *Y. pestis* with the vATPase. Since the vATPase can undergo reversible dissociation into its two domains, it is tempting to hypothesize that *Y. pestis* is blocking reassembly of the vATPase domains, thus rendering the vATPase

inactive. Utilizing an antibody to the membrane-bound V_o domain in colocalization studies may help resolve this possibility. If this were the case, the bacteria or a bacterial protein could be either directly blocking contact sites where the two domains come together, such as subunit a, or it could be binding to the RAVE complex chaperone necessary for reassembly of the vATPase (139). If *Y. pestis* is sequestering the RAVE complex to prevent reassembly of the vATPase, a yeast two hybrid screen may be used to identify the bacterial factor involved. It is also possible that *Y. pestis* could be secreting a factor to block the V_1 subunit A-B interface, thus blocking the ATP hydrolysis required for the vATPase to pump proteins. There is some evidence for secretion systems being required to block phagolysosomal fusion, which would indirectly affect the vATPase (149). Thus, it is not inconceivable that a secretion system may be required to prevent phagosomal maturation.

Is inhibition of phagosome acidification required for the survival of *Y. pestis* in macrophages?

Although *phoP* is required for *Y. pestis* to survive in macrophages, a *phoP* mutant does not colocalize with Lysotracker Red during infection. This suggests that inhibition of phagosomal acidification is not sufficient to promote survival of *Y. pestis* in macrophages. PhoP regulates genes responsible for promoting resistance to antimicrobial peptides, and this resistance is due to modification of lipid A component of the LPS (LOS in *Y. pestis*) (47). These findings concerning PhoP suggest that resistance to antimicrobial peptides plays a key role in the survival of *Y. pestis* in macrophages, and hint at the possibility that bacterial resistance to antimicrobial peptides may be more important to

the bacterium's intracellular survival strategy than the inhibition of phagosomal acidification. However, this does not preclude the possibility that the genes responsible for inhibiting phagosomal acidification are also critically important for the survival of the bacteria in macrophages. To best examine this question, the factor would need to be identified. Mutants defective for production of this factor could then be infected into macrophages for CFU assays, and also into mice to examine the effects on virulence.

Does the YCV interact with endocytic Rab GTPases?

My preliminary Rab colocalization experiments showed a low level of colocalization of Rab7 with YCVs. Though there is some concern about antibody specificity, it is possible that *Y. pestis* interferes with intracellular trafficking events by removing Rab7 from the phagosomal surface. The generation of stable cell lines expressing dominant-negative versions of the endocytic Rabs may elucidate any interactions between these proteins and the YCV. In addition, these types of experiments could lead to a better understanding of which endocytic compartments fuse with the YCV, since Rabs are key regulatory proteins of endocytic vacuoles. Generation of more specific antibodies would be of great assistance in furthering the knowledge of how Rabs localize to the YCV.

Genes contributing to *Y. pestis* survival in macrophages.

The negative selection screen performed in BMMs identified a number of potential candidates involved in promoting the intracellular survival of *Y. pestis*. Unfortunately, the genes tested to date, with the exception of *galU*, are not required for

survival in macrophages. This suggests that the screen has a high false positive rate and may not be stringent enough. Passaging the bacteria several times through the selection condition has been shown to enrich for genes that participate in intracellular survival (20), and may be useful in the context of this screen. A more advantageous strategy may be to select for conditions that are already known to affect the intracellular survival of *Y. pestis*, such as promoting resistance to antimicrobial peptides, and see if further genes are identified. As a radical idea, it may be possible that most of the genes that exhibit a major effect on the survival of *Y. pestis* in macrophages are already identified.

Investigation of interactions of *Y. pestis* with antimicrobial peptides.

The identification of *galU* from the negative selection screen, as well as its subsequent characterization, indicated that the *galU* gene product contributes to the survival of *Y. pestis* in macrophages, in part by promoting resistance to antimicrobial peptides. It would be interesting to extend this result, as other recently identified genes, like those from the PhoP regulon, also seem to have a similar effect (47). Recent research has found that resistance to antimicrobial peptides is important for the virulence of *Y. pseudotuberculosis* (3). Since *Y. pestis* and *Y. pseudotuberculosis* are close genetic relatives, a similar result is likely to be found in *Y. pestis*. Further experiments are needed to investigate the role of antimicrobial peptides in the YCV. Analysis of antimicrobial peptides such as CRAMP via fluorescence microscopy could help determine if and how these peptides are localized to the YCV as compared to phagosomes containing inert material. The use of CRAMP $^{-/-}$ mice (5) may also further elucidate the role of lysosomal antimicrobial peptides in the context of *Y. pestis* infection

in macrophages. Screening of a bacterial mutant library utilizing a panel of antimicrobial peptides may further reveal more genes involved in peptide resistance. This examination will also help further define the environment in which *Y. pestis* resides intracellularly, as it could help resolve whether or not the YCV interacts with lysosomes, a main source for these peptides.

References

1. **Achtman, M., K. Zurth, G. Morelli, G. Torrea, A. Guiyoule, and E. Carniel.** 1999. *Yersinia pestis*, the cause of plague, is a recently emerged clone of *Yersinia pseudotuberculosis*. Proc Natl Acad Sci U S A **96:**14043-8.
2. **Akasaki, K., A. Michihara, K. Mibuka, Y. Fujiwara, and H. Tsuji.** 1995. Biosynthetic transport of a major lysosomal membrane glycoprotein, lamp-1: convergence of biosynthetic and endocytic pathways occurs at three distinctive points. Exp Cell Res **220:**464-73.
3. **Arafah, S., M. L. Rosso, L. Rehaume, R. E. Hancock, M. Simonet, and M. Marceau.** 2009. An iron-regulated LysR-type element mediates antimicrobial peptide resistance and virulence in Yersinia pseudotuberculosis. Microbiology **155:**2168-81.
4. **Autenrieth, S. E., and I. B. Autenrieth.** 2008. Yersinia enterocolitica: subversion of adaptive immunity and implications for vaccine development. Int J Med Microbiol **298:**69-77.
5. **Bergman, P., L. Johansson, H. Wan, A. Jones, R. L. Gallo, G. H. Gudmundsson, T. Hokfelt, A. B. Jonsson, and B. Agerberth.** 2006. Induction of the antimicrobial peptide CRAMP in the blood-brain barrier and meninges after meningococcal infection. Infect Immun **74:**6982-91.
6. **Bergman, T., S. Hakansson, A. Forsberg, L. Norlander, A. Macellaro, A. Backman, I. Bolin, and H. Wolf-Watz.** 1991. Analysis of the V antigen lcrGVH-yopBD operon of Yersinia pseudotuberculosis: evidence for a regulatory role of LcrH and LcrV. J Bacteriol **173:**1607-16.
7. **Birmingham, C. L., V. Canadien, N. A. Kaniuk, B. E. Steinberg, D. E. Higgins, and J. H. Brumell.** 2008. Listeriolysin O allows *Listeria monocytogenes* replication in macrophage vacuoles. Nature **451:**350-4.
8. **Birmingham, C. L., X. Jiang, M. B. Ohlson, S. I. Miller, and J. H. Brumell.** 2005. Salmonella-induced filament formation is a dynamic phenotype induced by rapidly replicating Salmonella enterica serovar typhimurium in epithelial cells. Infect Immun **73:**1204-8.
9. **Blander, J. M., and R. Medzhitov.** 2004. Regulation of phagosome maturation by signals from toll-like receptors. Science **304:**1014-8.
10. **Bliska, J. B., and D. S. Black.** 1995. Inhibition of the Fc receptor-mediated oxidative burst in macrophages by the Yersinia pseudotuberculosis tyrosine phosphatase. Infect Immun **63:**681-5.
11. **Boland, A., and G. R. Cornelis.** 1998. Role of YopP in suppression of tumor necrosis factor alpha release by macrophages during Yersinia infection. Infect Immun **66:**1878-84.
12. **Boman, H. G., B. Agerberth, and A. Boman.** 1993. Mechanisms of action on Escherichia coli of cecropin P1 and PR-39, two antibacterial peptides from pig intestine. Infect Immun **61:**2978-84.
13. **Brubaker, R. R.** 1970. Interconversion of Purine Mononucleotides in Pasteurella pestis. Infect Immun **1:**446-454.

14. **Brumell, J. H., and S. Grinstein.** 2004. Salmonella redirects phagosomal maturation. Curr Opin Microbiol **7:**78-84.
15. **Brumell, J. H., P. Tang, S. D. Mills, and B. B. Finlay.** 2001. Characterization of Salmonella-induced filaments (Sifs) reveals a delayed interaction between Salmonella-containing vacuoles and late endocytic compartments. Traffic **2:**643-53.
16. **Bucci, C., R. G. Parton, I. H. Mather, H. Stunnenberg, K. Simons, B. Hoflack, and M. Zerial.** 1992. The small GTPase rab5 functions as a regulatory factor in the early endocytic pathway. Cell **70:**715-28.
17. **Bucci, C., P. Thomsen, P. Nicoziani, J. McCarthy, and B. van Deurs.** 2000. Rab7: a key to lysosome biogenesis. Mol Biol Cell **11:**467-80.
18. **Burrack, L. S., and D. E. Higgins.** 2007. Genomic approaches to understanding bacterial virulence. Curr Opin Microbiol **10:**4-9.
19. **Cavanaugh, D. C., and R. Randall.** 1959. The role of multiplication of *Pasteurella pestis* in mononuclear phagocytes in the pathogenesis of flea-borne plague. J Immunol **83:**348-63.
20. **Chan, K., C. C. Kim, and S. Falkow.** 2005. Microarray-based detection of *Salmonella enterica* serovar Typhimurium transposon mutants that cannot survive in macrophages and mice. Infect Immun **73:**5438-49.
21. **Chang, H. Y., J. H. Lee, W. L. Deng, T. F. Fu, and H. L. Peng.** 1996. Virulence and outer membrane properties of a *galU* mutant of *Klebsiella pneumoniae* CG43. Microb Pathog **20:**255-61.
22. **Chen, Y. A., and R. H. Scheller.** 2001. SNARE-mediated membrane fusion. Nat Rev Mol Cell Biol **2:**98-106.
23. **Cherepanov, P. A., T. G. Mikhailova, G. A. Karimova, N. M. Zakharova, V. Ershov Iu, and K. I. Volkovoi.** 1991. [Cloning and detailed mapping of the fra-ymt region of the Yersinia pestis pFra plasmid]. Mol Gen Mikrobiol Virusol**:**19-26.
24. **Churchill, G. A.** 2002. Fundamentals of experimental design for cDNA microarrays. Nat Genet **32 Suppl:**490-5.
25. **Collyn, F., M. A. Lety, S. Nair, V. Escuyer, A. Ben Younes, M. Simonet, and M. Marceau.** 2002. Yersinia pseudotuberculosis harbors a type IV pilus gene cluster that contributes to pathogenicity. Infect Immun **70:**6196-205.
26. **Cornelis, G. R., A. Boland, A. P. Boyd, C. Geuijen, M. Iriarte, C. Neyt, M. P. Sory, and I. Stainier.** 1998. The virulence plasmid of Yersinia, an antihost genome. Microbiol Mol Biol Rev **62:**1315-52.
27. **Curtis, L. M., and S. Gluck.** 2005. Distribution of Rab GTPases in mouse kidney and comparison with vacuolar H+-ATPase. Nephron Physiol **100:**p31-42.
28. **Datsenko, K. A., and B. L. Wanner.** 2000. One-step inactivation of chromosomal genes in *Escherichia coli* K-12 using PCR products. Proc Natl Acad Sci U S A **97:**6640-5.
29. **De Smet, K., and R. Contreras.** 2005. Human antimicrobial peptides: defensins, cathelicidins and histatins. Biotechnol Lett **27:**1337-47.

30. **Derbise, A., B. Lesic, D. Dacheux, J. M. Ghigo, and E. Carniel.** 2003. A rapid and simple method for inactivating chromosomal genes in *Yersinia*. FEMS Immunol Med Microbiol **38:**113-6.
31. **Deretic, V., S. Singh, S. Master, J. Harris, E. Roberts, G. Kyei, A. Davis, S. de Haro, J. Naylor, H. H. Lee, and I. Vergne.** 2006. *Mycobacterium tuberculosis* inhibition of phagolysosome biogenesis and autophagy as a host defence mechanism. Cell Microbiol **8:**719-27.
32. **Desjardins, M.** 1995. Biogenesis of phagolysosomes: the 'kiss and run' hypothesis. Trends Cell Biol **5:**183-6.
33. **Devignat, R.** 1951. [Varieties of Pasteurella pestis; new hypothesis.]. Bull World Health Organ **4:**247-63.
34. **Ernst, R. K., T. Guina, and S. I. Miller.** 1999. How intracellular bacteria survive: surface modifications that promote resistance to host innate immune responses. J Infect Dis **179 Suppl 2:**S326-30.
35. **Feng, Y., B. Press, and A. Wandinger-Ness.** 1995. Rab 7: an important regulator of late endocytic membrane traffic. J Cell Biol **131:**1435-52.
36. **Forgac, M.** 2007. Vacuolar ATPases: rotary proton pumps in physiology and pathophysiology. Nat Rev Mol Cell Biol **8:**917-29.
37. **Frigui, W., D. Bottai, L. Majlessi, M. Monot, E. Josselin, P. Brodin, T. Garnier, B. Gicquel, C. Martin, C. Leclerc, S. T. Cole, and R. Brosch.** 2008. Control of M. tuberculosis ESAT-6 secretion and specific T cell recognition by PhoP. PLoS Pathog **4:**e33.
38. **Gabay, J. E., J. M. Heiple, Z. A. Cohn, and C. F. Nathan.** 1986. Subcellular location and properties of bactericidal factors from human neutrophils. J Exp Med **164:**1407-21.
39. **Galimand, M., A. Guiyoule, G. Gerbaud, B. Rasoamanana, S. Chanteau, E. Carniel, and P. Courvalin.** 1997. Multidrug resistance in *Yersinia pestis* mediated by a transferable plasmid. N Engl J Med **337:**677-80.
40. **Garcia Vescovi, E., F. C. Soncini, and E. A. Groisman.** 1996. Mg2+ as an extracellular signal: environmental regulation of Salmonella virulence. Cell **84:**165-74.
41. **Garvis, S. G., C. R. Beuzon, and D. W. Holden.** 2001. A role for the PhoP/Q regulon in inhibition of fusion between lysosomes and Salmonella-containing vacuoles in macrophages. Cell Microbiol **3:**731-44.
42. **Geisow, M. J., P. D'Arcy Hart, and M. R. Young.** 1981. Temporal changes of lysosome and phagosome pH during phagolysosome formation in macrophages: studies by fluorescence spectroscopy. J Cell Biol **89:**645-52.
43. **Gennaro, R., and M. Zanetti.** 2000. Structural features and biological activities of the cathelicidin-derived antimicrobial peptides. Biopolymers **55:**31-49.
44. **Gong, S., S. W. Bearden, V. A. Geoffroy, J. D. Fetherston, and R. D. Perry.** 2001. Characterization of the *Yersinia pestis* Yfu ABC inorganic iron transport system. Infect Immun **69:**2829-37.
45. **Grabenstein, J. P.** 2005. Identification and characterization of genes involved in survival and replication of *Yersinia* pestis and *Yersinia* pseudotuberculosis in macrophages. Unpublished dissertation (Ph.D.) Stony Brook University.

46. **Grabenstein, J. P., H. S. Fukuto, L. E. Palmer, and J. B. Bliska.** 2006. Characterization of phagosome trafficking and identification of PhoP-regulated genes important for survival of *Yersinia pestis* in macrophages. Infect Immun **74:**3727-41.
47. **Groisman, E. A.** 2001. The pleiotropic two-component regulatory system PhoP-PhoQ. J Bacteriol **183:**1835-42.
48. **Grosdent, N., I. Maridonneau-Parini, M. P. Sory, and G. R. Cornelis.** 2002. Role of Yops and adhesins in resistance of Yersinia enterocolitica to phagocytosis. Infect Immun **70:**4165-76.
49. **Grosshans, B. L., D. Ortiz, and P. Novick.** 2006. Rabs and their effectors: achieving specificity in membrane traffic. Proc Natl Acad Sci U S A **103:**11821-7.
50. **Guo, L., K. B. Lim, J. S. Gunn, B. Bainbridge, R. P. Darveau, M. Hackett, and S. I. Miller.** 1997. Regulation of lipid A modifications by Salmonella typhimurium virulence genes phoP-phoQ. Science **276:**250-3.
51. **Guo, L., K. B. Lim, C. M. Poduje, M. Daniel, J. S. Gunn, M. Hackett, and S. I. Miller.** 1998. Lipid A acylation and bacterial resistance against vertebrate antimicrobial peptides. Cell **95:**189-98.
52. **Gwinn, M. R., and V. Vallyathan.** 2006. Respiratory burst: role in signal transduction in alveolar macrophages. J Toxicol Environ Health B Crit Rev **9:**27-39.
53. **Haag, H., K. Hantke, H. Drechsel, I. Stojiljkovic, G. Jung, and H. Zahner.** 1993. Purification of yersiniabactin: a siderophore and possible virulence factor of Yersinia enterocolitica. J Gen Microbiol **139:**2159-65.
54. **Hansen, L. T., and T. A. Gill.** 2000. Solubility and antimicrobial efficacy of protamine on Listeria monocytogenes and Escherichia coli as influenced by pH. J Appl Microbiol **88:**1049-55.
55. **Hashim, S., K. Mukherjee, M. Raje, S. K. Basu, and A. Mukhopadhyay.** 2000. Live Salmonella modulate expression of Rab proteins to persist in a specialized compartment and escape transport to lysosomes. J Biol Chem **275:**16281-8.
56. **Higuchi, R.** 1990. Recombinant PCR., p. 177-183. *In* D. H. G. M.A. Innis, J.J. Snisky & T.J. White (ed.), PCR Protocols: A Guide in Methods and Applications. Academic Press, New York.
57. **Hirata, R., L. A. Graham, A. Takatsuki, T. H. Stevens, and Y. Anraku.** 1997. VMA11 and VMA16 encode second and third proteolipid subunits of the Saccharomyces cerevisiae vacuolar membrane H+-ATPase. J Biol Chem **272:**4795-803.
58. **Holmstrom, A., R. Rosqvist, H. Wolf-Watz, and A. Forsberg.** 1995. Virulence plasmid-encoded YopK is essential for Yersinia pseudotuberculosis to cause systemic infection in mice. Infect Immun **63:**2269-76.
59. **Hurtado-Lorenzo, A., M. Skinner, J. El Annan, M. Futai, G. H. Sun-Wada, S. Bourgoin, J. Casanova, A. Wildeman, S. Bechoua, D. A. Ausiello, D. Brown, and V. Marshansky.** 2006. V-ATPase interacts with ARNO and Arf6 in

early endosomes and regulates the protein degradative pathway. Nat Cell Biol **8:**124-36.

60. **Inglesby, T. V., D. T. Dennis, D. A. Henderson, J. G. Bartlett, M. S. Ascher, E. Eitzen, A. D. Fine, A. M. Friedlander, J. Hauer, J. F. Koerner, M. Layton, J. McDade, M. T. Osterholm, T. O'Toole, G. Parker, T. M. Perl, P. K. Russell, M. Schoch-Spana, and K. Tonat.** 2000. Plague as a biological weapon: medical and public health management. Working Group on Civilian Biodefense. JAMA **283:**2281-90.
61. **Izumi, T.** 2007. Physiological roles of Rab27 effectors in regulated exocytosis. Endocr J **54:**649-57.
62. **Jancic, C., A. Savina, C. Wasmeier, T. Tolmachova, J. El-Benna, P. M. Dang, S. Pascolo, M. A. Gougerot-Pocidalo, G. Raposo, M. C. Seabra, and S. Amigorena.** 2007. Rab27a regulates phagosomal pH and NADPH oxidase recruitment to dendritic cell phagosomes. Nat Cell Biol **9:**367-78.
63. **Janeway, C.** 2001. Immunobiology : the immune system in health and disease, 5th ed, vol. Garland Pub., New York.
64. **Kaniga, K., J. C. Bossio, and J. E. Galan.** 1994. The *Salmonella typhimurium* invasion genes *invF* and *invG* encode homologues of the AraC and PulD family of proteins. Mol Microbiol **13:**555-68.
65. **Kawahara, K., H. Tsukano, H. Watanabe, B. Lindner, and M. Matsuura.** 2002. Modification of the structure and activity of lipid A in Yersinia pestis lipopolysaccharide by growth temperature. Infect Immun **70:**4092-8.
66. **Kawasaki-Nishi, S., T. Nishi, and M. Forgac.** 2001. Arg-735 of the 100-kDa subunit a of the yeast V-ATPase is essential for proton translocation. Proc Natl Acad Sci U S A **98:**12397-402.
67. **Kinchen, J. M., and K. S. Ravichandran.** 2008. Phagosome maturation: going through the acid test. Nat Rev Mol Cell Biol **9:**781-95.
68. **Knirel, Y. A., S. V. Dentovskaya, S. N. Senchenkova, R. Z. Shaikhutdinova, N. A. Kocharova, and A. P. Anisimov.** 2006. Structural features and structural variability of the lipopolysaccharide of Yersinia pestis, the cause of plague. J Endotoxin Res **12:**3-9.
69. **Kukkonen, M., M. Suomalainen, P. Kyllonen, K. Lahteenmaki, H. Lang, R. Virkola, I. M. Helander, O. Holst, and T. K. Korhonen.** 2004. Lack of O-antigen is essential for plasminogen activation by Yersinia pestis and Salmonella enterica. Mol Microbiol **51:**215-25.
70. **Kumar, Y., and R. H. Valdivia.** 2009. Leading a sheltered life: intracellular pathogens and maintenance of vacuolar compartments. Cell Host Microbe **5:**593-601.
71. **Kurosaka, K., Q. Chen, F. Yarovinsky, J. J. Oppenheim, and D. Yang.** 2005. Mouse cathelin-related antimicrobial peptide chemoattracts leukocytes using formyl peptide receptor-like 1/mouse formyl peptide receptor-like 2 as the receptor and acts as an immune adjuvant. J Immunol **174:**6257-65.
72. **Kwiatkowska, K., and A. Sobota.** 1999. Signaling pathways in phagocytosis. Bioessays **21:**422-31.

73. **Lahteenmaki, K., R. Virkola, A. Saren, L. Emody, and T. K. Korhonen.** 1998. Expression of plasminogen activator pla of Yersinia pestis enhances bacterial attachment to the mammalian extracellular matrix. Infect Immun **66:**5755-62.
74. **Landolt-Marticorena, C., K. M. Williams, J. Correa, W. Chen, and M. F. Manolson.** 2000. Evidence that the NH2 terminus of vph1p, an integral subunit of the V0 sector of the yeast V-ATPase, interacts directly with the Vma1p and Vma13p subunits of the V1 sector. J Biol Chem **275:**15449-57.
75. **Lathem, W. W., S. D. Crosby, V. L. Miller, and W. E. Goldman.** 2005. Progression of primary pneumonic plague: a mouse model of infection, pathology, and bacterial transcriptional activity. Proc Natl Acad Sci U S A **102:**17786-91.
76. **Liberati, N. T., J. M. Urbach, S. Miyata, D. G. Lee, E. Drenkard, G. Wu, J. Villanueva, T. Wei, and F. M. Ausubel.** 2006. An ordered, nonredundant library of *Pseudomonas aeruginosa* strain PA14 transposon insertion mutants. Proc Natl Acad Sci U S A **103:**2833-8.
77. **Ligon, B. L.** 2006. Plague: a review of its history and potential as a biological weapon. Semin Pediatr Infect Dis **17:**161-70.
78. **Lill, H., S. Engelbrecht, G. Schonknecht, and W. Junge.** 1986. The proton channel, CF0, in thylakoid membranes. Only a low proportion of CF1-lacking CF0 is active with a high unit conductance (169 fS). Eur J Biochem **160:**627-34.
79. **Lilo, S., Y. Zheng, and J. B. Bliska.** 2008. Caspase-1 activation in macrophages infected with Yersinia pestis KIM requires the type III secretion system effector YopJ. Infect Immun **76:**3911-23.
80. **Liu, Q., X. H. Leng, P. R. Newman, E. Vasilyeva, P. M. Kane, and M. Forgac.** 1997. Site-directed mutagenesis of the yeast V-ATPase A subunit. J Biol Chem **272:**11750-6.
81. **Lopez-Garcia, B., P. H. Lee, K. Yamasaki, and R. L. Gallo.** 2005. Anti-fungal activity of cathelicidins and their potential role in Candida albicans skin infection. J Invest Dermatol **125:**108-15.
82. **Lukaszewski, R. A., D. J. Kenny, R. Taylor, D. G. Rees, M. G. Hartley, and P. C. Oyston.** 2005. Pathogenesis of *Yersinia pestis* infection in BALB/c mice: effects on host macrophages and neutrophils. Infect Immun **73:**7142-50.
83. **Ma, J., T. Chen, J. Mandelin, A. Ceponis, N. E. Miller, M. Hukkanen, G. F. Ma, and Y. T. Konttinen.** 2003. Regulation of macrophage activation. Cell Mol Life Sci **60:**2334-46.
84. **Martin-Orozco, N., N. Touret, M. L. Zaharik, E. Park, R. Kopelman, S. Miller, B. B. Finlay, P. Gros, and S. Grinstein.** 2006. Visualization of vacuolar acidification-induced transcription of genes of pathogens inside macrophages. Mol Biol Cell **17:**498-510.
85. **Martin, C., A. Williams, R. Hernandez-Pando, P. J. Cardona, E. Gormley, Y. Bordat, C. Y. Soto, S. O. Clark, G. J. Hatch, D. Aguilar, V. Ausina, and B. Gicquel.** 2006. The live Mycobacterium tuberculosis phoP mutant strain is more attenuated than BCG and confers protective immunity against tuberculosis in mice and guinea pigs. Vaccine **24:**3408-19.

86. **Matsuzaki, K.** 2009. Control of cell selectivity of antimicrobial peptides. Biochim Biophys Acta **1788:**1687-92.
87. **McNeil, P. L., L. Tanasugarn, J. B. Meigs, and D. L. Taylor.** 1983. Acidification of phagosomes is initiated before lysosomal enzyme activity is detected. J Cell Biol **97:**692-702.
88. **Menasche, G., E. Pastural, J. Feldmann, S. Certain, F. Ersoy, S. Dupuis, N. Wulffraat, D. Bianchi, A. Fischer, F. Le Deist, and G. de Saint Basile.** 2000. Mutations in RAB27A cause Griscelli syndrome associated with haemophagocytic syndrome. Nat Genet **25:**173-6.
89. **Meresse, S., O. Steele-Mortimer, B. B. Finlay, and J. P. Gorvel.** 1999. The rab7 GTPase controls the maturation of Salmonella typhimurium-containing vacuoles in HeLa cells. EMBO J **18:**4394-403.
90. **Miller, S. I., R. K. Ernst, and M. W. Bader.** 2005. LPS, TLR4 and infectious disease diversity. Nat Rev Microbiol **3:**36-46.
91. **Miller, S. I., A. M. Kukral, and J. J. Mekalanos.** 1989. A two-component regulatory system (phoP phoQ) controls Salmonella typhimurium virulence. Proc Natl Acad Sci U S A **86:**5054-8.
92. **Monack, D. M., J. Mecsas, N. Ghori, and S. Falkow.** 1997. Yersinia signals macrophages to undergo apoptosis and YopJ is necessary for this cell death. Proc Natl Acad Sci U S A **94:**10385-90.
93. **Mu, F. T., J. M. Callaghan, O. Steele-Mortimer, H. Stenmark, R. G. Parton, P. L. Campbell, J. McCluskey, J. P. Yeo, E. P. Tock, and B. H. Toh.** 1995. EEA1, an early endosome-associated protein. EEA1 is a conserved alpha-helical peripheral membrane protein flanked by cysteine "fingers" and contains a calmodulin-binding IQ motif. J Biol Chem **270:**13503-11.
94. **Nagaoka, I., S. Hirota, S. Yomogida, A. Ohwada, and M. Hirata.** 2000. Synergistic actions of antibacterial neutrophil defensins and cathelicidins. Inflamm Res **49:**73-9.
95. **Nathan, C. F., H. W. Murray, M. E. Wiebe, and B. Y. Rubin.** 1983. Identification of interferon-gamma as the lymphokine that activates human macrophage oxidative metabolism and antimicrobial activity. J Exp Med **158:**670-89.
96. **Nesper, J., C. M. Lauriano, K. E. Klose, D. Kapfhammer, A. Kraiss, and J. Reidl.** 2001. Characterization of *Vibrio cholerae* O1 El tor *galU* and *galE* mutants: influence on lipopolysaccharide structure, colonization, and biofilm formation. Infect Immun **69:**435-45.
97. **Okan, N. A., J. B. Bliska, and A. W. Karzai.** 2006. A Role for the SmpB-SsrA system in *Yersinia pseudotuberculosis* pathogenesis. PLoS Pathog **2:**e6.
98. **Oyston, P. C., N. Dorrell, K. Williams, S. R. Li, M. Green, R. W. Titball, and B. W. Wren.** 2000. The response regulator PhoP is important for survival under conditions of macrophage-induced stress and virulence in *Yersinia pestis*. Infect Immun **68:**3419-25.
99. **Pendrak, M. L., and R. D. Perry.** 1991. Characterization of a hemin-storage locus of Yersinia pestis. Biol Met **4:**41-7.

100. **Perez-Gutierrez, C., C. M. Llompart, M. Skurnik, and J. A. Bengoechea.** 2007. Expression of the Yersinia enterocolitica pYV-encoded type III secretion system is modulated by lipopolysaccharide O-antigen status. Infect Immun **75:**1512-6.
101. **Perry, R. D., and J. D. Fetherston.** 1997. *Yersinia pestis*--etiologic agent of plague. Clin Microbiol Rev **10:**35-66.
102. **Perry, R. D., M. L. Pendrak, and P. Schuetze.** 1990. Identification and cloning of a hemin storage locus involved in the pigmentation phenotype of *Yersinia pestis*. J Bacteriol **172:**5929-37.
103. **Philips, J. A.** 2008. Mycobacterial manipulation of vacuolar sorting. Cell Microbiol **10:**2408-15.
104. **Pinheiro da Silva, F., R. L. Gallo, and V. Nizet.** 2009. Differing effects of exogenous or endogenous cathelicidin on macrophage toll-like receptor signaling. Immunol Cell Biol.
105. **Pitt, A., L. S. Mayorga, P. D. Stahl, and A. L. Schwartz.** 1992. Alterations in the protein composition of maturing phagosomes. J Clin Invest **90:**1978-83.
106. **Powell, B., L. A. Graham, and T. H. Stevens.** 2000. Molecular characterization of the yeast vacuolar H+-ATPase proton pore. J Biol Chem **275:**23654-60.
107. **Prentice, M. B., and L. Rahalison.** 2007. Plague. Lancet **369:**1196-207.
108. **Prior, J. L., J. Parkhill, P. G. Hitchen, K. L. Mungall, K. Stevens, H. R. Morris, A. J. Reason, P. C. Oyston, A. Dell, B. W. Wren, and R. W. Titball.** 2001. The failure of different strains of Yersinia pestis to produce lipopolysaccharide O-antigen under different growth conditions is due to mutations in the O-antigen gene cluster. FEMS Microbiol Lett **197:**229-33.
109. **Pujol, C., and J. B. Bliska.** 2003. The ability to replicate in macrophages is conserved between *Yersinia pestis* and *Yersinia pseudotuberculosis*. Infect Immun **71:**5892-9.
110. **Pujol, C., and J. B. Bliska.** 2005. Turning *Yersinia* pathogenesis outside in: subversion of macrophage function by intracellular yersiniae. Clin Immunol **114:**216-26.
111. **Pujol, C., J. P. Grabenstein, R. D. Perry, and J. B. Bliska.** 2005. Replication of *Yersinia pestis* in interferon gamma-activated macrophages requires *ripA*, a gene encoded in the pigmentation locus. Proc Natl Acad Sci U S A **102:**12909-14.
112. **Pujol, C., K. A. Klein, G. A. Romanov, L. E. Palmer, C. Cirota, Z. Zhao, and J. B. Bliska.** 2009. *Yersinia pestis* can reside in autophagosomes and avoid xenophagy in murine macrophages by preventing vacuole acidification. Infect Immun **77:**2251-61.
113. **Radtke, A. L., and M. X. O'Riordan.** 2006. Intracellular innate resistance to bacterial pathogens. Cell Microbiol **8:**1720-9.
114. **Raj, P. A., K. J. Antonyraj, and T. Karunakaran.** 2000. Large-scale synthesis and functional elements for the antimicrobial activity of defensins. Biochem J **347 Pt 3:**633-41.
115. **Rink, J., E. Ghigo, Y. Kalaidzidis, and M. Zerial.** 2005. Rab conversion as a mechanism of progression from early to late endosomes. Cell **122:**735-49.

116. **Risso, A.** 2000. Leukocyte antimicrobial peptides: multifunctional effector molecules of innate immunity. J Leukoc Biol **68:**785-92.
117. **Roberts, R. L., M. A. Barbieri, K. M. Pryse, M. Chua, J. H. Morisaki, and P. D. Stahl.** 1999. Endosome fusion in living cells overexpressing GFP-rab5. J Cell Sci **112 (Pt 21):**3667-75.
118. **Roberts, R. L., M. A. Barbieri, J. Ullrich, and P. D. Stahl.** 2000. Dynamics of rab5 activation in endocytosis and phagocytosis. J Leukoc Biol **68:**627-32.
119. **Rosen, G. M., S. Pou, C. L. Ramos, M. S. Cohen, and B. E. Britigan.** 1995. Free radicals and phagocytic cells. FASEB J **9:**200-9.
120. **Rosqvist, R., I. Bolin, and H. Wolf-Watz.** 1988. Inhibition of phagocytosis in Yersinia pseudotuberculosis: a virulence plasmid-encoded ability involving the Yop2b protein. Infect Immun **56:**2139-43.
121. **Rosqvist, R., A. Forsberg, M. Rimpilainen, T. Bergman, and H. Wolf-Watz.** 1990. The cytotoxic protein YopE of Yersinia obstructs the primary host defence. Mol Microbiol **4:**657-67.
122. **Rosqvist, R., K. E. Magnusson, and H. Wolf-Watz.** 1994. Target cell contact triggers expression and polarized transfer of Yersinia YopE cytotoxin into mammalian cells. EMBO J **13:**964-72.
123. **Rotz, L. D., A. S. Khan, S. R. Lillibridge, S. M. Ostroff, and J. M. Hughes.** 2002. Public health assessment of potential biological terrorism agents. Emerg Infect Dis **8:**225-30.
124. **Roy, C. R., K. H. Berger, and R. R. Isberg.** 1998. Legionella pneumophila DotA protein is required for early phagosome trafficking decisions that occur within minutes of bacterial uptake. Mol Microbiol **28:**663-74.
125. **Rubin, E. J., B. J. Akerley, V. N. Novik, D. J. Lampe, R. N. Husson, and J. J. Mekalanos.** 1999. *In vivo* transposition of *mariner*-based elements in enteric bacteria and mycobacteria. Proc Natl Acad Sci U S A **96:**1645-50.
126. **Sano, G., Y. Takada, S. Goto, K. Maruyama, Y. Shindo, K. Oka, H. Matsui, and K. Matsuo.** 2007. Flagella facilitate escape of Salmonella from oncotic macrophages. J Bacteriol **189:**8224-32.
127. **Sansonetti, P. J., and A. Phalipon.** 1999. M cells as ports of entry for enteroinvasive pathogens: mechanisms of interaction, consequences for the disease process. Semin Immunol **11:**193-203.
128. **Sassetti, C. M., D. H. Boyd, and E. J. Rubin.** 2001. Comprehensive identification of conditionally essential genes in mycobacteria. Proc Natl Acad Sci U S A **98:**12712-7.
129. **Sato, S. B., and S. Toyama.** 1994. Interference with the endosomal acidification by a monoclonal antibody directed toward the 116 (100)-kD subunit of the vacuolar type proton pump. J Cell Biol **127:**39-53.
130. **Schnaitman, C. A., and J. D. Klena.** 1993. Genetics of lipopolysaccharide biosynthesis in enteric bacteria. Microbiol Rev **57:**655-82.
131. **Schotte, P., G. Denecker, A. Van Den Broeke, P. Vandenabeele, G. R. Cornelis, and R. Beyaert.** 2004. Targeting Rac1 by the Yersinia effector protein YopE inhibits caspase-1-mediated maturation and release of interleukin-1beta. J Biol Chem **279:**25134-42.

132. **Shi, Y., M. J. Cromie, F. F. Hsu, J. Turk, and E. A. Groisman.** 2004. PhoP-regulated Salmonella resistance to the antimicrobial peptides magainin 2 and polymyxin B. Mol Microbiol **53:**229-41.
133. **Shirakawa, R., T. Higashi, A. Tabuchi, A. Yoshioka, H. Nishioka, M. Fukuda, T. Kita, and H. Horiuchi.** 2004. Munc13-4 is a GTP-Rab27-binding protein regulating dense core granule secretion in platelets. J Biol Chem **279:**10730-7.
134. **Simonet, M., and S. Falkow.** 1992. Invasin expression in *Yersinia pseudotuberculosis*. Infect Immun **60:**4414-7.
135. **Skrzypek, E., C. Cowan, and S. C. Straley.** 1998. Targeting of the Yersinia pestis YopM protein into HeLa cells and intracellular trafficking to the nucleus. Mol Microbiol **30:**1051-65.
136. **Skurnik, M., and J. A. Bengoechea.** 2003. The biosynthesis and biological role of lipopolysaccharide O-antigens of pathogenic Yersiniae. Carbohydr Res **338:**2521-9.
137. **Skurnik, M., M. Biedzka-Sarek, P. S. Lubeck, T. Blom, J. A. Bengoechea, C. Perez-Gutierrez, P. Ahrens, and J. Hoorfar.** 2007. Characterization and biological role of the O-polysaccharide gene cluster of *Yersinia enterocolitica* serotype O:9. J Bacteriol **189:**7244-53.
138. **Smardon, A. M., and P. M. Kane.** 2007. RAVE is essential for the efficient assembly of the C subunit with the vacuolar H(+)-ATPase. J Biol Chem **282:**26185-94.
139. **Smardon, A. M., M. Tarsio, and P. M. Kane.** 2002. The RAVE complex is essential for stable assembly of the yeast V-ATPase. J Biol Chem **277:**13831-9.
140. **Smyth, G. K.** 2004. Linear models and empirical bayes methods for assessing differential expression in microarray experiments. Stat Appl Genet Mol Biol **3:**Article3.
141. **Sodeinde, O. A., and J. D. Goguen.** 1988. Genetic analysis of the 9.5-kilobase virulence plasmid of Yersinia pestis. Infect Immun **56:**2743-8.
142. **Sory, M. P., and G. R. Cornelis.** 1994. Translocation of a hybrid YopE-adenylate cyclase from Yersinia enterocolitica into HeLa cells. Mol Microbiol **14:**583-94.
143. **Steele-Mortimer, O., J. H. Brumell, L. A. Knodler, S. Meresse, A. Lopez, and B. B. Finlay.** 2002. The invasion-associated type III secretion system of Salmonella enterica serovar Typhimurium is necessary for intracellular proliferation and vacuole biogenesis in epithelial cells. Cell Microbiol **4:**43-54.
144. **Stenmark, H., R. G. Parton, O. Steele-Mortimer, A. Lutcke, J. Gruenberg, and M. Zerial.** 1994. Inhibition of rab5 GTPase activity stimulates membrane fusion in endocytosis. EMBO J **13:**1287-96.
145. **Stewart, G. R., J. Patel, B. D. Robertson, A. Rae, and D. B. Young.** 2005. Mycobacterial mutants with defective control of phagosomal acidification. PLoS Pathog **1:**269-78.
146. **Stinchcombe, J. C., D. C. Barral, E. H. Mules, S. Booth, A. N. Hume, L. M. Machesky, M. C. Seabra, and G. M. Griffiths.** 2001. Rab27a is required for regulated secretion in cytotoxic T lymphocytes. J Cell Biol **152:**825-34.

147. **Straley, S. C., and P. A. Harmon.** 1984. Growth in mouse peritoneal macrophages of *Yersinia pestis* lacking established virulence determinants. Infect Immun **45:**649-54.
148. **Straley, S. C., and P. A. Harmon.** 1984. *Yersinia pestis* grows within phagolysosomes in mouse peritoneal macrophages. Infect Immun **45:**655-9.
149. **Tan, T., W. L. Lee, D. C. Alexander, S. Grinstein, and J. Liu.** 2006. The ESAT-6/CFP-10 secretion system of Mycobacterium marinum modulates phagosome maturation. Cell Microbiol **8:**1417-29.
150. **Tapper, H., and R. Sundler.** 1995. Bafilomycin A1 inhibits lysosomal, phagosomal, and plasma membrane H(+)-ATPase and induces lysosomal enzyme secretion in macrophages. J Cell Physiol **163:**137-44.
151. **Territo, M. C., T. Ganz, M. E. Selsted, and R. Lehrer.** 1989. Monocyte-chemotactic activity of defensins from human neutrophils. J Clin Invest **84:**2017-20.
152. **Tsukano, H., F. Kura, S. Inoue, S. Sato, H. Izumiya, T. Yasuda, and H. Watanabe.** 1999. *Yersinia pseudotuberculosis* blocks the phagosomal acidification of B10.A mouse macrophages through the inhibition of vacuolar H(+)-ATPase activity. Microb Pathog **27:**253-63.
153. **Uchiya, K., M. A. Barbieri, K. Funato, A. H. Shah, P. D. Stahl, and E. A. Groisman.** 1999. A Salmonella virulence protein that inhibits cellular trafficking. EMBO J **18:**3924-33.
154. **Via, L. E., D. Deretic, R. J. Ulmer, N. S. Hibler, L. A. Huber, and V. Deretic.** 1997. Arrest of mycobacterial phagosome maturation is caused by a block in vesicle fusion between stages controlled by rab5 and rab7. J Biol Chem **272:**13326-31.
155. **Viboud, G. I., and J. B. Bliska.** 2005. *Yersinia* outer proteins: role in modulation of host cell signaling responses and pathogenesis. Annu Rev Microbiol **59:**69-89.
156. **Vieira, O. V., R. J. Botelho, and S. Grinstein.** 2002. Phagosome maturation: aging gracefully. Biochem J **366:**689-704.
157. **Vieira, O. V., C. Bucci, R. E. Harrison, W. S. Trimble, L. Lanzetti, J. Gruenberg, A. D. Schreiber, P. D. Stahl, and S. Grinstein.** 2003. Modulation of Rab5 and Rab7 recruitment to phagosomes by phosphatidylinositol 3-kinase. Mol Cell Biol **23:**2501-14.
158. **Wang, J., T. Takeuchi, H. Yokota, and T. Izumi.** 1999. Novel rabphilin-3-like protein associates with insulin-containing granules in pancreatic beta cells. J Biol Chem **274:**28542-8.
159. **Warrens, A. N., M. D. Jones, and R. I. Lechler.** 1997. Splicing by overlap extension by PCR using asymmetric amplification: an improved technique for the generation of hybrid proteins of immunological interest. Gene **186:**29-35.
160. **Wren, B. W.** 2003. The yersiniae--a model genus to study the rapid evolution of bacterial pathogens. Nat Rev Microbiol **1:**55-64.
161. **Xu, J., O. Laine, M. Masciocchi, J. Manoranjan, J. Smith, S. J. Du, N. Edwards, X. Zhu, C. Fenselau, and L. Y. Gao.** 2007. A unique Mycobacterium ESX-1 protein co-secretes with CFP-10/ESAT-6 and is necessary for inhibiting phagosome maturation. Mol Microbiol **66:**787-800.

162. **Xu, T., and M. Forgac.** 2001. Microtubules are involved in glucose-dependent dissociation of the yeast vacuolar [H+]-ATPase in vivo. J Biol Chem **276:**24855-61.
163. **Yeaman, M. R., and N. Y. Yount.** 2003. Mechanisms of antimicrobial peptide action and resistance. Pharmacol Rev **55:**27-55.
164. **Yi, Z., H. Yokota, S. Torii, T. Aoki, M. Hosaka, S. Zhao, K. Takata, T. Takeuchi, and T. Izumi.** 2002. The Rab27a/granuphilin complex regulates the exocytosis of insulin-containing dense-core granules. Mol Cell Biol **22:**1858-67.
165. **Zanetti, M., L. Litteri, R. Gennaro, H. Horstmann, and D. Romeo.** 1990. Bactenecins, defense polypeptides of bovine neutrophils, are generated from precursor molecules stored in the large granules. J Cell Biol **111:**1363-71.
166. **Zhang, J., E. Vasilyeva, Y. Feng, and M. Forgac.** 1995. Inhibition and labeling of the coated vesicle V-ATPase by 2-azido-[32P]ATP. J Biol Chem **270:**15494-500.
167. **Zhang, Y., J. Murtha, M. A. Roberts, R. M. Siegel, and J. B. Bliska.** 2008. Type III secretion decreases bacterial and host survival following phagocytosis of Yersinia pseudotuberculosis by macrophages. Infect Immun **76:**4299-310.
168. **Zhang, Z., T. Inoue, M. Forgac, and S. Wilkens.** 2006. Localization of subunit C (Vma5p) in the yeast vacuolar ATPase by immuno electron microscopy. FEBS Lett **580:**2006-10.
169. **Zhou, D., Y. Han, L. Qin, Z. Chen, J. Qiu, Y. Song, B. Li, J. Wang, Z. Guo, Z. Du, X. Wang, and R. Yang.** 2005. Transcriptome analysis of the Mg2+-responsive PhoP regulator in Yersinia pestis. FEMS Microbiol Lett **250:**85-95.